Agenda - June 26th

1) Course presentation on Antenna measurements.
   - Antenna properties review
   - FF measurements
   - SNF measurements.

University of Aveiro
Training Course

Leandro de Haro, Cristian Martínez (ASYSOL)

June 26th , 2012

Centro de Empresas, Parque Científico y Tecnológico UPM
Campus de Montegancedo, 28223 Pozuelo de Alarcón, Madrid, Spain

Contacts

Jose Luis Besada/Leandro de Haro/Cristian Martínez

ANTENNA SYSTEMS SOLUTIONS S.L. (ASYSOL)
Despacho 01, Centro de Empresas,
Parque Científico y Tecnológico UPM
Campus de Montegancedo,
28223 Pozuelo de Alarcón, Madrid, SPAIN.

Tel: +34 91 452 48 26
WEB SITE: www.asysol.com
E-Mail: info@asysol.com

Far Field & Anecoich Chambers

Summary

- Field regions around a radiating antenna
- Antenna Parameters
- Far Field ranges: Design Criteria
- Elevated and ground reflection ranges
- Anechoic chambers for antenna measurements
- Classical measurements in Far Field
  - Patterns:
    - Errors due to reflections.
    - Range length effect
  - Gain:
    - Errors due to impedance and polarization.
  - Polarization:
    - Axis definition
    - Direct CP-XP measurements
    - Indirect measurements: Errors
    - Axial ration vs frequency measurements

Field Regions around an Antenna

- Around a radiating antenna, there are mainly three regions:
  - Reactive Near-Field Regions ($r<\lambda$)
    - Reactive energy is higher than radiating energy.
  - Radiating near field regions (including Fresnel's region)
    - Intermediate region between reactive and Far Field region. Radiating energy is higher but pattern is still function of distance.
  - Far Field Region (Radiation region, Fraunhofer's region)
    - Pattern is practically independent of distance.

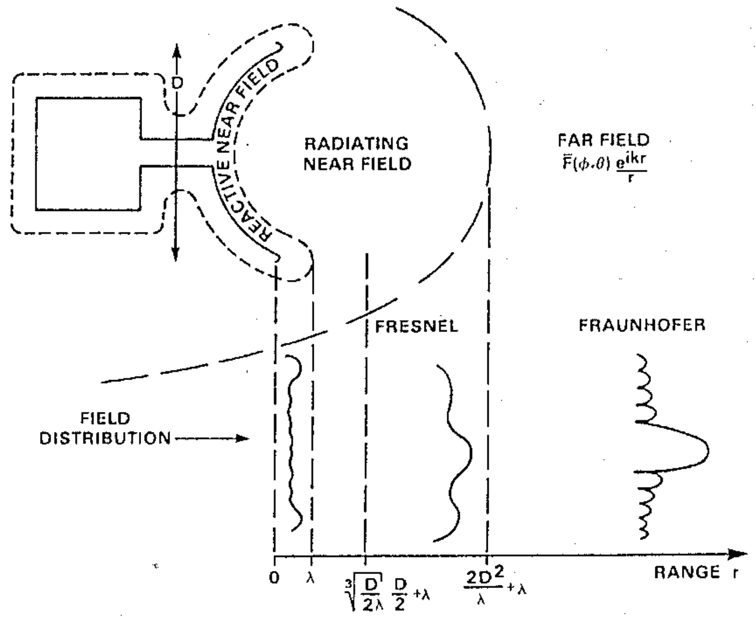

Standard Far-Field criteria is:

$$r \geq \frac{2D^2}{\lambda} \quad y \quad r >> \lambda$$

D: Maximum antenna size

ANTENNA Systems Solutions

Field Regions

- Radiation pattern simulation of an array of 9 vertical dipoles (base station antenna) at different ranges
  - Frequency: 900 MHz
  - Size : 2.1 m
  - Far Field criteria: 26.7 m

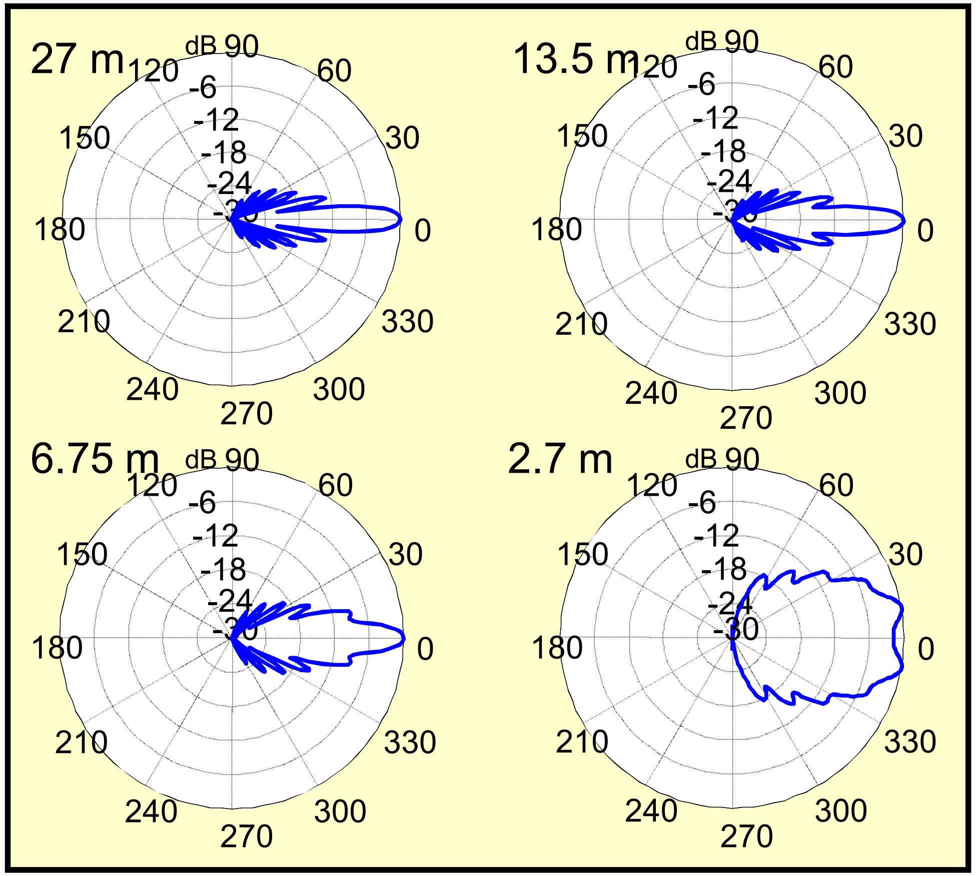

ANTENNA Systems Solutions

Antenna Measurement Ranges

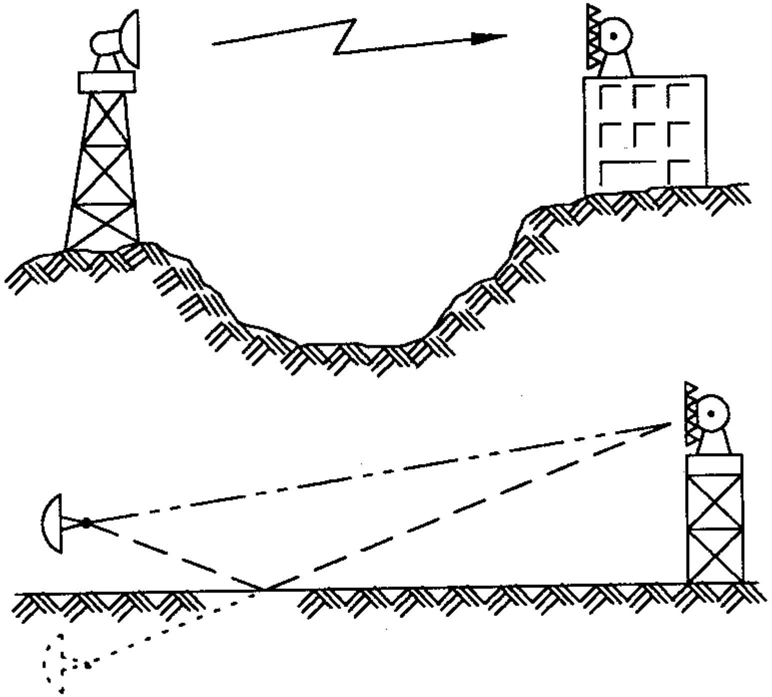

Far Field Ranges.
Elevated and Ground Reflection

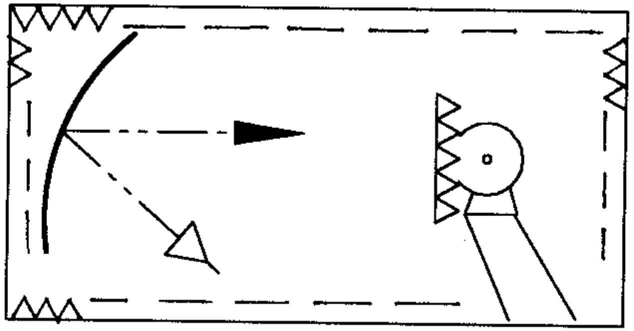

Compact Range

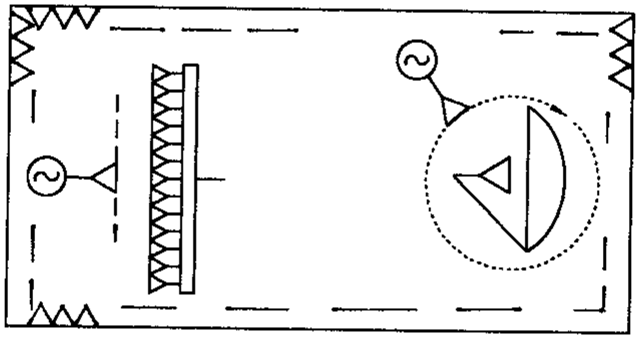

Near-Field Ranges: Plannar and Spherical

Antenna Radiating Field: Properties

- Radiating fields of an antenna follows:
  - Fields **E** y **H** depends on r as a spherical wave $e^{-jk_0 r}/r$.
  - Fields **E** y **H** depends on θ y ϕ due to the spherical wave is non homogeneous.
  - The radiated spherical wave performs locally as a plannar wave:

$$\vec{E} \perp \hat{r} \qquad \left|\vec{E}\right| = \eta \left|\vec{H}\right|$$
$$\vec{H} \perp \hat{r}$$

  - Fields **E** y **H** doe not have radial component:

$$\vec{E} = \frac{e^{-jk_o r}}{r}\left(\hat{\theta}\, F_\theta(\theta,\phi) + \hat{\phi}\, F_\phi(\theta,\phi)\right)$$

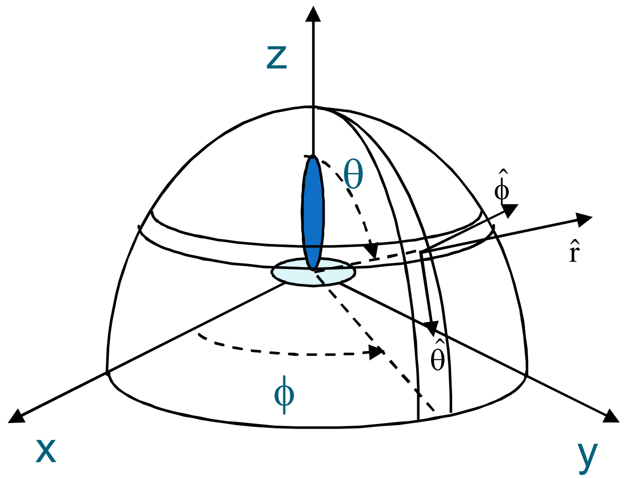

$0 \le \theta \le \pi$

$0 \le \phi < 2\pi$

Principal Plane Patterns

- Directive antenna are usually described with the principal planes:
  - Plane E: vector E and maximum radiation direction (YZ)
  - Plane H: vector H and maximum radiation direction (XZ)

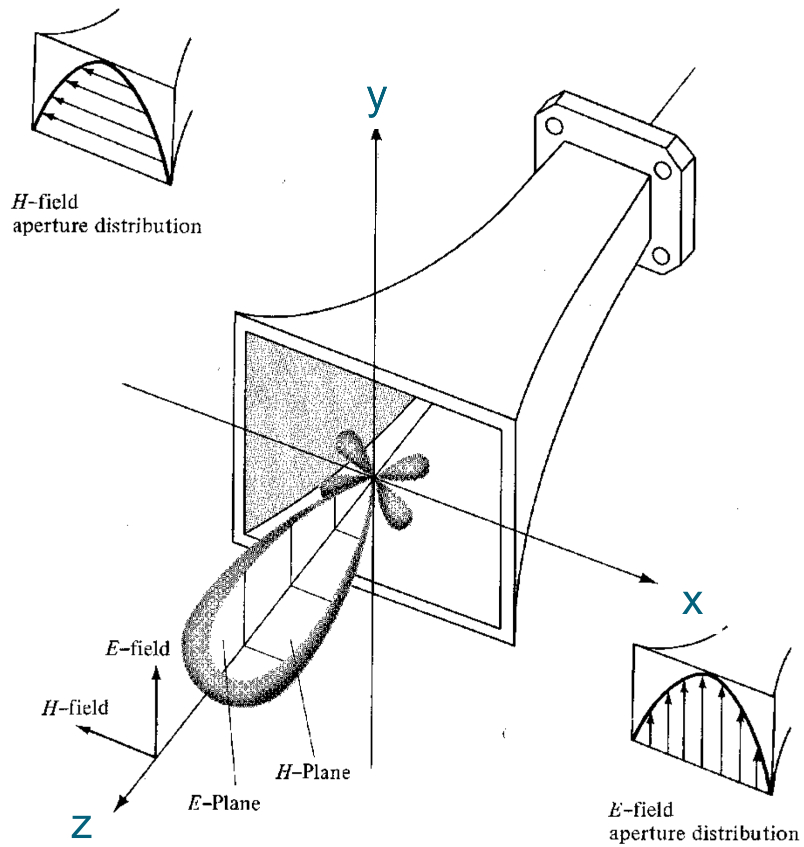

Figure 2.3 Principal *E*- and *H*-plane patterns for a pyramidal horn antenna.

Radiation Pattern Parameters

- LOBE: pattern region limited by lower radiation regiosns.
  - Main lobe: it contains main radiation
  - Secondary Lobe: non main lobes.
  - Side Lobes: adyacents to the main lobe
- Secondary Lobe Level (higher secondary lobe respect the main lobe)
- Main beam-width at -3dB (between half-power directions).
- Forward-Backward ratio, (ratio between main and backward lobes).

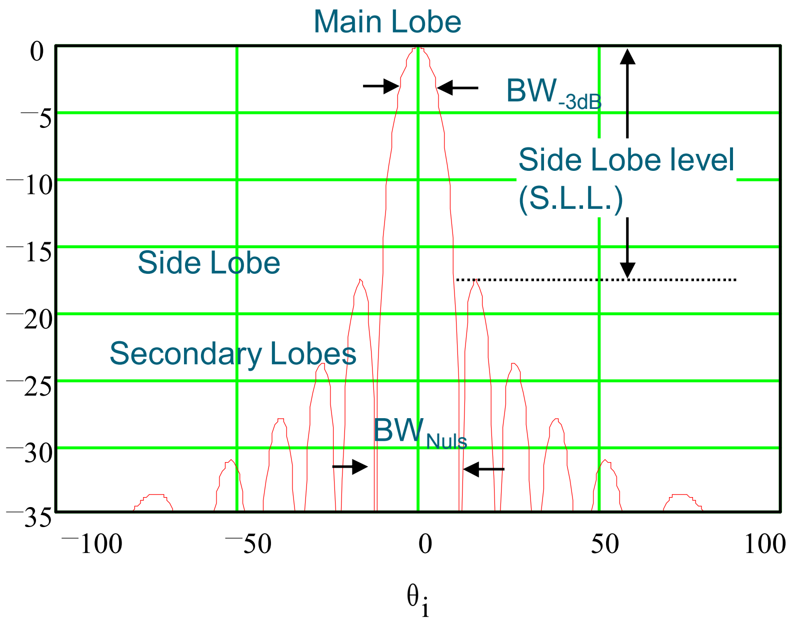

Directivity

- Directive Gain: $D(\theta,\phi)$
  - Ratio between radiation intensity at (θ,ϕ) and the radiation intensity of an isotropic antenna radiating the same total power.

$$D(\theta,\phi) \stackrel{\Delta}{=} \frac{U(\theta,\phi)}{U_{Isotropic}} = 4\pi \frac{U(\theta,\phi)}{P_{radiated}} = 4\pi r^2 \frac{\langle S(r,\theta,\phi)\rangle}{P_{radiated}}$$

$$P_{rad} = \int_{4\pi} U(\theta,\phi)\,d\Omega = \int_0^{\pi}\int_0^{2\pi} r^2 \langle S(r,\theta,\phi)\rangle sen\,\theta\, d\theta\, d\phi$$

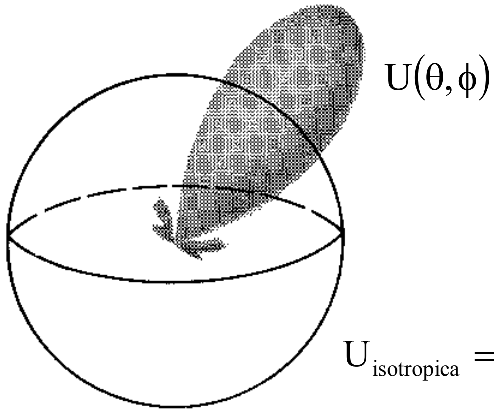

$$U_{isotropica} = \frac{P_{radiada}}{4\pi}$$

- Directivity: D_0.
  - Directive gain at the maximum radiation direction.
  - Higher or equal than 1 (0 dBi).
  - Described in dBi: $10 \log D_0$.

Gain & Efficiency

- Power Gain: G(θ,ϕ)

$$G(\theta,\phi) \stackrel{\Delta}{=} 4\pi \frac{U(\theta,\phi)}{P_{delivered}} = 4\pi r^2 \frac{\langle S(r,\theta,\phi)\rangle}{P_{delivered}}$$

- Gain: G_0.
  - Power gain at maximum radiation direction.
  - It cab be lower than 1
  - Described in dBi: 10 log G_0.

- Radiation efficiency

$$\eta_R = \frac{P_{radiated}}{P_{delivered}} = \frac{G_0}{D_0} \qquad \mathrm{G}(\theta,\phi) = \eta_R \cdot \mathrm{D}(\theta,\phi)$$

Polarization

- "Plot in terms of time for a direction, displayed by the edge of radiated field vector and its direction of rotation seen from the antenna"

$$\vec{E} = E_\theta \hat{\theta} + E_\phi \hat{\phi} \qquad \begin{cases} E_\theta = |E_\theta| e^{j\delta_\theta} \\ E_\phi = |E_\phi| e^{j\delta_\phi} \end{cases}$$

Time

$$E_{\theta i} = |E_\theta| \cos(\omega t + \delta_\theta)$$
$$E_{\phi i} = |E_\phi| \cos(\omega t + \delta_\phi)$$

Removing t

$$\left(\frac{E_{\theta i}}{|E_\theta|}\right)^2 - 2\frac{E_{\theta i}}{|E_\theta|}\frac{E_{\phi i}}{|E_\phi|}\cos\delta + \left(\frac{E_{\phi i}}{|E_\phi|}\right)^2 = \mathrm{sen}^2\,\delta$$

$$\delta = \delta_\phi - \delta_\theta \qquad \begin{array}{ll} \delta < 0 & \text{(CW)} \\ \delta > 0 & \text{(CCW)} \end{array}$$

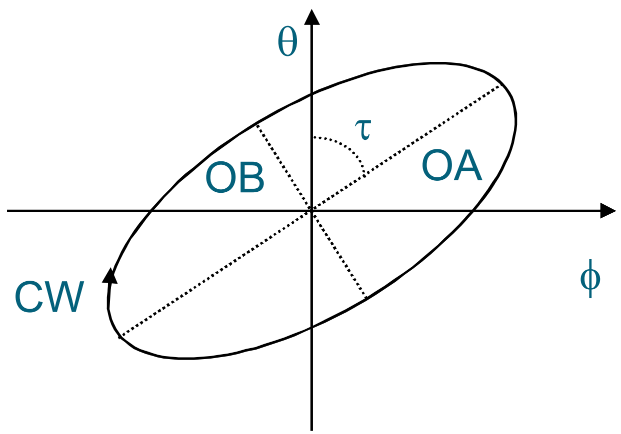

Polarization ellipse

Copolar & Crosspolar Pattern

$$\vec{E}(\theta,\phi) = E_\theta(\theta,\phi)\hat{\theta} + E_\phi(\theta,\phi)\hat{\phi}$$

$$\vec{E}(\theta,\phi) = E_{CP}(\theta,\phi)\hat{u}_{cp} + E_{XP}(\theta,\phi)\hat{u}_{xp}$$

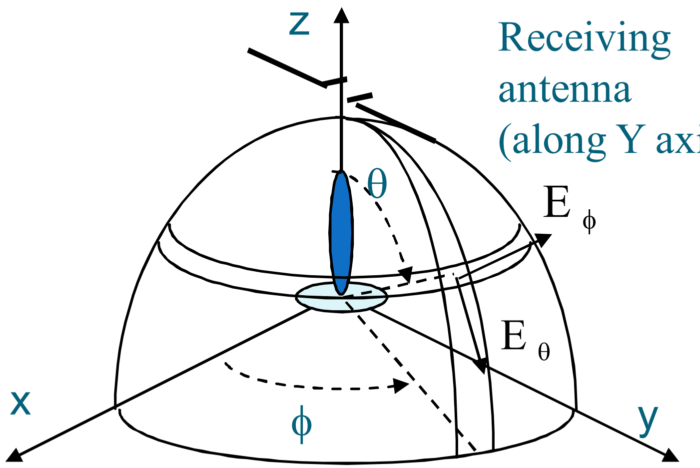

CP & XP Components :

- Linear: 3rd Ludwig's definition

$$E_Y(\theta,\phi) = E_\theta(\theta,\phi) sen\phi + E_\phi(\theta,\phi)\cos\phi \qquad E_{CP}(\theta,\phi) = E_Y(\theta,\phi)$$

$$E_X(\theta,\phi) = E_\theta(\theta,\phi)\cos\phi - E_\phi(\theta,\phi) sen\phi \qquad E_{XP}(\theta,\phi) = E_X(\theta,\phi)$$

- Circular

$$E_{RHC}(\theta,\phi) = \frac{1}{\sqrt{2}}\left(E_\theta(\theta,\phi) + jE_\phi(\theta,\phi)\right)e^{-j\phi}$$

$$E_{LHC}(\theta,\phi) = \frac{1}{\sqrt{2}}\left(E_\theta(\theta,\phi) - jE_\phi(\theta,\phi)\right)e^{j\phi}$$

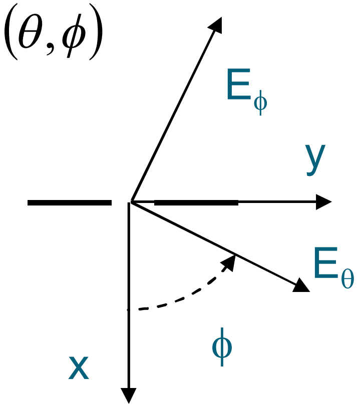

Polarization Relationships

<u>Circular relationships for circular polarization</u>

$$\rho \stackrel{\Delta}{=} \frac{|E_{RHC}|}{|E_{LHC}|} \qquad 0 \le \rho \le \infty \qquad \begin{cases} \rho = 0 & \text{Circular Left.} \\ \rho = 1 & \text{Lineal} \\ \rho = \infty & \text{Circular Right} \end{cases}$$

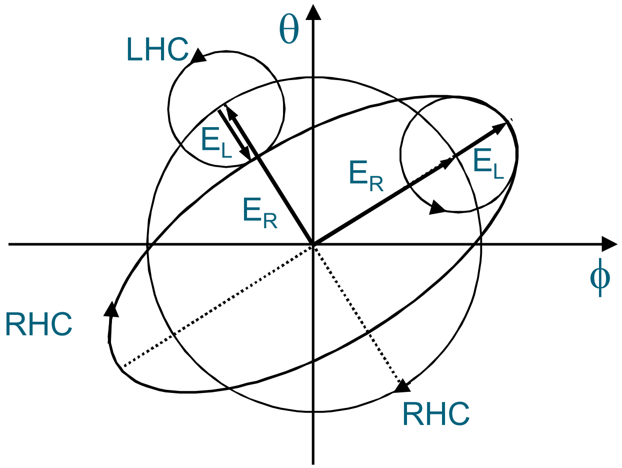

<u>Axial Ratio</u>

$$r = \frac{|E_{RHC}| + |E_{LHC}|}{|E_{RHC}| - |E_{LHC}|} \qquad AR = |r| \qquad 1 \le AR \le \infty \qquad \begin{cases} r > 0 & \text{CW} \\ r < 0 & \text{CCW} \end{cases}$$

AR=1 Polarización Circular

AR=∞ Polarización Lineal

<u>Relationships</u>

$$r = \frac{\rho + 1}{\rho - 1} \qquad \rho = \frac{r + 1}{r - 1}$$

CP-XP typical patterns

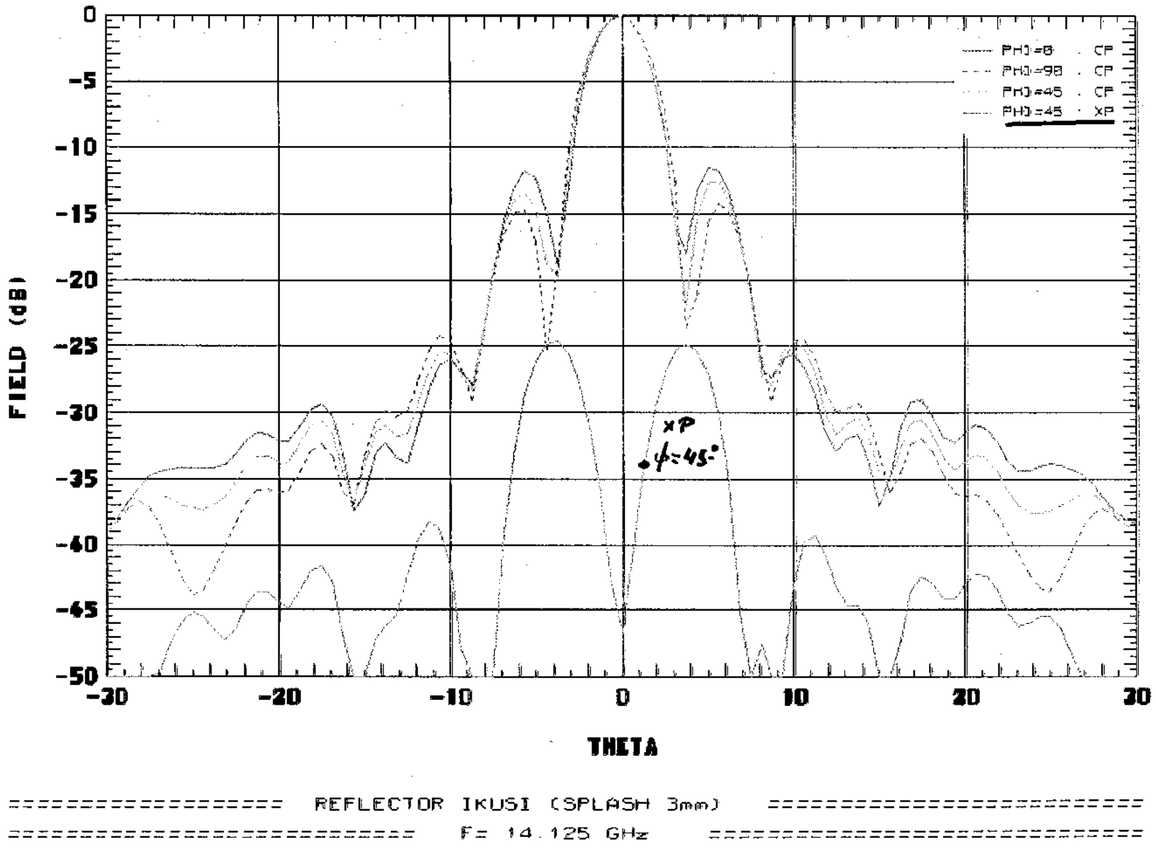

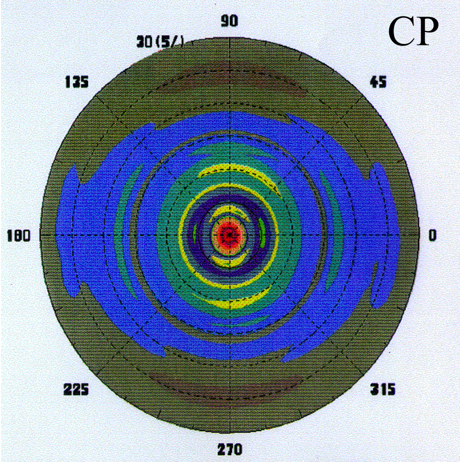

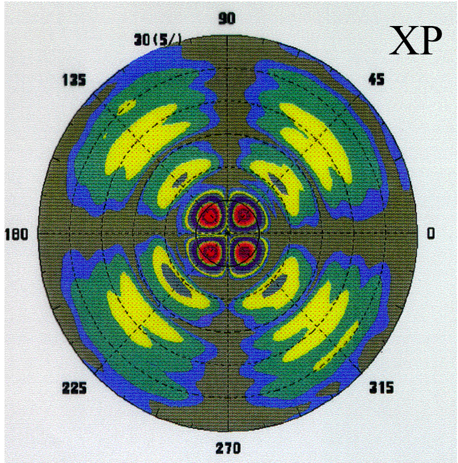

Classical Far Field Ranges

- ANTENNA UNDER TEST (usually receiving) is illuminated by a SOURCE ANTENNA.
  - The source antenna must be far away enough in order the arriving wave were a planar one:
    - Amplitude and phase constant on a volume covering the full antenna under test.

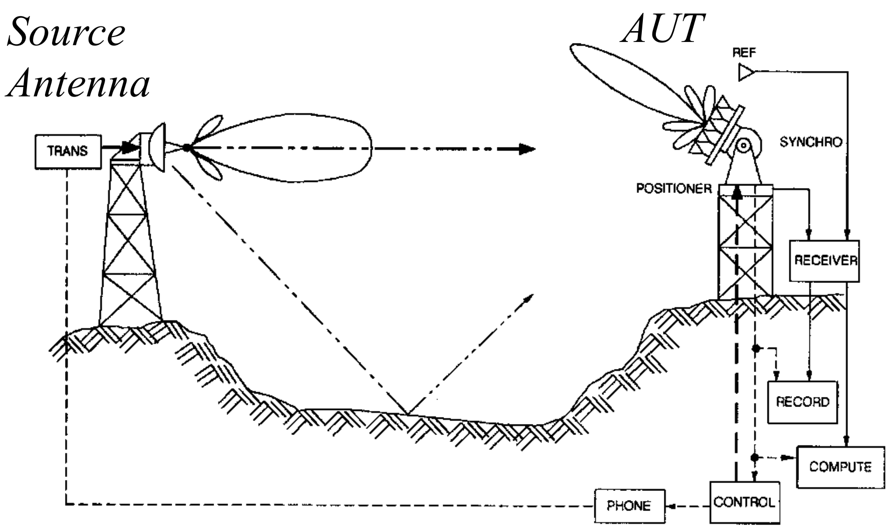

NOTE:
AUT can be tested both in reception as well as in transmission (source antenna transmitting).
Patterns and parameters have the same values according the Reciprocity theorem.

Far Field Ranges: Design Criteria

- Criteria to define source antenna properties and the minimum range (R) between antennas.

① Reactive coupling

- Important at low frequency.

$$R \geq 10\lambda \quad \Rightarrow \quad \frac{E_{1/r^2}}{E_{1/r}} \leq -36\text{dB}$$

Relationship computed for a short dipole

② Reradiation between antennas.

- Important if antennas have a high mismatch or there are metallic beams not properly covered with absorbent.

③ Amplitude Variation along the antenna.

- $R \geq 10$ L (L antenna length) $\Leftrightarrow$ Variation ≤ 1 dB

ANTENNA Systems Solutions

Far Field Ranges: Design Criteria

④ Amplitude taper of the incident wave, related to the main lobe of the source antenna (illuminating at AUT).

- Reducing the measured gain and SLL
- According an illumination "cosine over a pedestal of -10dB", typical of a parabolic reflector
  - Δ=-0.5 dB $\Rightarrow$ ΔG=-0.15 dB.

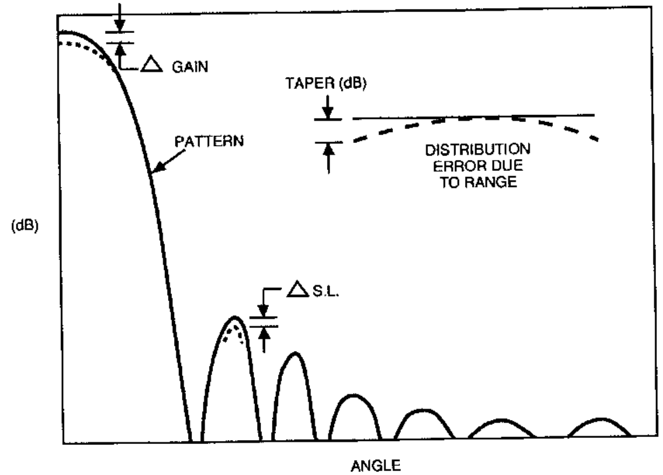

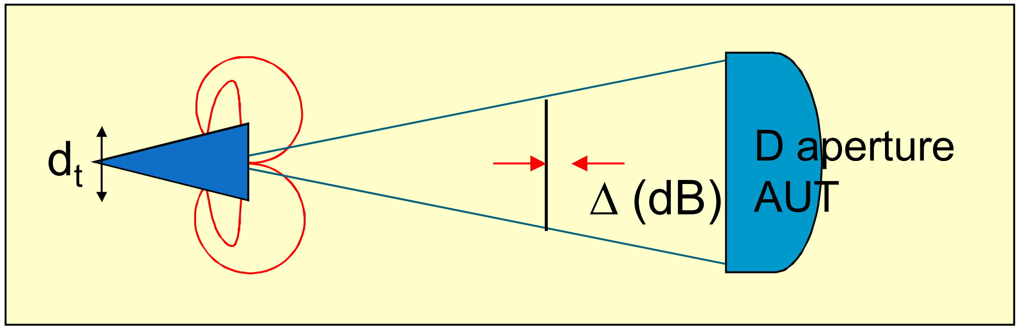

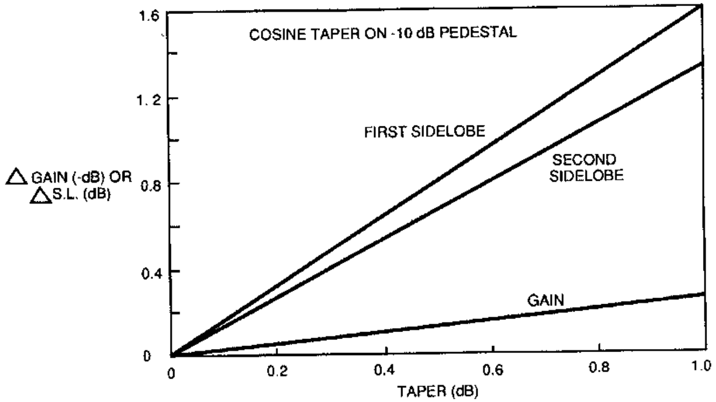

- **CRITERIUM $\Delta \approx$ -0.25 dB$\Rightarrow$ d_t.**

Estimation of Errors by Amplitude Taper

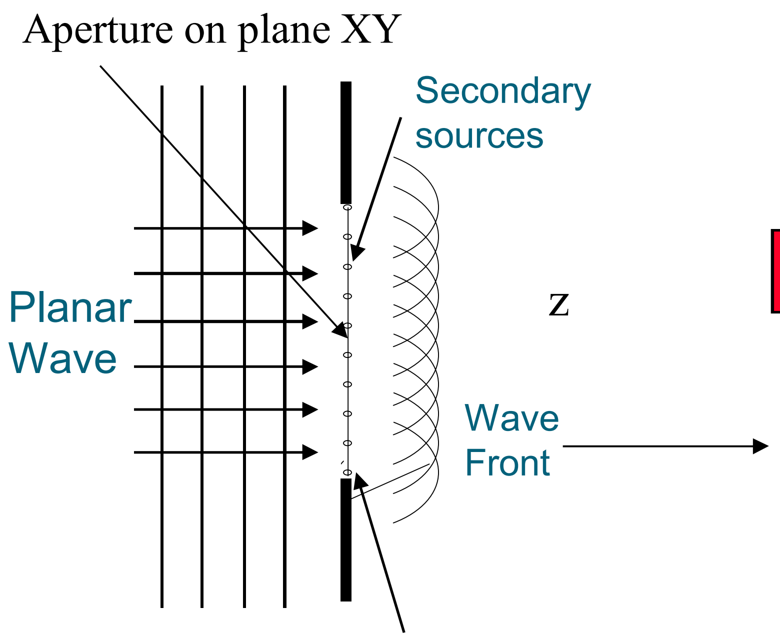

Aperture Field:

$$\vec{E}_a = \hat{x}\, E_{ax}(x', y') + \hat{y}\, E_{ay}(x', y')$$

Radiated Field:

$$E_\theta(r,\theta,\phi) = jk\frac{e^{-jkr}}{2\pi r}\left(P_x \cos\phi + P_y \operatorname{sen}\phi\right)$$

$$E_\phi(r,\theta,\phi) = -jk\frac{e^{-jkr}}{2\pi r}\cos\theta\left(P_x \operatorname{sen}\phi - P_y \cos\phi\right)$$

$$P_{x,y}(u,v) = \iint_{S_a} E_{ax,ay}(x', y')\, e^{j\frac{2\pi}{\lambda}(ux'+vy')}\, dx'dy'$$

Pattern $\approx$ Inverse Fourier Transform of Aperture Field $P_{x,y}(u,v)$

If the aperture is illuminated in reception by a field $\vec{E}'(x', y')$ with an amplitude taper and a polarization mismatch with aperture field $\vec{E}_a$, the really measured pattern is the Fourier transform of the dot product of both fields.

Far Field Ranges: Design Criteria

⑤ Phase taper on the AUT aperture.

- Gain is reduced.
- Side lobes are higher and nulls are filled.

$$\Delta R \approx \frac{D^2}{8R} \qquad \Delta\Phi = \frac{2\pi}{\lambda}\Delta R \approx \frac{\pi D^2}{4\lambda R}$$

- MINIMUM DISTANCE CRITERIUM

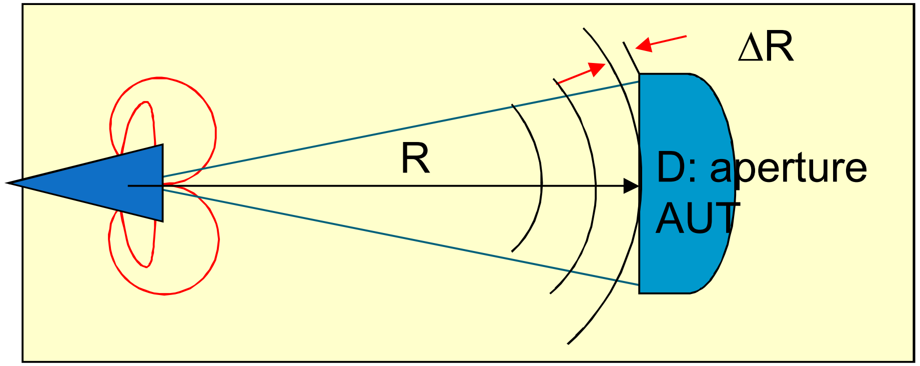

$$\boxed{\begin{array}{l}\Delta\Phi \le \dfrac{\pi}{8} \\ R \ge \dfrac{2D^2}{\lambda}\end{array}} \Rightarrow$$

Source antenna in Far Field region of AUT (reciprocity)

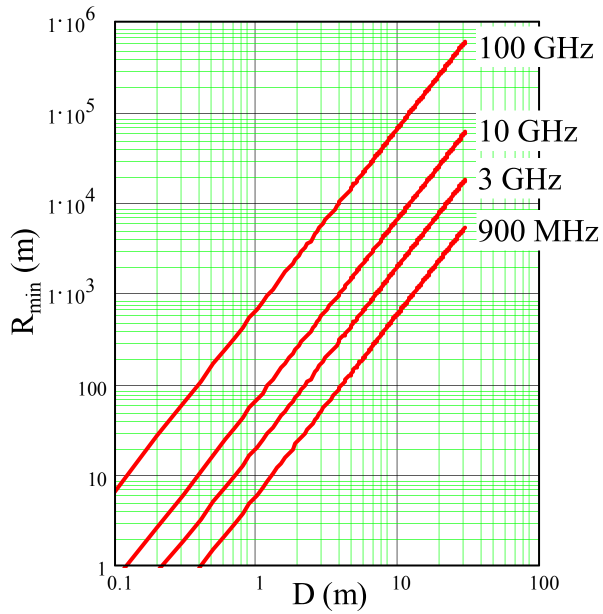

Range Length Effect

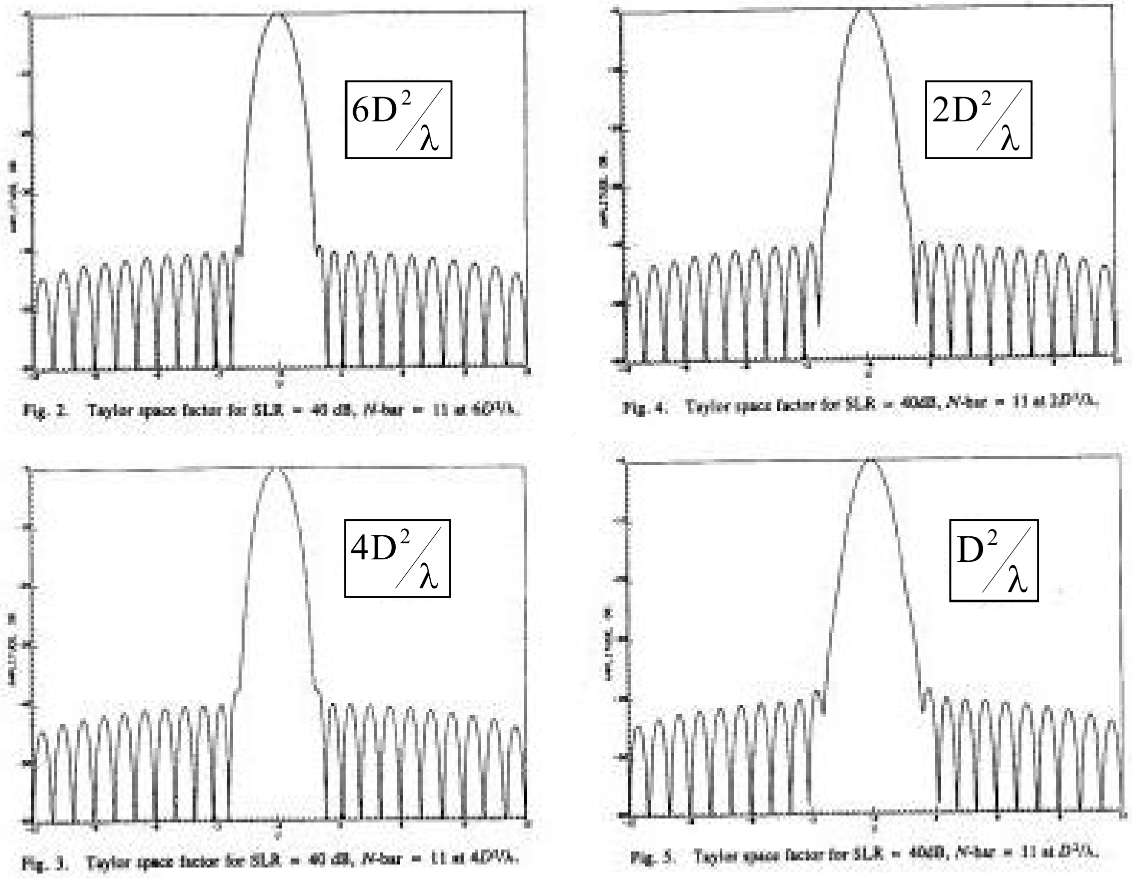

Fig. 2. Taylor space factor for SLR = 40 dB, N-bar = 11 at $6D^2/\lambda$.

Fig. 4. Taylor space factor for SLR = 40dB, N-bar = 11 at $2D^2/\lambda$.

Fig. 3. Taylor space factor for SLR = 40 dB, N-bar = 11 at $4D^2/\lambda$.

Fig. 5. Taylor space factor for SLR = 40dB, N-bar = 11 at D^2/λ.

Simulactions on the measurements of the antenna of AWACS RADAR

Elevated Range: Typical Design

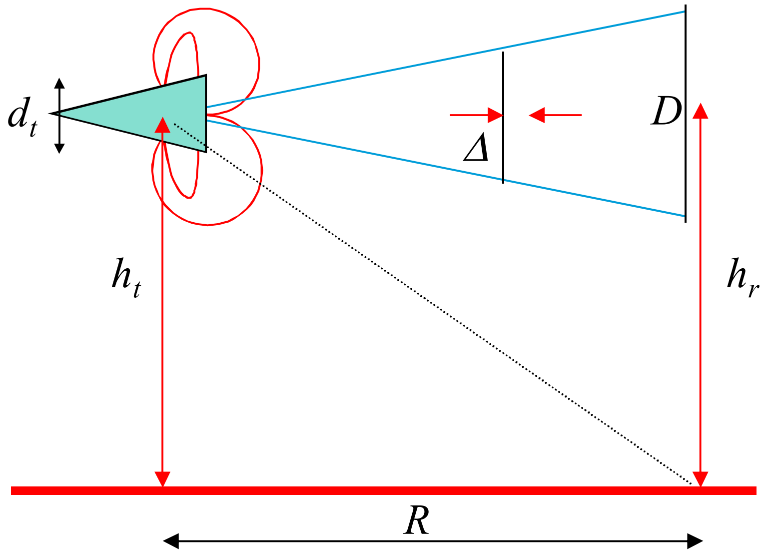

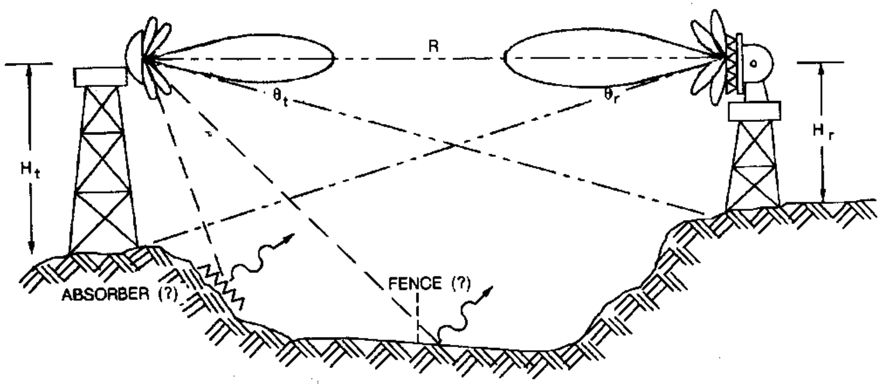

- *Phase condition: (Error in SLL)*

$$R = k\frac{D^2}{\lambda} \qquad (k \geq 2)$$

- *Taper Condition $\Delta \leq 0,25$ dB*

$$d_t \leq \frac{\lambda R}{4D}$$

- *Condition of (Non) Ground Illumination*

Main Lobe: $h_t = h_r \geq 4D$

1st Side Lobe: $h_t = h_r \geq 6D$

- *Source antennas have usually low SLL*

- *Ranges are placed on a valley to reduce ground reflections.*

Carabaña's Range (RYMSA) on Tajuña's valley

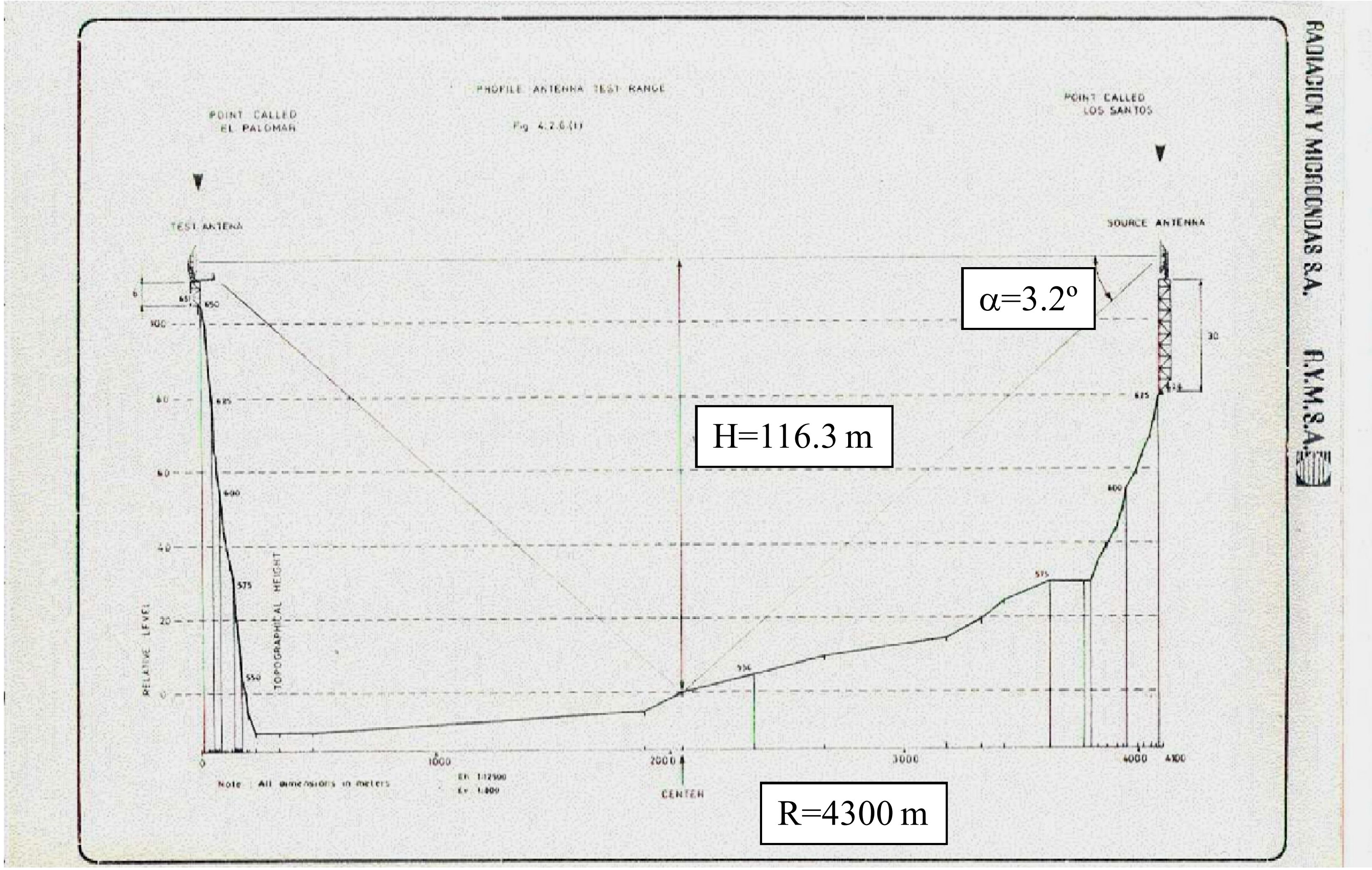

Ground Reflection Ranges: Design

- Typical for VHF & UHF

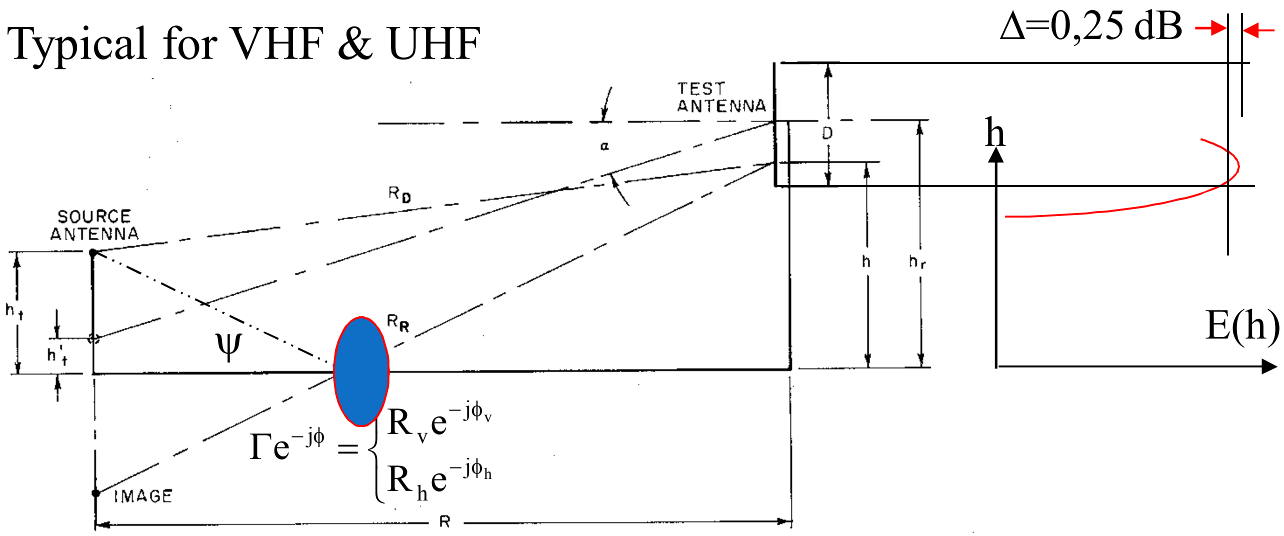

$$\Gamma e^{-j\phi} = \begin{cases} R_v e^{-j\phi_v} \\ R_h e^{-j\phi_h} \end{cases}$$

$$\psi \to 0$$

$$\Delta h_{rms} = \text{roughness}$$

$$\Delta h_{rms} < \frac{\lambda_{min}}{16 \operatorname{sen} \psi}$$

$$\phi_v, \phi_h \to 180^o$$

$$R_v, R_h \to 1$$

$$\text{Si } \psi = 3^o \to \Delta h_{rms} = \lambda$$

- *Phase Condition: (Error in SLL)*

$$R = k\frac{D^2}{\lambda} \qquad (k \geq 2)$$

- *Condition of Taper of the interference pattern $\Delta \leq 0{,}25$ dB:* $h_r \geq 3.3D$

- *Setting of the maximum on the aperture center:*

$$h_t = \frac{\lambda R}{4h_r} \qquad h'_t = \frac{1-|\Gamma|}{1+|\Gamma|} h_t$$

Fixed at everyone frequency

- *Taper Condition on the horizontal plane $\Delta \leq 0{,}25$ dB:* $d_t \leq \frac{\lambda R}{4D}$

Far Field Range: Instrumentation

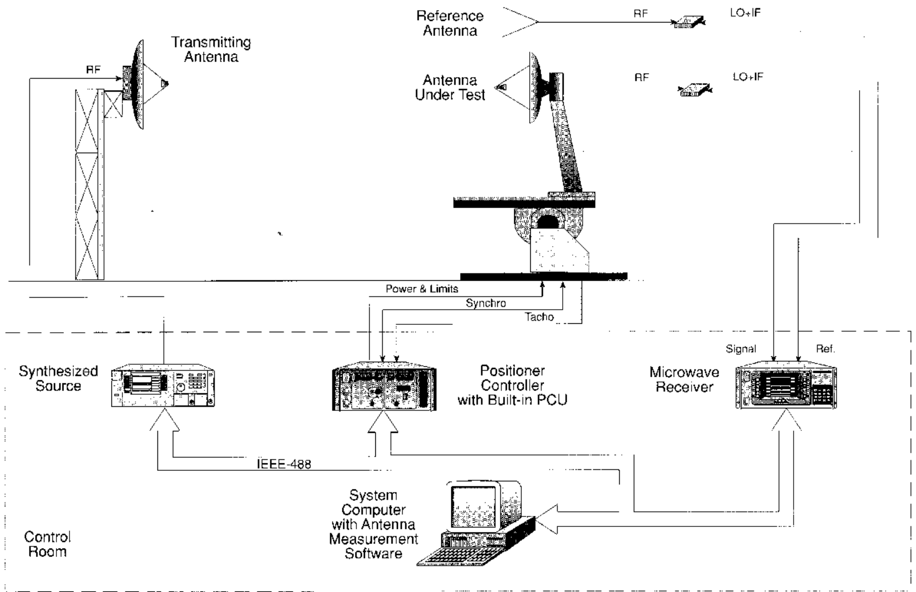

S/N	Taper Amp.	Phase Rip.
20 dB	±0.9 dB	±5.7 º
30 dB	±0.28 dB	±1.8º
40 dB	±0.09 dB	±0.57º

- Source Antenna
- Positioners
- Positioners Control
- RF Instrumentation
- Acquisition and Processes software
- Link budget and Dynamical Margin

$$P_{R\max}(dBm) = P_T(dBm) + 20\log\left(\frac{\lambda}{4\pi R}\right) + G_T(dBi) + G_R(dBi) \leq P_{Sat}$$

$$P_{R\min}(dBm) = Sensibility_{Rx}(dBm) + (S/N_0)(dB)$$

$$\begin{matrix}\text{Dynamical}\\ \text{Margin}\end{matrix}(dB) = P_{R\max}(dBm) - P_{R\min}(dBm) \geq G_{AUT}(dBi) + 10dB$$

Error bound due to Reflexions

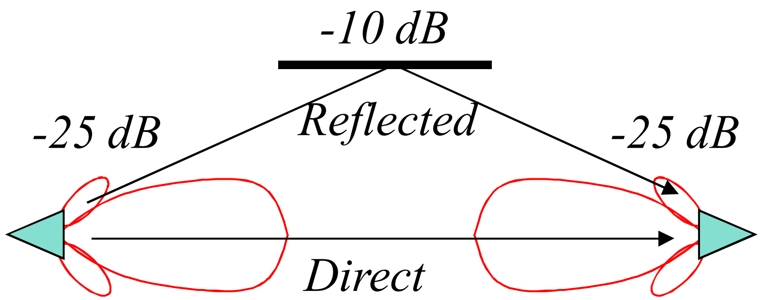

$$\left|\frac{E_R}{E_D}\right| = -60\ \text{dB} \qquad \text{Error=0,01 dB}$$

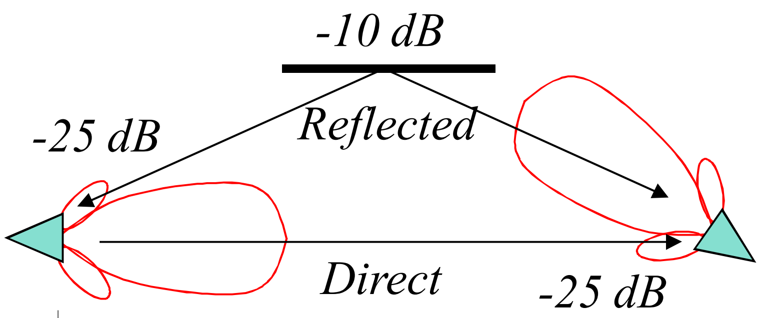

$$\left|\frac{E_R}{E_D}\right| = -10\ \text{dB} \qquad \text{Error=-3,3 dB a +2,4 dB}$$

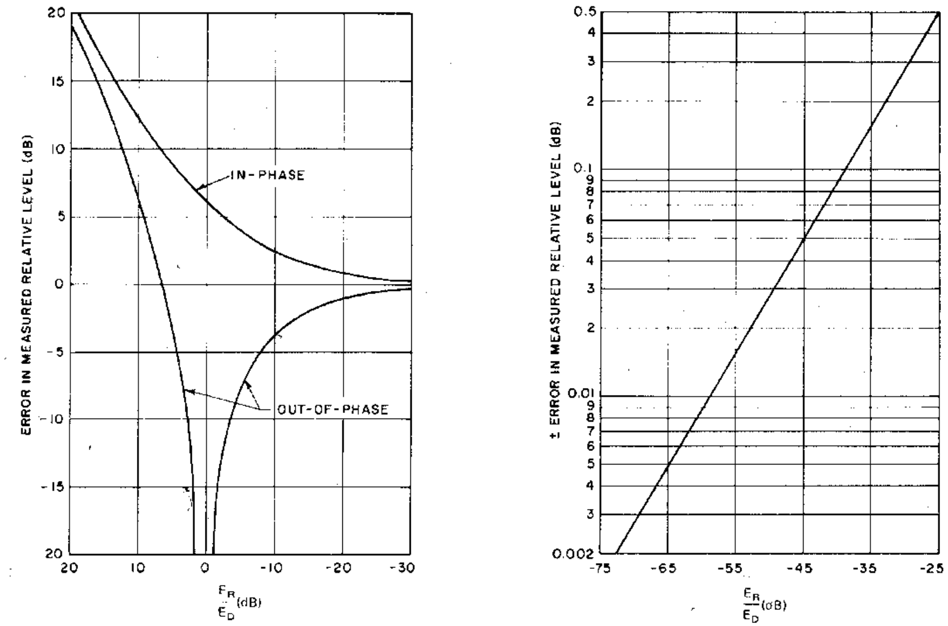

Fig 5

Possible Error in Measured Relative Pattern Level Due to Coherent Extraneous Signals

Linear Scales Are Employed for Signal Ratios of + 20 to –30 dB; the Plus-or-Minus Errors Are Essentially Equal for Ratios of – 25 dB or Less, as Indicated in the Logarithmic Plot for Ratios down to – 75 dB

Procedures to avoid Reflexions

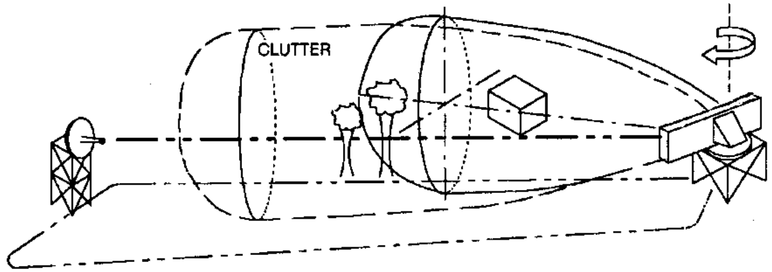

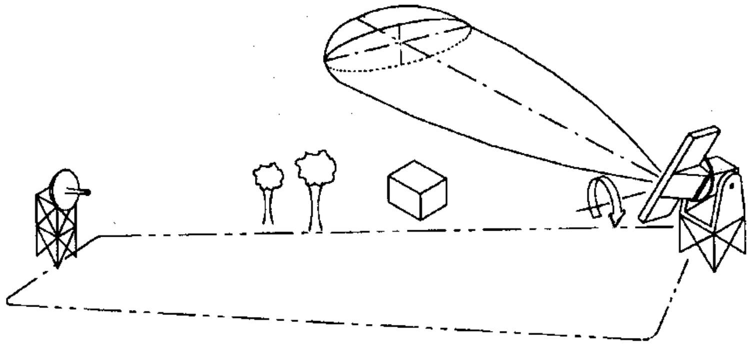

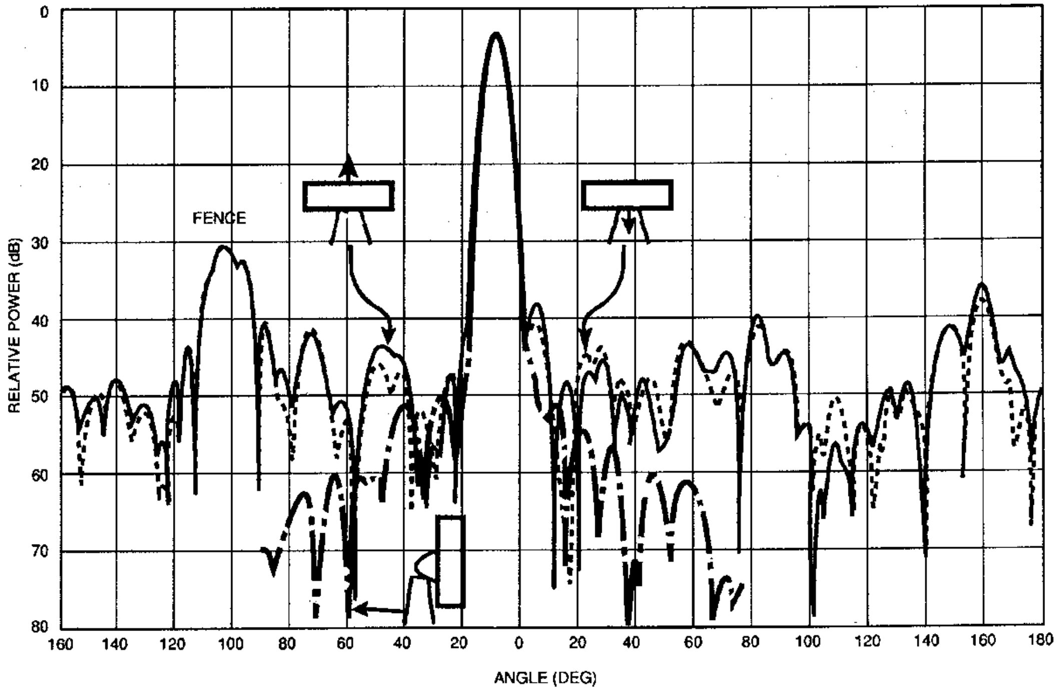

GOLDEN RULES

- *Main lobe must not be pointed toward the ground.*
- *Wide beams (like a fan) should be measured twice in elevation.*

Difractive Fences to reduce reflections

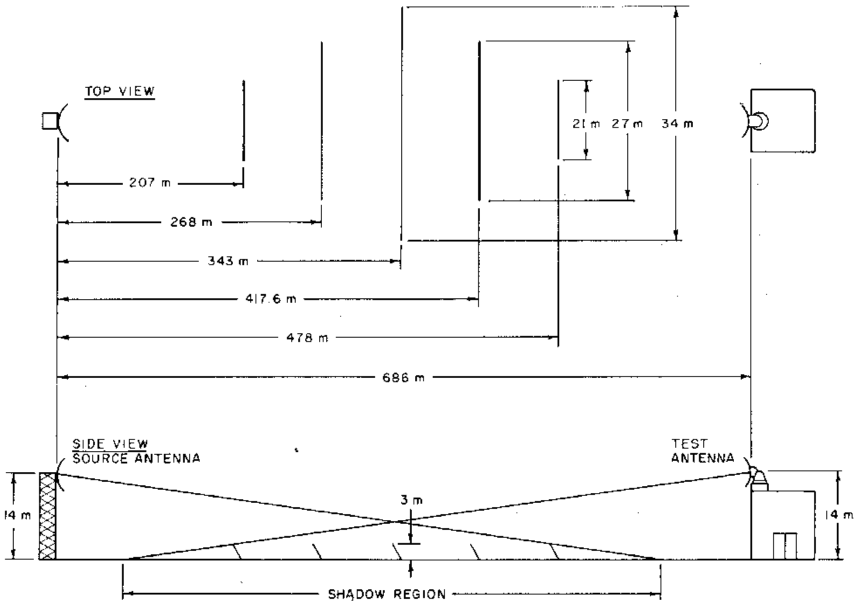

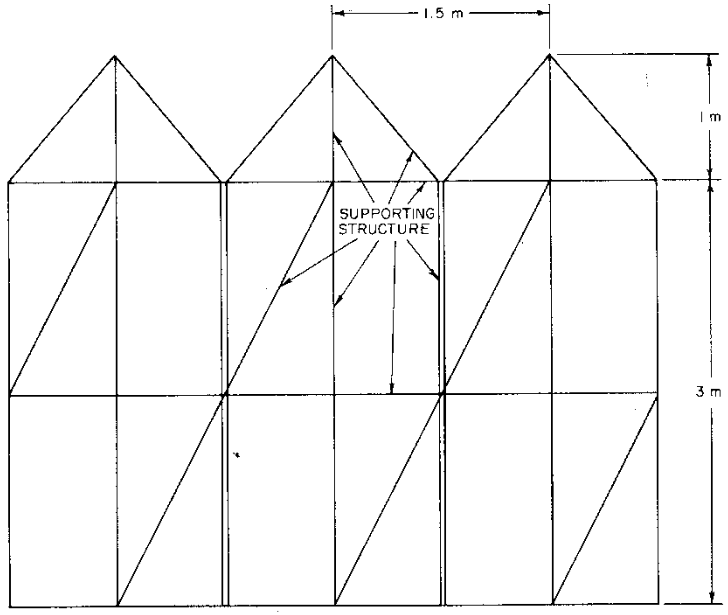

- Fences properties:
  - Zone is wider than 20 Fresnel's zones
  - Serrations should be deeper and wider than 5 to 10 λ at the lower frequency

Anecoic Chambers

- Closed rooms (usually shielded) with Radiation absorbent material simulating free space propagation (no-echoing) thanks to the absorption properties of RAM.

- Pros:
  - *Weather protection* ⇒ Improves time availability for measurement.
  - *Control of measurement ambient* (temperature, cleanliness ...) ⇒ Space or satellite antennas
  - *Saving in transportation expenses.*
  - *Avoiding security problems.*

ANTENNA Systems Solutions

Radiation Absorbent Material

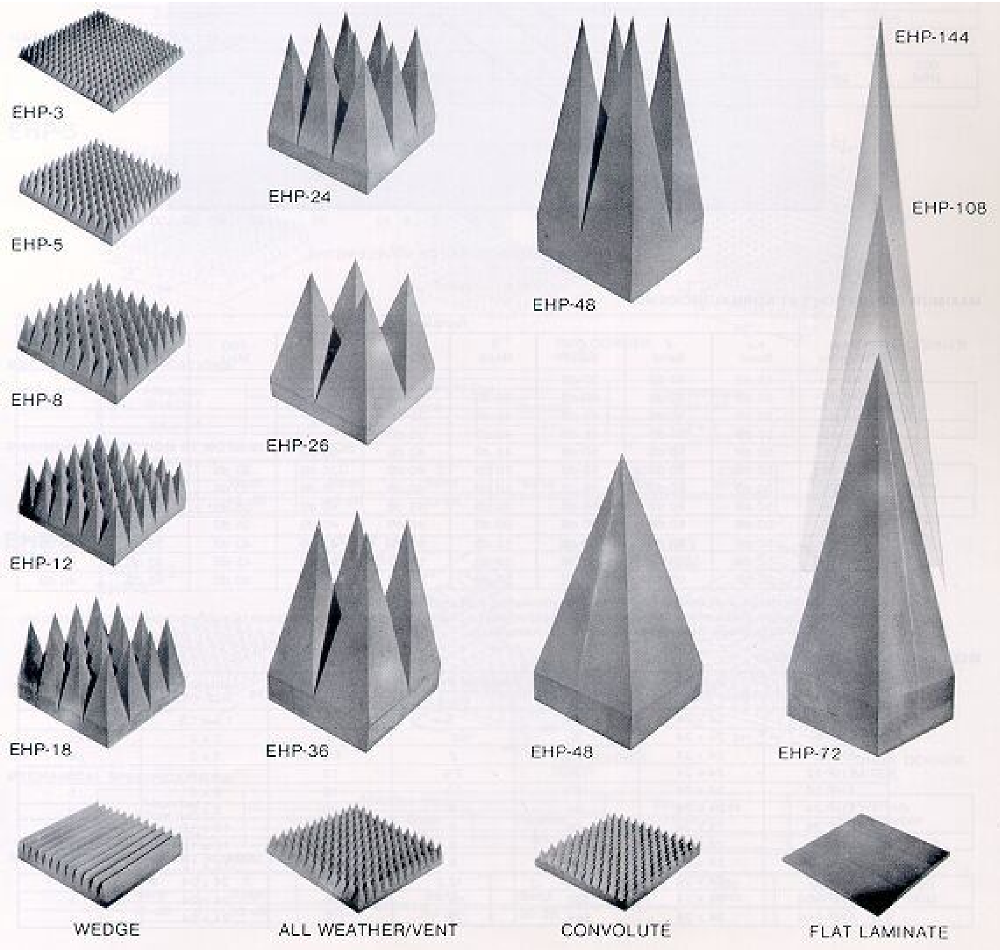

Shaping of RAM

- Pyramids (H>5l): r < -50 dB
- Convuluté: ρ < -50 dB for mm-waves
- Flat: ρ < -25 dB (towers...)
- Foot able: (pyramidal + foam + protective sheet)
- Ventilation, in the open...
- Wedge: specifically for compact range systems.

Radiation Absorbent Material

SPECIFIED MINIMUM REFLECTIVITY OF ECCOSORB VHP GRADES IN dB FOR ANGLES NEAR NORMAL INCIDENCE

	120 MHz	200 MHz	300 MHz	500 MHz	1 GHz	3 GHz	5 GHz	10 GHz	15 GHz	24 GHz
VHP-2							30	40	45	50
VHP-4						30	40	45	50	50
VHP-8					30	40	50	50	50	50
VHP-12					35	40	50	50	50	50
VHP-18				30	40	45	50	50	50	50
VHP-26			30	35	40	50	50	50	50	50
VHP-45		30	35	40	45	50	50	50	50	50
VHP-70	30	35	40	45	50	50	50	50	50	50

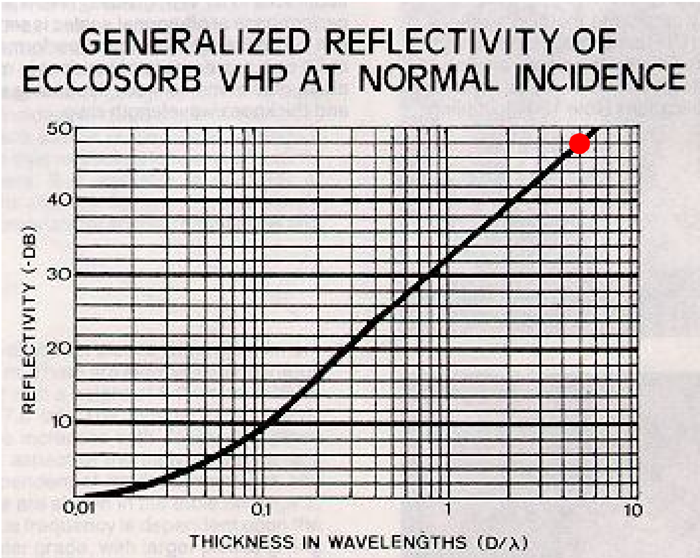

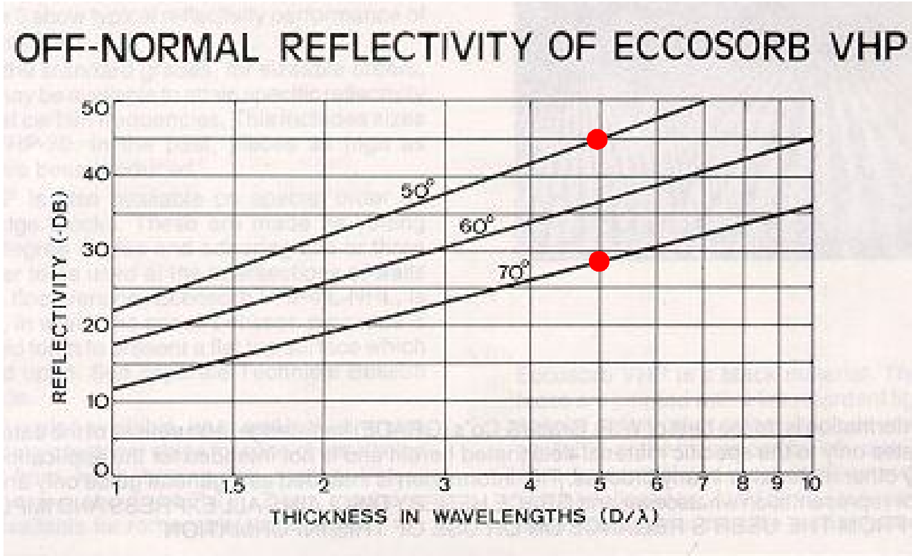

Anechoic Chambers

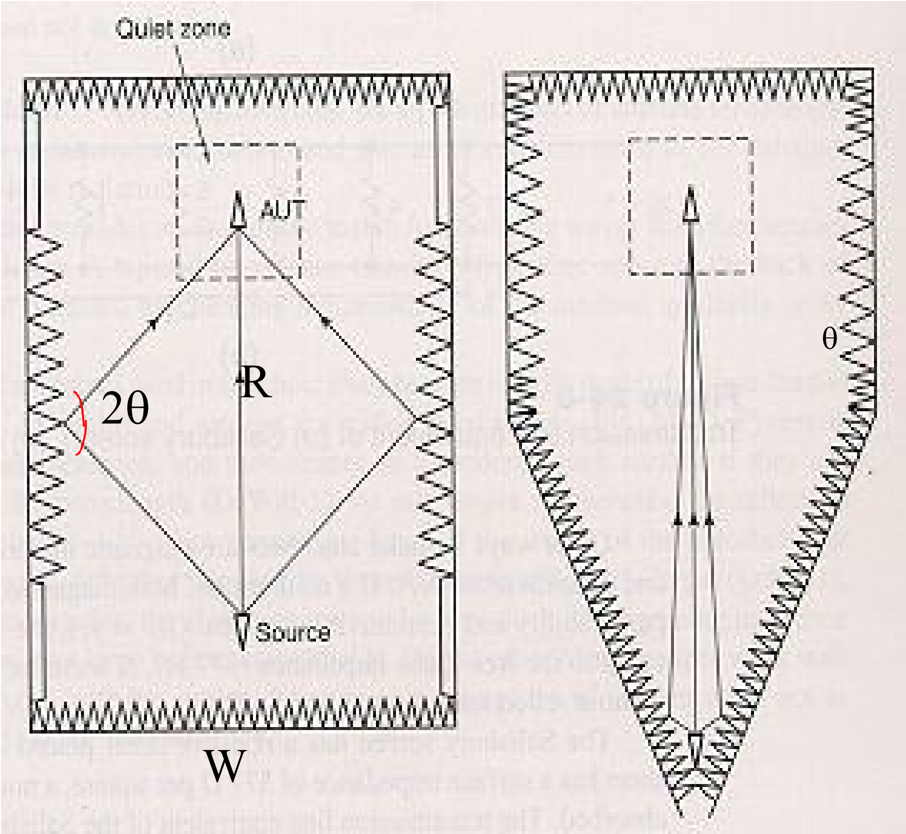

a) *Rectangular*

$\theta_{max} < 70^{\circ} \Rightarrow W/R > 1/2.75$

- Source antenna (horn) with main lobe not covering lateral walls, floor or ceiling.

b) *Tapered*

- Interfering signals are in phase to avoid the rippling in the quiet zone
- Applied at VHF and UHF
- Source must be fixed at every frequency

c) *Semi-opened*

- A wall of the chamber is opened, so the AUT is inside the chamber (protected from the inclemency of the weather) from a far away source antenna in the open.
- Examples: MBB and INTA (12x12x12 m and the source at 800 m.

Design based on Ray tracing

Model to estimate quit zone quality

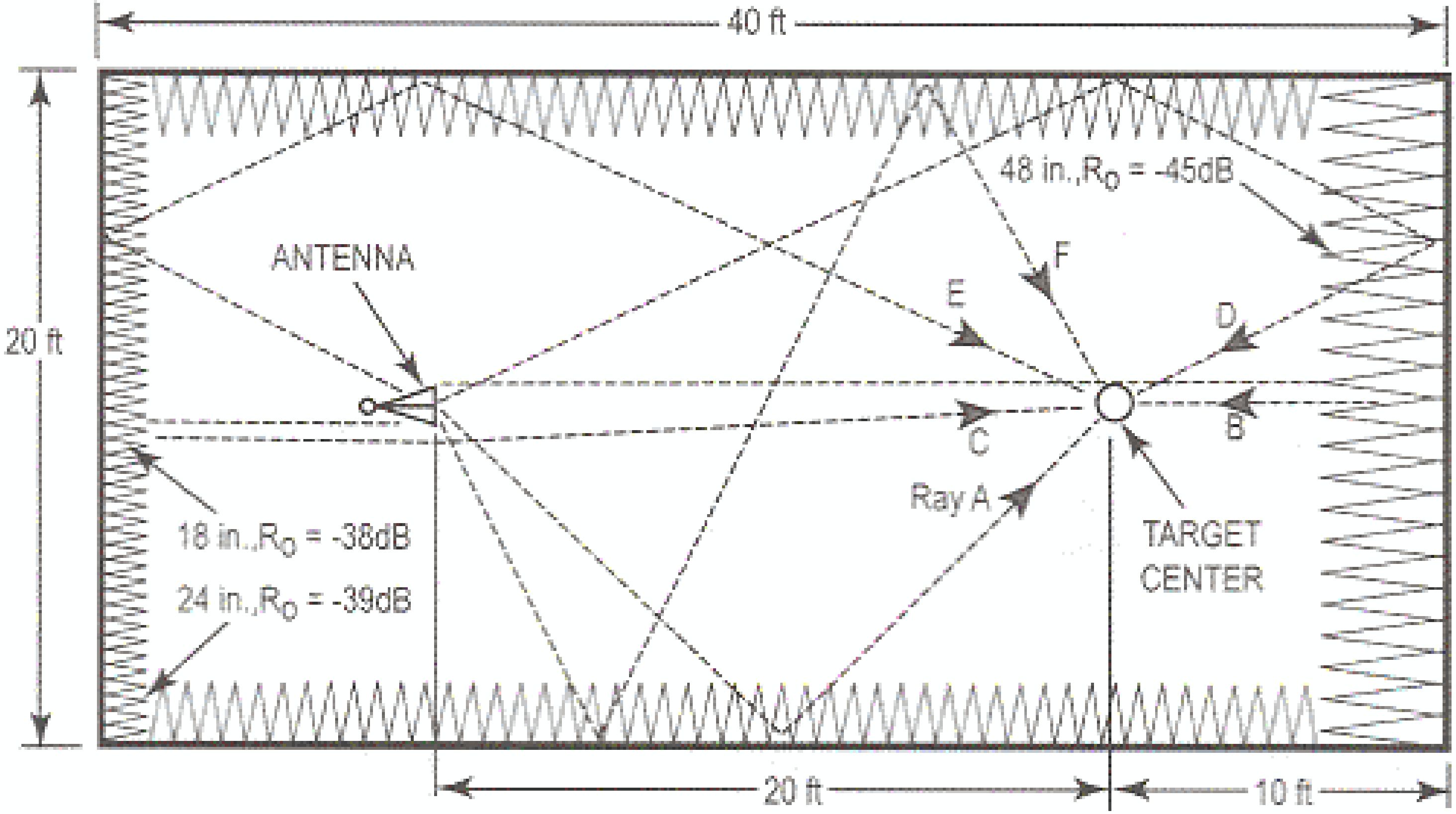

Quality Evaluation: Stationary Wave Method

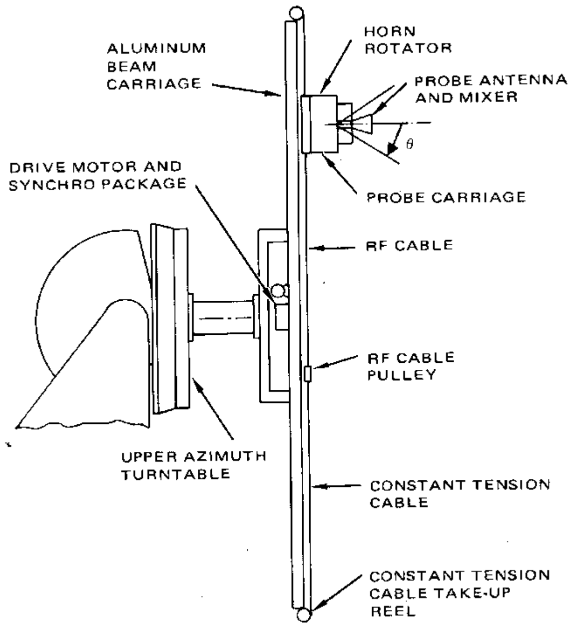

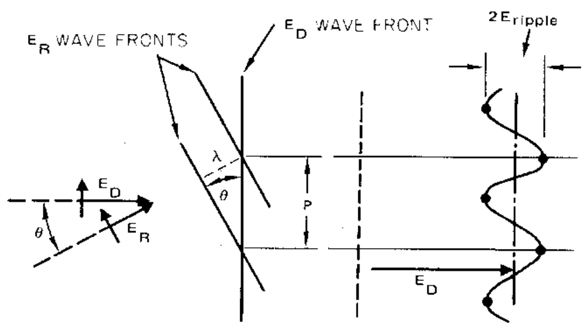

$$P = \lambda / \sin\theta$$

- An sliding probe tests that the source maximum radiation (or the interference lobe) points at the measurement aperture centre.
- The illumination field may help to detect spurious reflections and its level:

$$\frac{E_R}{E_D}(\mathrm{dB}) = 20\log\left(\frac{-1+10^{\sigma/20}}{1+10^{\sigma/20}}\right)$$

σ = Peak-to-peak riple in dB

Quality Evaluation: Pattern Comparison

- Pattern comparison detects large angle reflections (or, at least, the correct test realization).
- The same antenna is measured in different positions along the fiel axis of the range, so the direct signal and the reflected waves arrives the AUT with different electrical (and different relative phases).

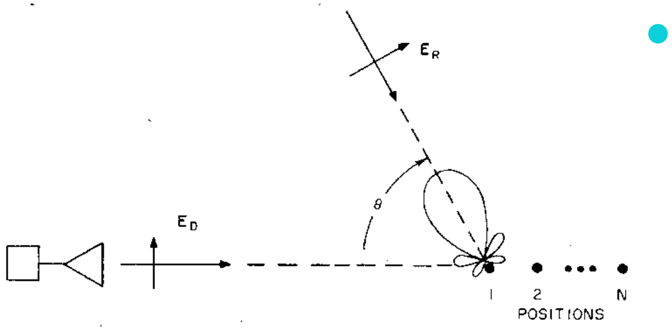

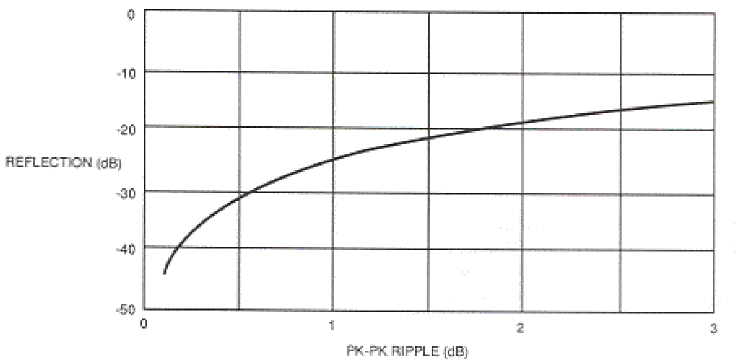

- Reflected wave is obtained by the peak-to-peak difference and the average value.

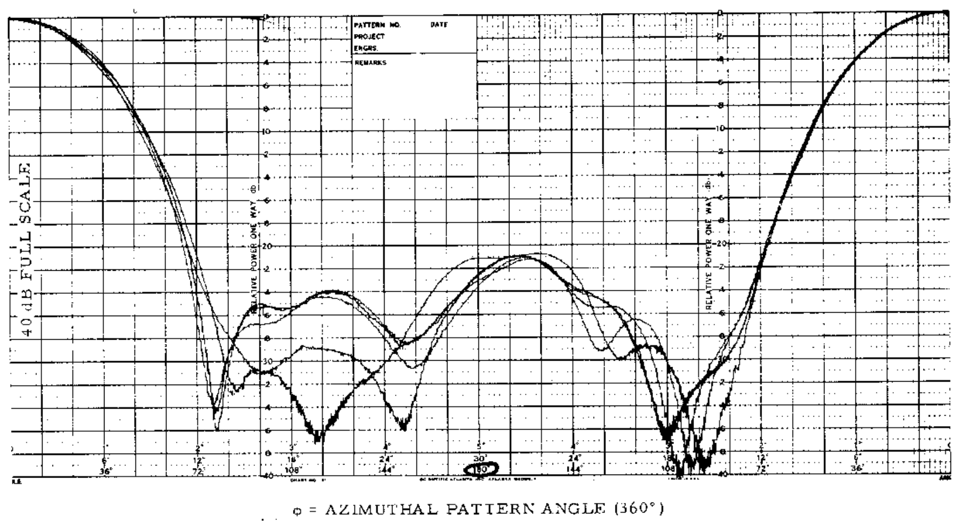

Polarization Pattern Measurement

- Direct CP-XP Measurement:
  - Source antenna is polarised with the copolar components:
    - Linear for CP-XP
    - Circular for CPC-XPC
  - Acquisition is realised according the co-cross polarization:
    - Linear for CP-XP
    - Circular for CPC-XPC

- Indirect Measurement:
  - Acquisition is realised in E_θ y E_ϕ components
  - Co-Cross polarization are obtained by processing:
    - E_{CP}-E_{XP},
    - E_{CPC} y E_{XPC}

Polarization Pattern Measurement

Axis correspondence for Roll over Azimuth

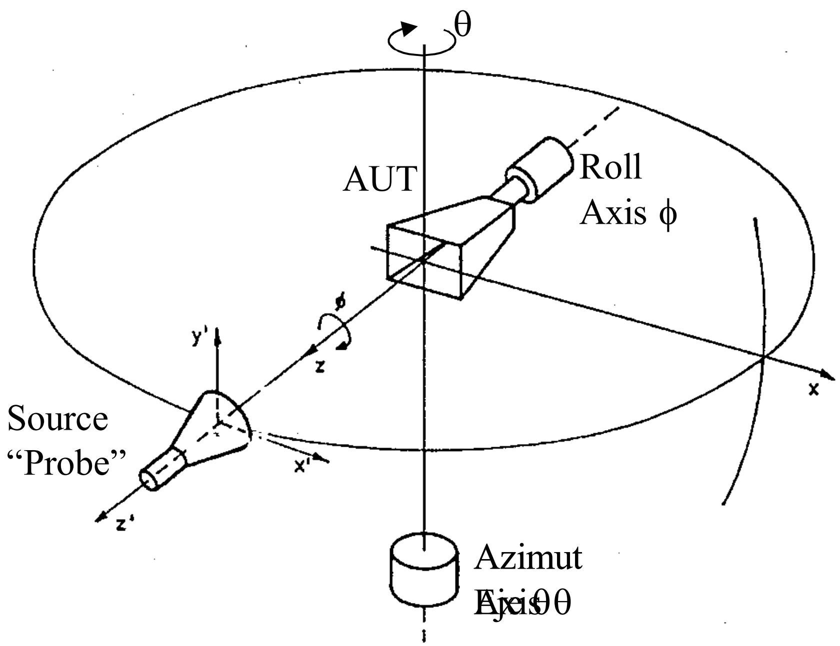

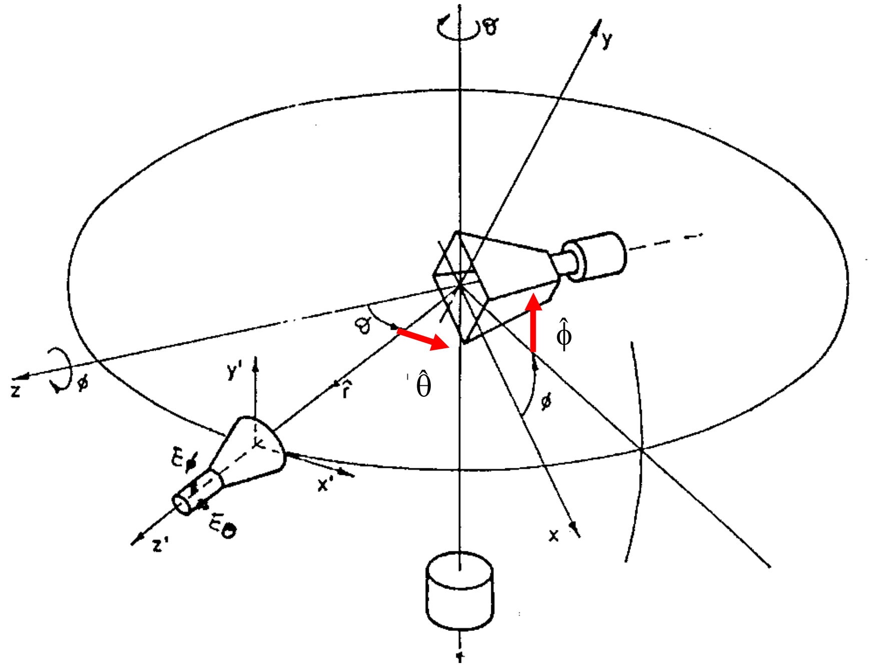

- **Double Polarization probe**: E_θ y E_ϕ components are acquired simultaneously, but a pre-calibration of probe and ports (with a highly pure polarization probe) is necessary.
- **Simple Polarization Probe**: Every component is acquired at each scan rotating the probe 90º.
- CP-XP, CPC-XPC components are computed using conversion formulas.
- Best polarization plane fitting by “Polarization positioner”.

Direct Measurement of CP-XP Patterns

- Typical measurement for horns
- AUT is pointed towards source antenna (along Z-axis) to acquire the cut ϕ=45º with an azimuth scan.
- Polarization plane or source antenna (polarization standard) is fixed to find the minimum value. XP pattern at cut ϕ=45º is acquired with an azimuth scan.
- Source antenna is rotated 90º and the CP component at ϕ=45º is acquired.
- Then, CP components at ϕ=0º and 90º is acquired.

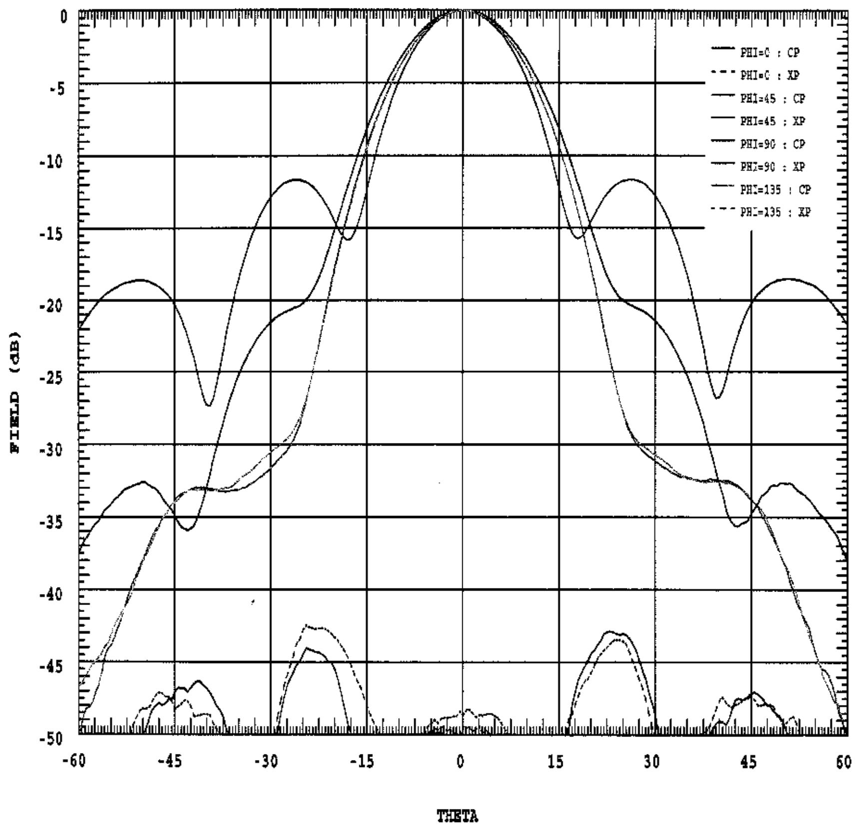

B. PIRAMIDAL de niquel (Sonda Corrugada)
F=13.00 GHz

Absolute Gain Measurements

A) Two antenna Procedure:

- Based on two identical antenna measurement and Friis' formulas

$$P_R(\text{dBm}) = P_T(\text{dBm}) + 20\log\left(\frac{\lambda}{4\pi R}\right) + G_T(\text{dBi}) + G_R(\text{dBi})$$

B) Three antenna Procedure:

- Three antennas (two by two) are compared (measured) solving the three equations based on g Friis' formula.

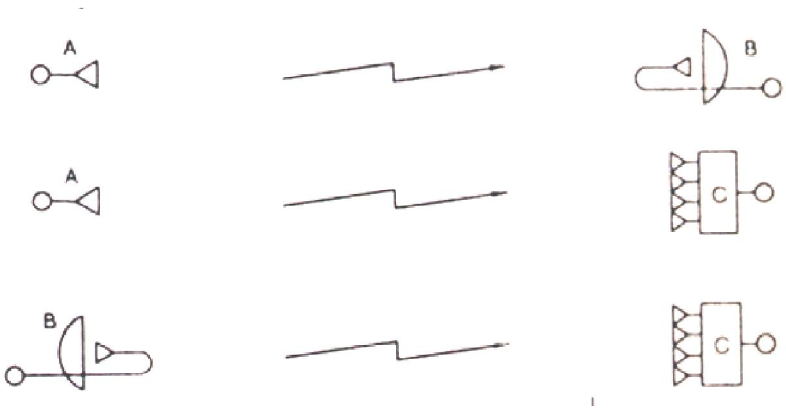

Gain Comparison Technique

- AUT gain is measured by comparison with a standard antenna, using the same source antenna.
  - In case of perfect impedance and polarization matching:

$$G_{AUT}(dB) = G_{SGH}(dB) + 10\log\left(\frac{P_{RAUT}}{P_{RSGH}}\right)$$

  - Correction by impedance mismatch:

$$\Delta G(dB) = -10\log\left|\frac{\left(1-|\Gamma_{AUT}|^2\right)\left(1-|\Gamma_{Rx}|^2\right)}{|1-\Gamma_{AUT}\Gamma_{Rx}|^2}\right| + 10\log\left|\frac{\left(1-|\Gamma_{SGH}|^2\right)\left(1-|\Gamma_{Rx}|^2\right)}{|1-\Gamma_{SGH}\Gamma_{Rx}|^2}\right|$$

    - A well matched attenuator at the receiver side (close to the antenna) improves correction due to $\Gamma_{Rx} \approx 0$.

Gain Measurement

Polarization Requirements of Source Antenna

- Gain of circular polarized antennas is measured by partial gain procedure, that is to say, adding the gain for the both linear polarizations (V & H) of the source antenna.

$$G_{AUT}(dB) = 10\log(G_{AUTV} + G_{AUTH})$$

- In case the polarization purity of source antenna is low, some measurement errors appear:

Errors in the Measured Gain of a Purely Circularly Polarized Antenna Due to a Finite Axial Ratio of the Transmitting Antenna

Transmitting Antenna Axial Ratio (dB)	Measurement Error [dB]	
	Same Sense	Opposite Sense
20	+0.828	−0.915
25	+0.475	−0.503
30	+0.270	−0.279
35	+0.153	−0.156
40	+0.086	−0.109
45	+0.049	−0.049
50	+0.027	−0.028

Errors in the Measured Gain of a Linearly Polarized Antenna Due to a Finite Axial Ratio of the Transmitting Antenna*

Transmitting Antenna Axial Ratio (dB)	Measurement Error [dB]	
	Same Sense	Opposite Sense
20	−0.035	+0.063
25	−0.014	+0.041
30	−0.002	+0.003
35	+0.005	+0.022
40	+0.009	+0.019
45	+0.011	+0.016
50	+0.012	+0.015

*The test antenna has an axial ratio of 25 dB. The gain standard is purely linearly polarized.

Gain Standards

- Pyramidal horns (SGH) are used as standards at Microwave bandwidth.
- Theoretical value (provided by the manufacturer) is usually used.
  - Difference between theoretical and real value is lower than ± 0.3 dB.
- If a large accuracy is needed, the standard horn has to be calibrated, using an absolute gain procedure.
- A simpler and accurate procedure is:
  - Directivity is computed by integration of pattern measured in a spherical system.
  - Gain is computes as $G=\eta_{rad} D_o$ where $\eta_{rad} \approx 0.02$ dB.
  - Typical error $3\sigma < \pm 0.1$ dB

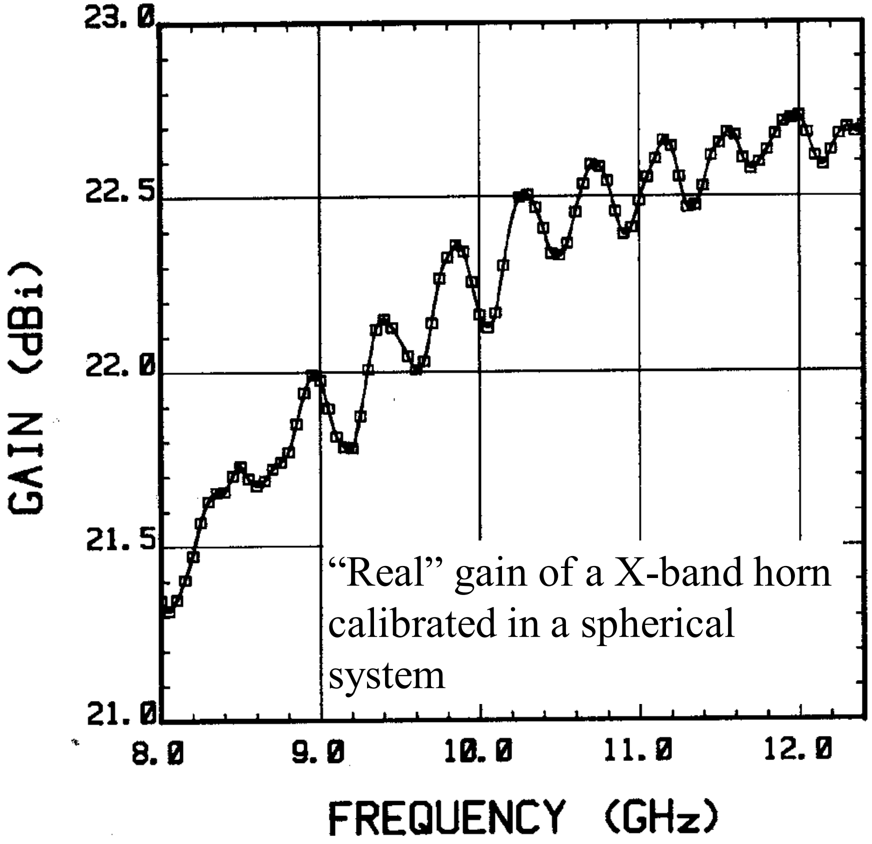

Polarization Measurement

Rotating Linear Source Method

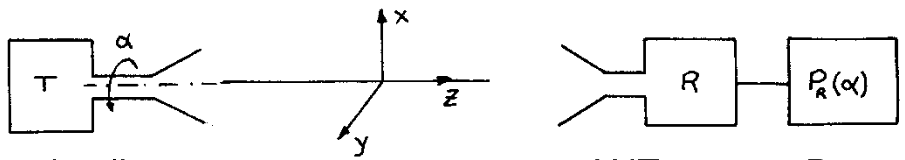

Rotating linear polarization antenna

AUT

Power

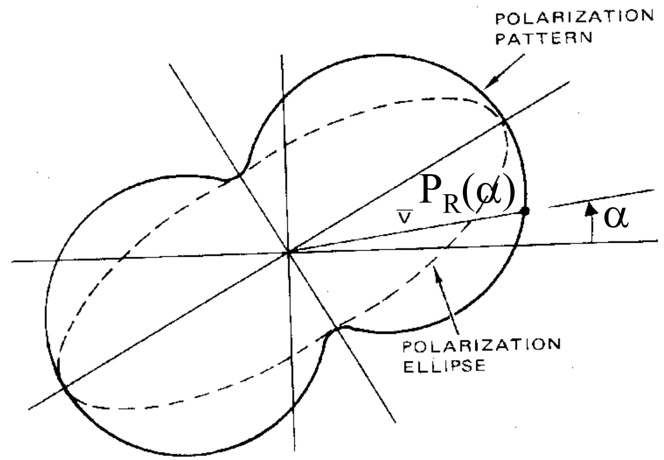

- Axial ratio is the difference between the maximum and the minimum registered plots in terms of α, and the tilt angle (corresponding to the mayor axis).
- The sense of rotation is not measured.
  - In case of linear AUTs, it is not important
  - In case of circular polarization, the sense of rotation is usually know a priori, or it can be measured with two helix with opposite windings (CW and CCW).

Measurements of Axial Ratio vs Frequency

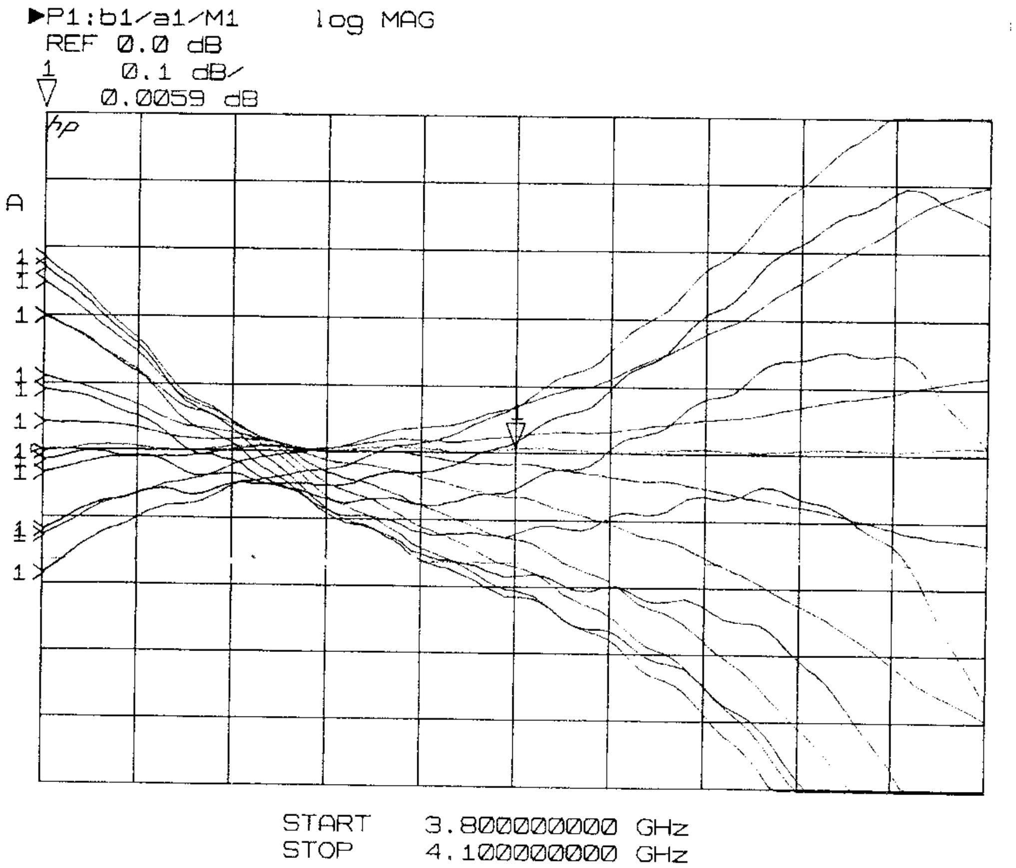

- A linear rotating source provides the axial ratio vs frequency. Axial ratio is registered in terms of trequency for different discrete value of α ($\Delta\alpha$<15º)
- Axial ratio is the peak-to-peak diference between the envelopes of all the plots.
- Low AR is limited by the rotary joint performance. It shall be veryfied.

Polarization Requeriments of Source Antenna

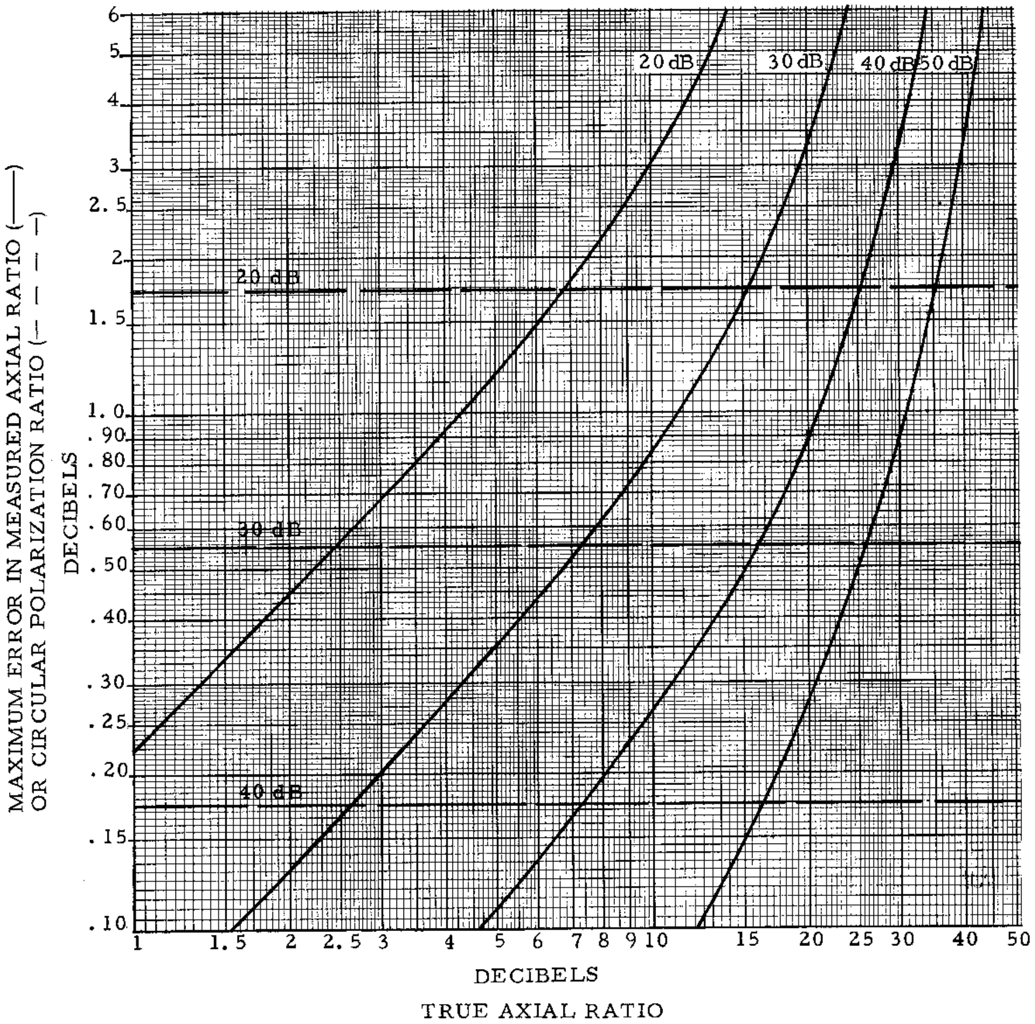

- The solid line shows the error corresponding to the AUT Axial Ratio in terms of the axial ratio of the source antenna.
- The broken line shows the error corresponding to the measurement of the AUT circular polarization ratio in terms of the axial ratio of the source antenna.

Polarization Standard

- Pyramidal horns (manufactured by electroformed to provide high accuracy and perpendicularity between faces) providing a very high AR> 50 dB.

- A very simpler procedure to bound the minimum AR of a standard consists on:
  - Perform three measurements using 3 standards two by two.
  - In case the apparent measured axial ratio are RA_1, RA_2, y RA_3, the worst standard has a real axial ratio bounded as:

$$\frac{1}{2}\left(\frac{1}{RA_1}+\frac{1}{RA_2}-\frac{1}{RA_3}\right)\leq\frac{1}{\min\left(RA_{true}\right)}\leq\frac{1}{2}\left(\frac{1}{RA_1}+\frac{1}{RA_2}+\frac{1}{RA_3}\right)$$

and $RA_3 > RA_1 \ y \ RA_2$

  - It can be tested that: $RA_{v\min}(dB) \geq RA_{worst\ aparent}(dB) - 3{,}5\,dB$

Calibration of Polarization Standard by the 3 Antennas Procedure

- Using three antennas the three axial ratios, the senses of rotation, and the tilt angle (respect to a geometry reference)
- They are very accurate procedures but long ones. See for instance:
  - [Newell, 1988] "Improved Polarization Measurements Using a Modified Three-Antenna Technique". IEEE Trans. AP. Vol. 36, no. 6. Junio 1988.

Error in Polarization Measurement

- Measurement of the two orthogonal components (in amplitude and phase) and the computation of linear and circular co-polar and cross-polar components and the axial ratio.

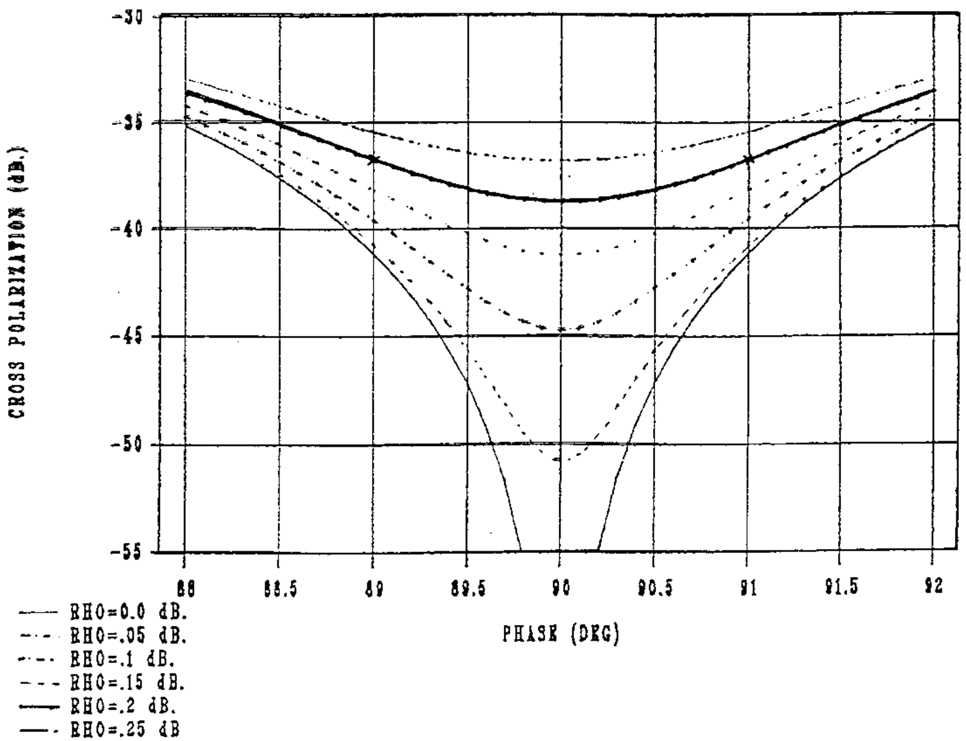

Measurement error of a "pure" circular polarization in function of the measurement errors of the linear polarization (amplitude and phase)

Error Sources Far at Far Field Measurements

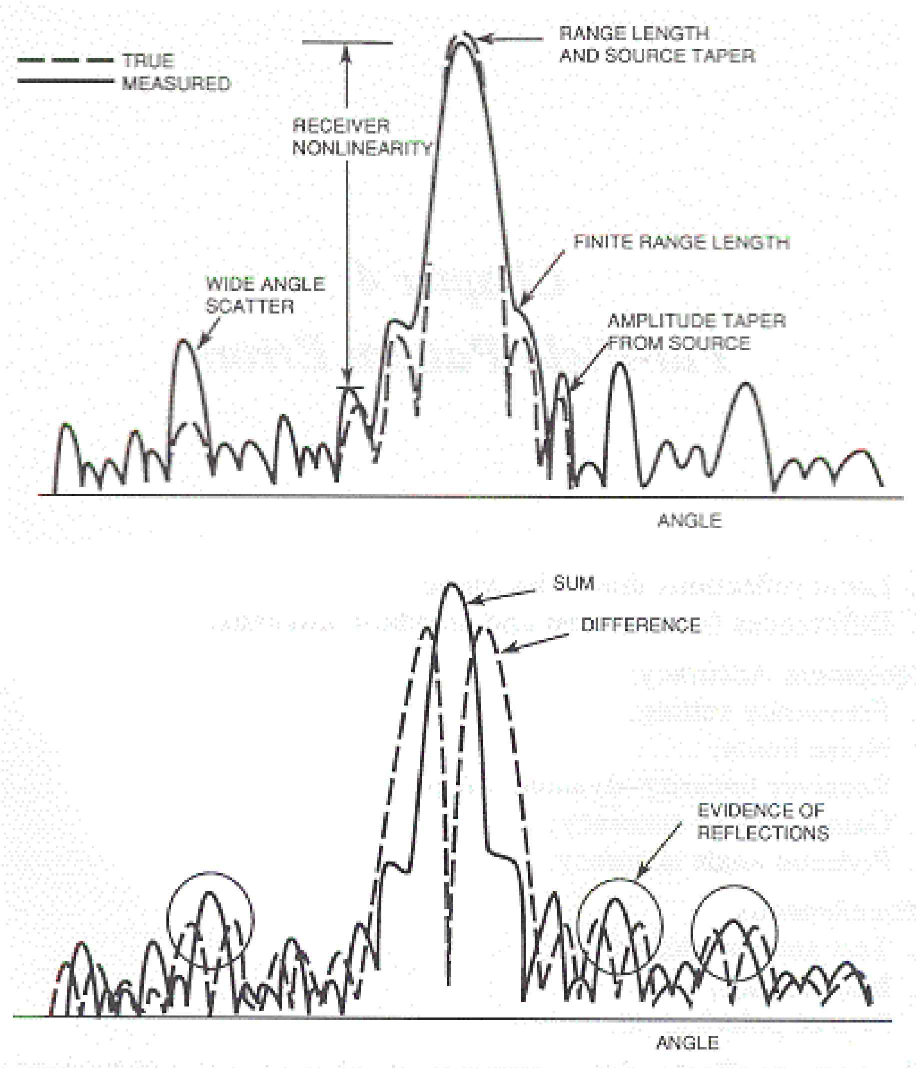

Main reasons of error:

- Range length
- Illumination Amplitude Taper
- Non symmetric illumination
- Reflexions
- Non-linearity of the receiver
- Lack of dynamic range (noise floor)
- Gain measurement, inaccuracy of SGH, impedance mismatch Typical accuracy ±0.5dB.

Typical Problems on Reflectors and Arrays

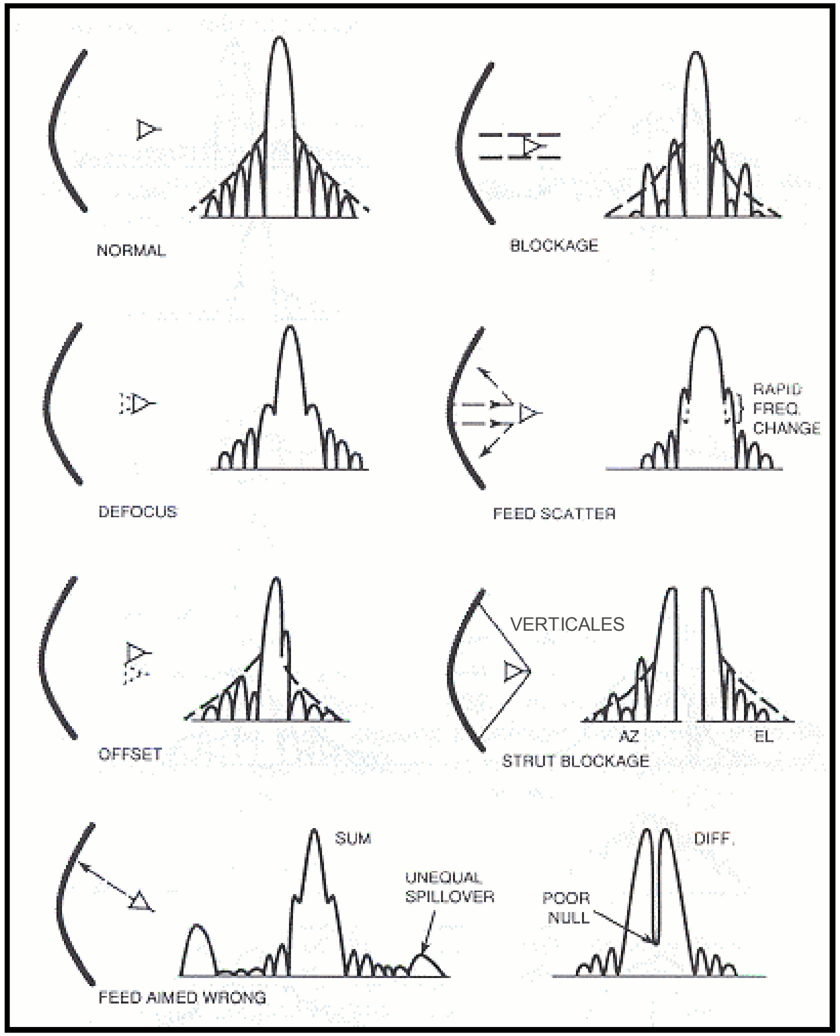

Reflectors

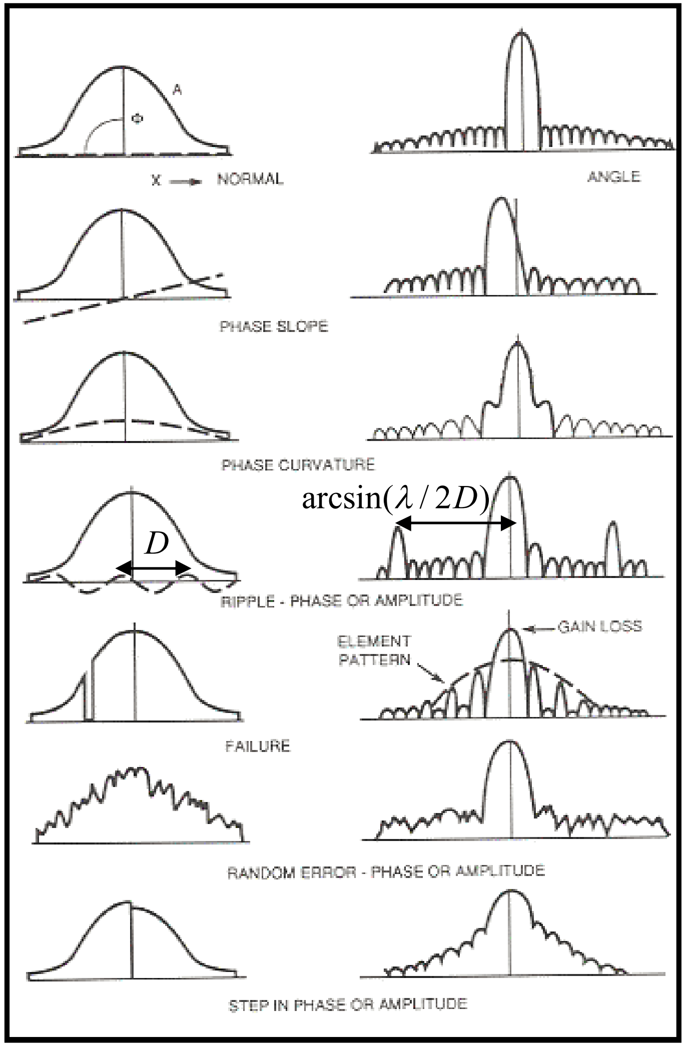

Arrays

Large antenna Measurement "in-situ"

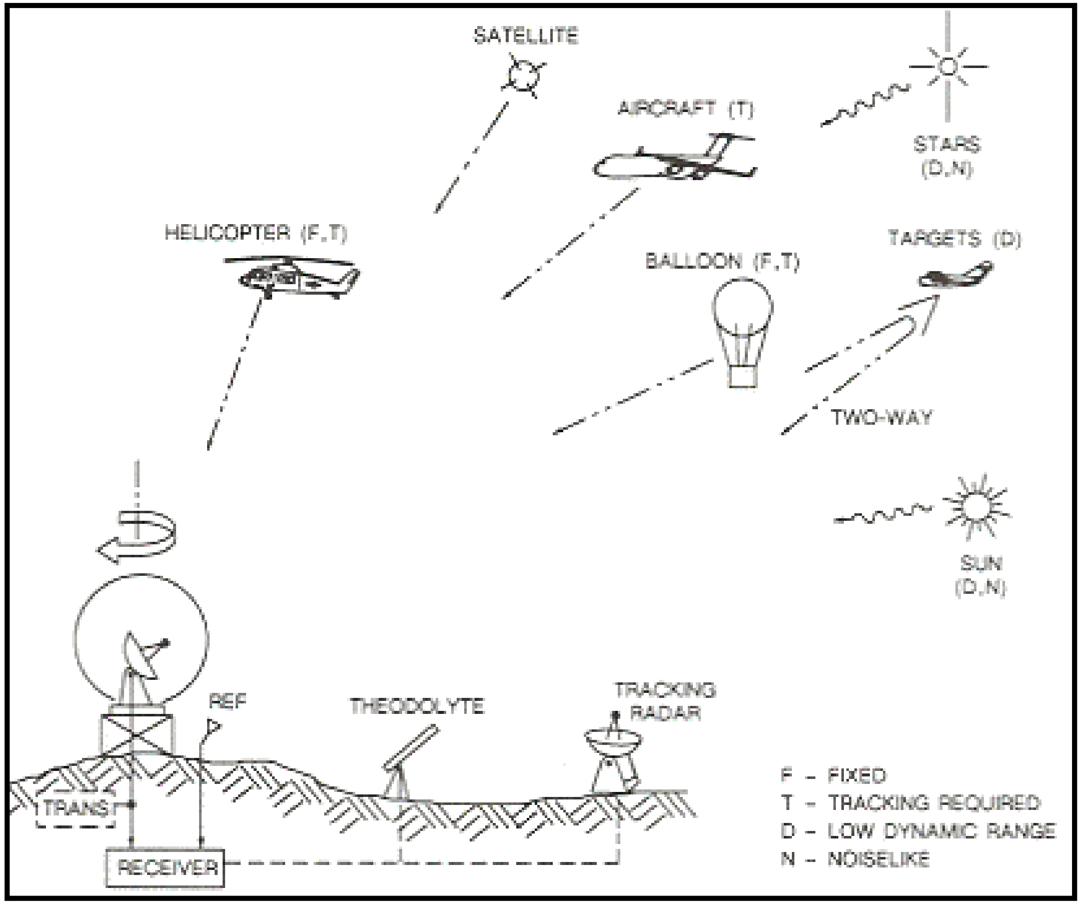

Gain measurement using radio sources (cyg A, Casiopea, Virgo, …) with espectral flux density *S(λ)* known

$$\Delta P_R = \frac{S(\lambda)}{2}\frac{\lambda^2}{4\pi}G_T = k\Delta T_A \quad [W/Hz]$$

$$G_T = \frac{8\pi k \Delta T_A}{\lambda^2 S(\lambda)}$$

- *k* : Boltzman's constant
- ΔT_A : Antenna Noise Temperature increment (radiosource temperature minus background temperature). Measured with a calibrated radiometer with cold and hot loads

Special Measurement Systems

Systems to measure on-board ship antennas (scaled)

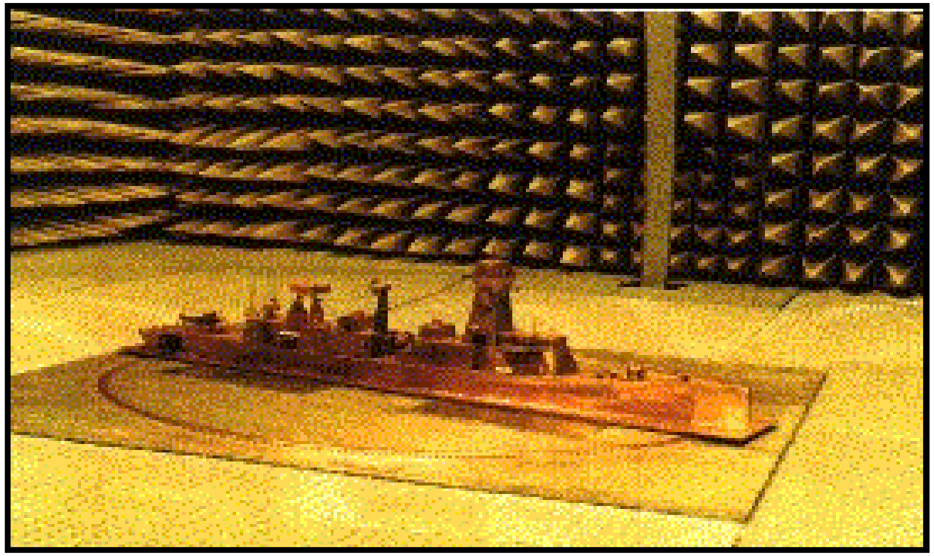

Semi-Anechoic Arc System to measure on board ship antennas (LEHA-UPM)

Length:	$l'=l/n$
Time:	$t'=t/n$
Wavelength:	$\lambda' = \lambda/n$
Capacity:	$C'=C/n$
Inductance:	$L'=L/n$
Reflexion Surface:	$A_e'=A_e/n^2$
Frequency:	$f'=n \cdot f$
Conductivity:	$\sigma'=n \cdot \sigma$
Permitivity:	$\varepsilon' = \varepsilon$
Permeability	$\mu' = \mu$
Propagation Speed:	$v'=v$
Impedance:	$Z'=Z$
Antenna Gain:	$G_o'=G_o$

Special Measurement Systems

Systems based on Termography

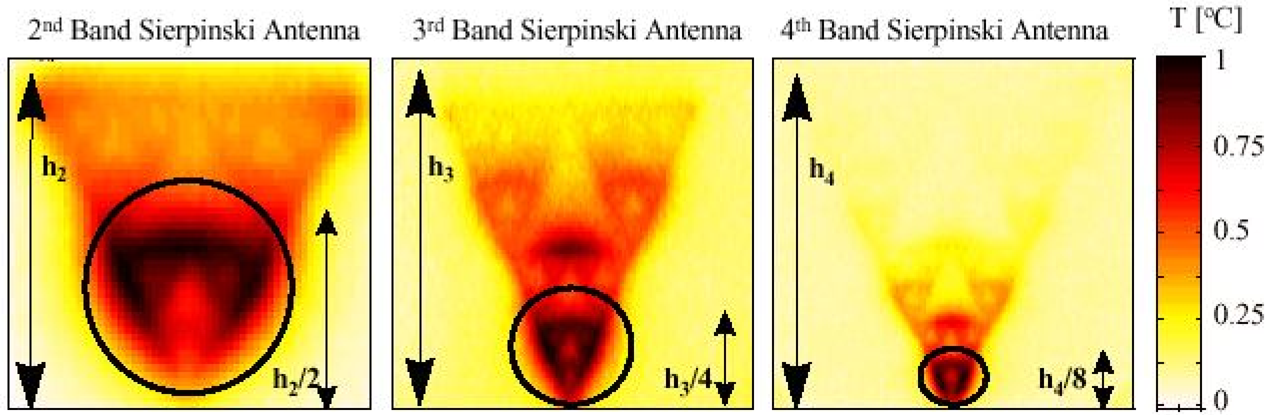

Fig. 5. Thermograms of Fractal-Sierpinki Antennas of 2^{nd}, 3^{rd}, and 4^{th} band: h_2=6 cm; h_3=12 cm and h_4=22 cm.

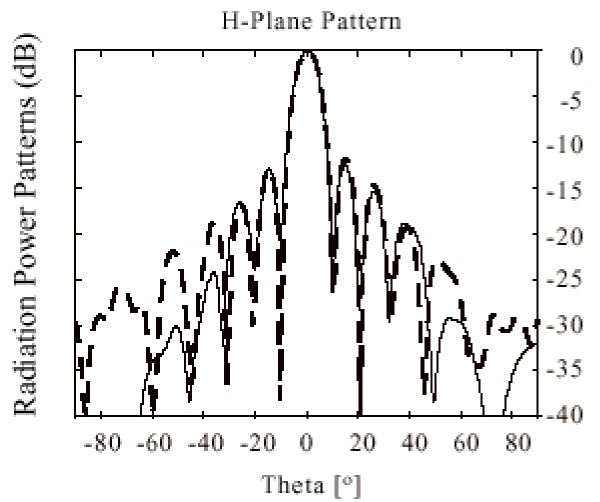

- Thermal intensity measurement in a planar system
- Phase reconstruction
- Computation of radiation pattern

(J.M. González Arbesu. UPC. AP-2000)

Special Measurement Systems

Small antenna Measurement Systems (cellular)

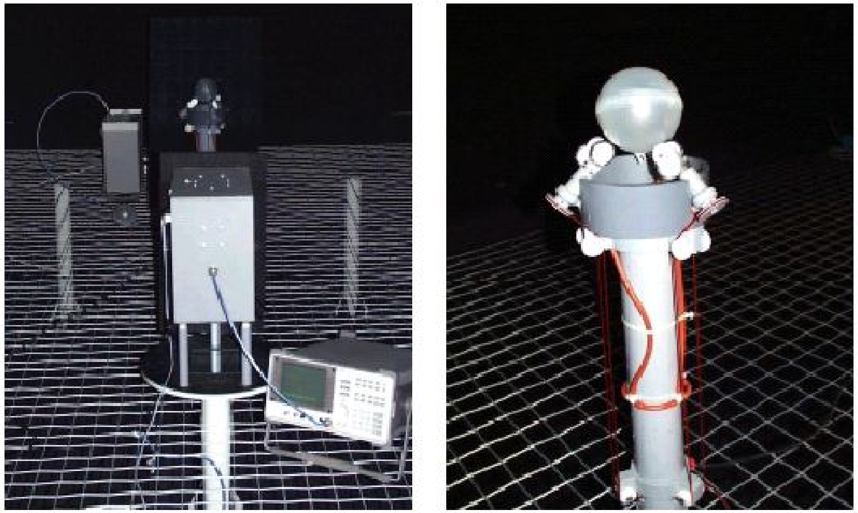
Figure 2 : general view of the measurement

Figure 3 : view of the positionner

EPFL-LEMA (Lausanne - Switzerland)

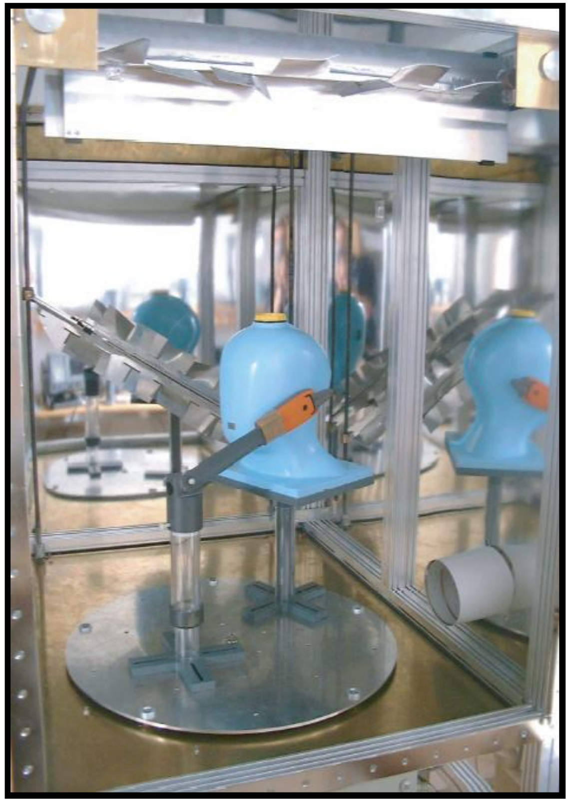

Chalmers-Bluetest
(Göteborg – Sweden)

Special Measurement Systems

Small antenna Measurement Systems (cellular)

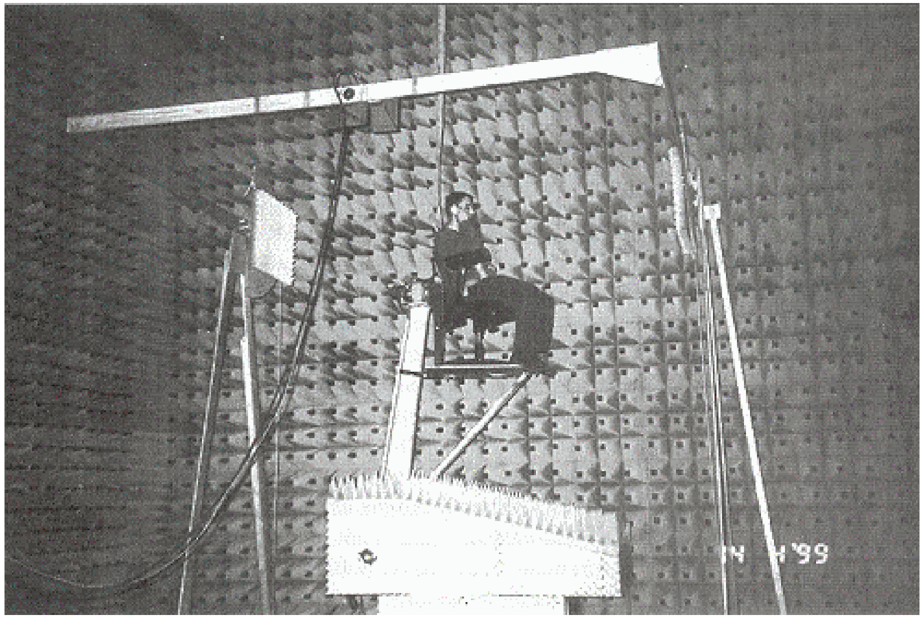

“Gantry” System (Aarlborg – The Netherlands)

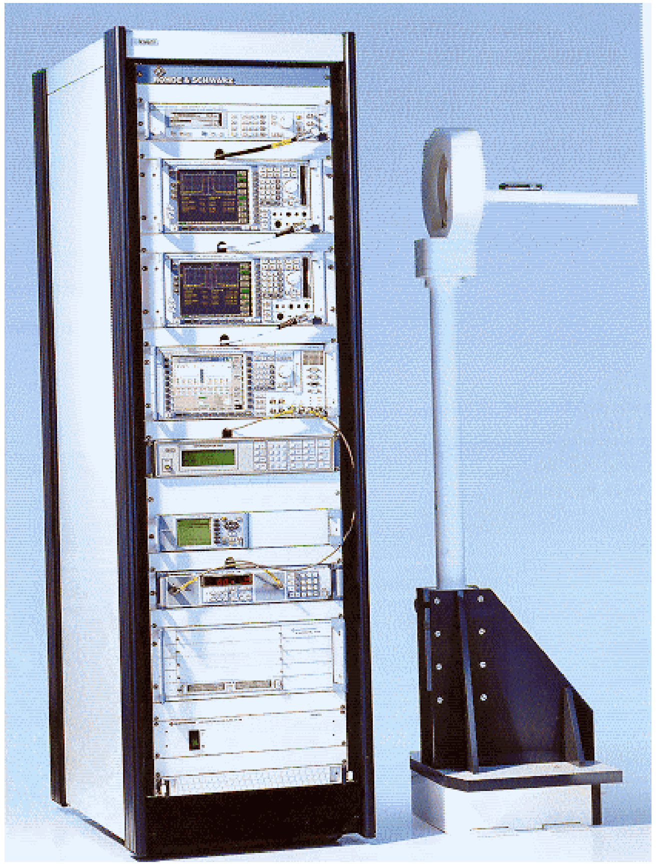

TS9970 System (Rohde Schwarz)

Special Measurement Systems

Stargate (SATIMO)

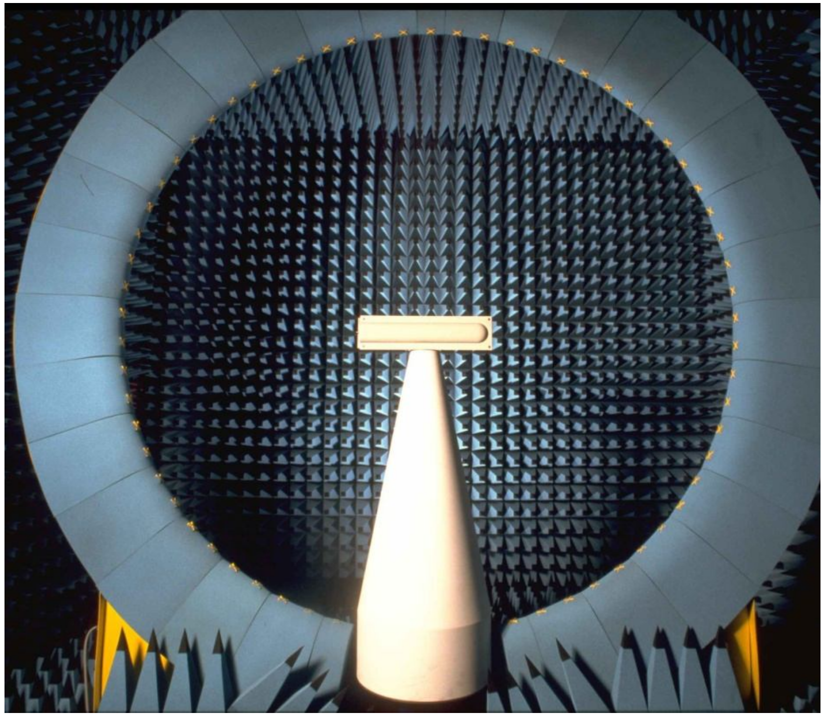

Stargate system with 64 probes

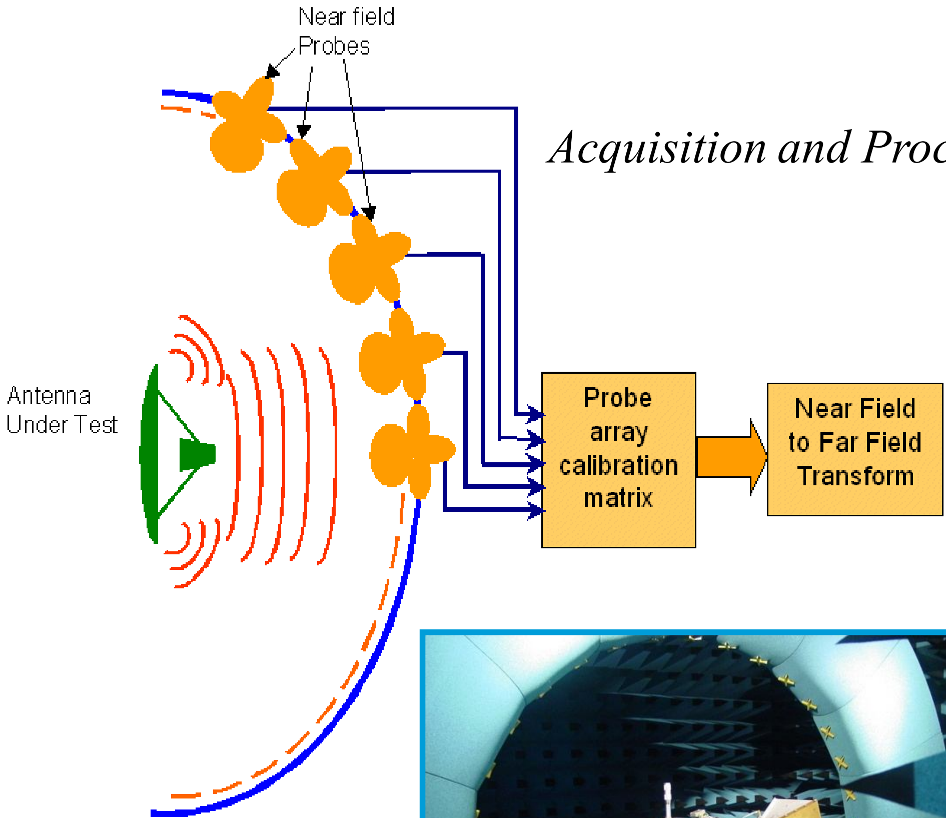

Acquisition and Process

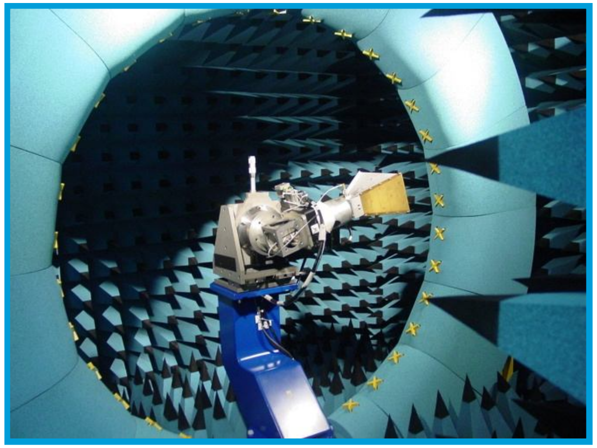

Probe calibration

References

- Hollis J.S., Lyon T.J. and Clayton L Microwaves Antenna Measurements. Scientific Atlanta. 1970 (1983)
- Microwave Antenna Measurements “Blue Book”. 3ª Edición. MI Technologies.
- IEEE Standards Test Procedures for Antennas. IEEE Std. 149-1979 John Wiley
- The Handbook of Antenna Design. Chapter 8. A.W. Rudge et al (Ed.), Appel-Hansen J, et al. Peter Pelegrinus Ltd 1982
- G.E. Evans. Antenna Measurement Techniques. Artech House Inc. 1990.
- AMTA Proceedings.
- Leland H. Hemming. Electromagnetic Anechoic Chambers: a fundamental design and specification guide.. IEEE Press. John Wiley Interscience. 2002
- P.S. Hacker. Range Distance Requirements for Measuring Low and Ultralow Sidelobe Antenna Patterns. IEEE Trans. AP. Sept. 1982.
- J.D. Kraus, R.J. Marhefka. Antennas for all applications. McGraw-Hill. 3rd Ed. 2002.
- NSI Antenna Measurements Products Catalogue. www.nearfield.com
- Emerson and Cumming Microwave Products. Eccosorb: www.eccosorb.com
- System TS9970: www.rohde-schwarz.com

Near Field Measurement Techniques

- Near field is measured in amplitude and phase on a surface (plane, cylinder o sphere) close to the AUT. Far field is computed using a transformation algorithm.

- Pros
  - Lower measurement volume (RAM save)
  - More security and control of the measurements
  - Far fields does not has the error related with the range length R
  - Random measured errors are averaged.
- Cons
  - Scanning systems must be more accurate than far field ones
  - Transformation software is needed (Software is based on spectral decomposition of the near field in planar, cylindrical or spherical waves)
  - The probe must be calibrated in pattern (directivity) and polarization)
  - **The full surface must be measured.**

Near Field Ranges

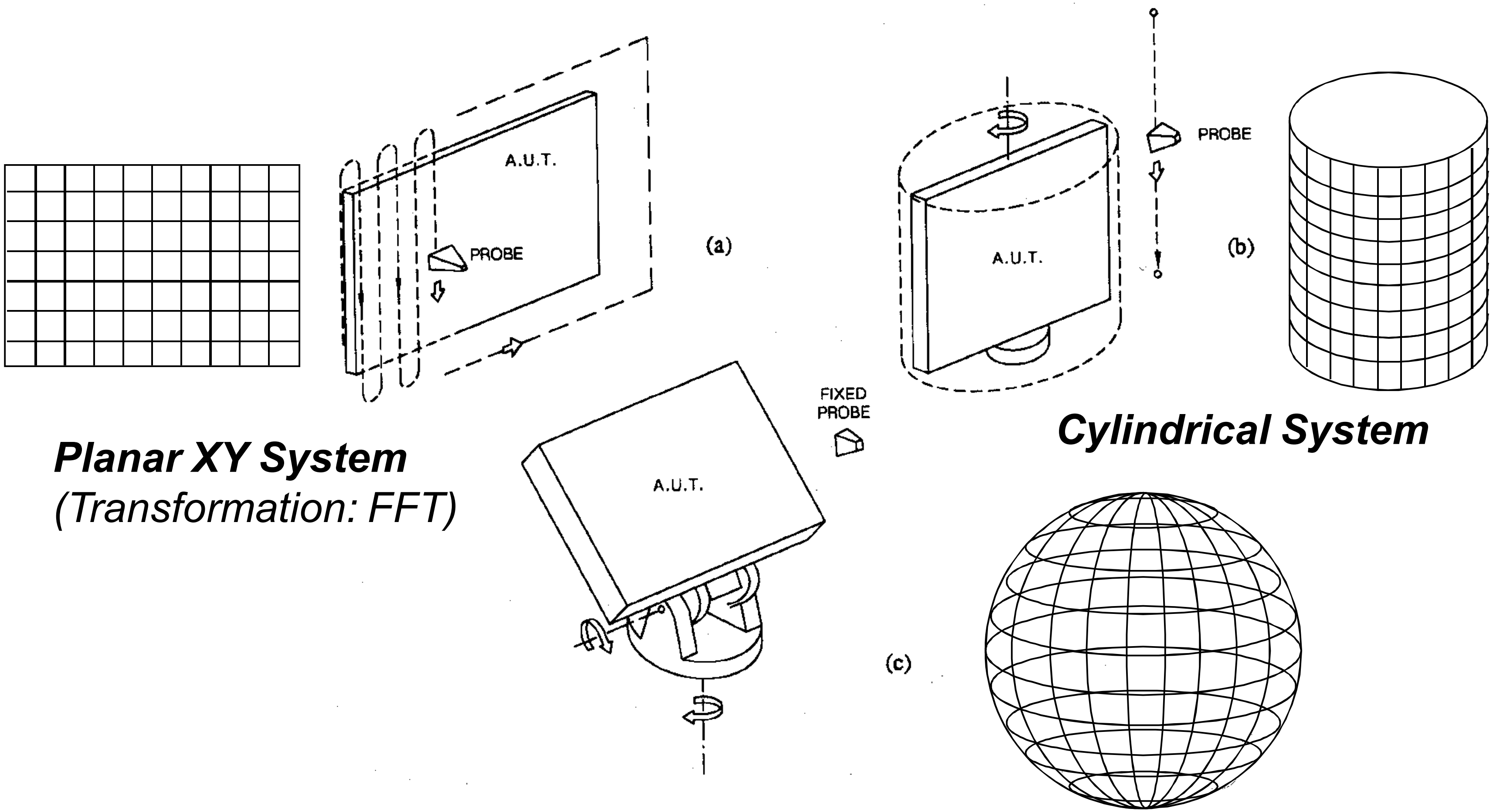

Planar XY System
(Transformation: FFT)

Cylindrical System

Spherical System

Near Field Ranges

- ***Plane-Polar System*** *(Transfomation: Bessel-Jacobi)*

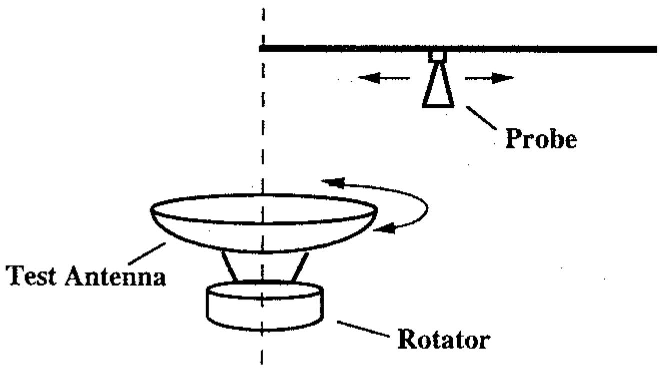

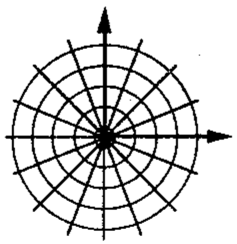

Plane-Polar
Data Grid

- ***Plane-Bi-polar System*** *(Interpolation+ FFT)*

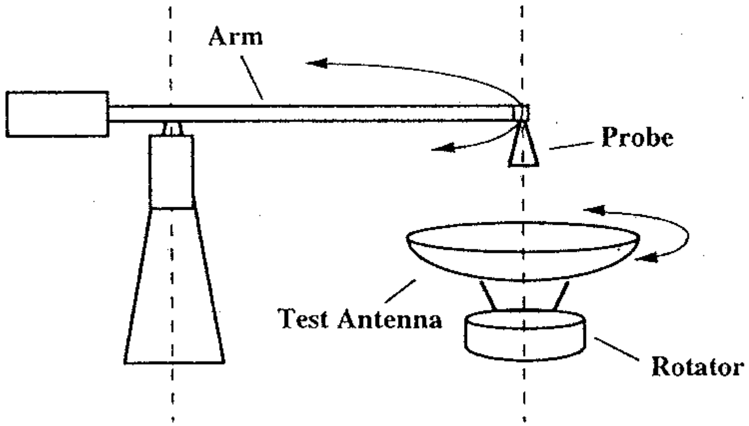

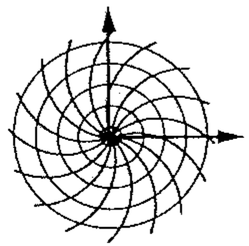

Bi-Polar
Data Grid

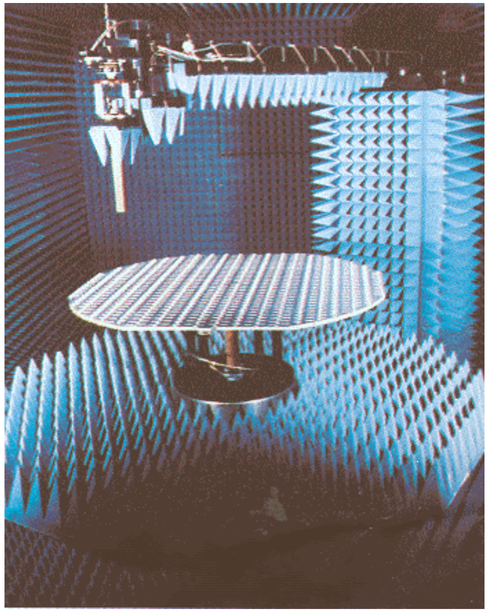

Bi-polar S. UCLA

ANTENNA Systems Solutions

Near Field Ranges: Comparison

- Planar System:
  - Conical coverage
  - Narrow beam antennas (apertures and planar arrays)
  - Direct diagnosis
  - Large space antennas
- Cylindrical System:
  - Toroidal coverage
  - Omni-directional antennas or with “fan” beam (Base station antennas)
  - Radar antennas
- Spherical System:
  - Full Coverage
  - Generic antennas (“general purpose”)
  - Well fitted for directivity computation.

Spherical Near Field Mesurements

Summary

- Spherical system Foundations.
  - System Geometry.
  - Radiated fields in spherical modes.
- Formulation with Probe correction.
  - Coupling equation.
  - Modal properties. Minimum sphere of measurement. Sampling.
  - Polarization and pattern correction.
- Practical Topics
  - Truncation.
  - Probe selection.
  - Alignment.
  - Mechanical errors effect

Spherical System Geometry

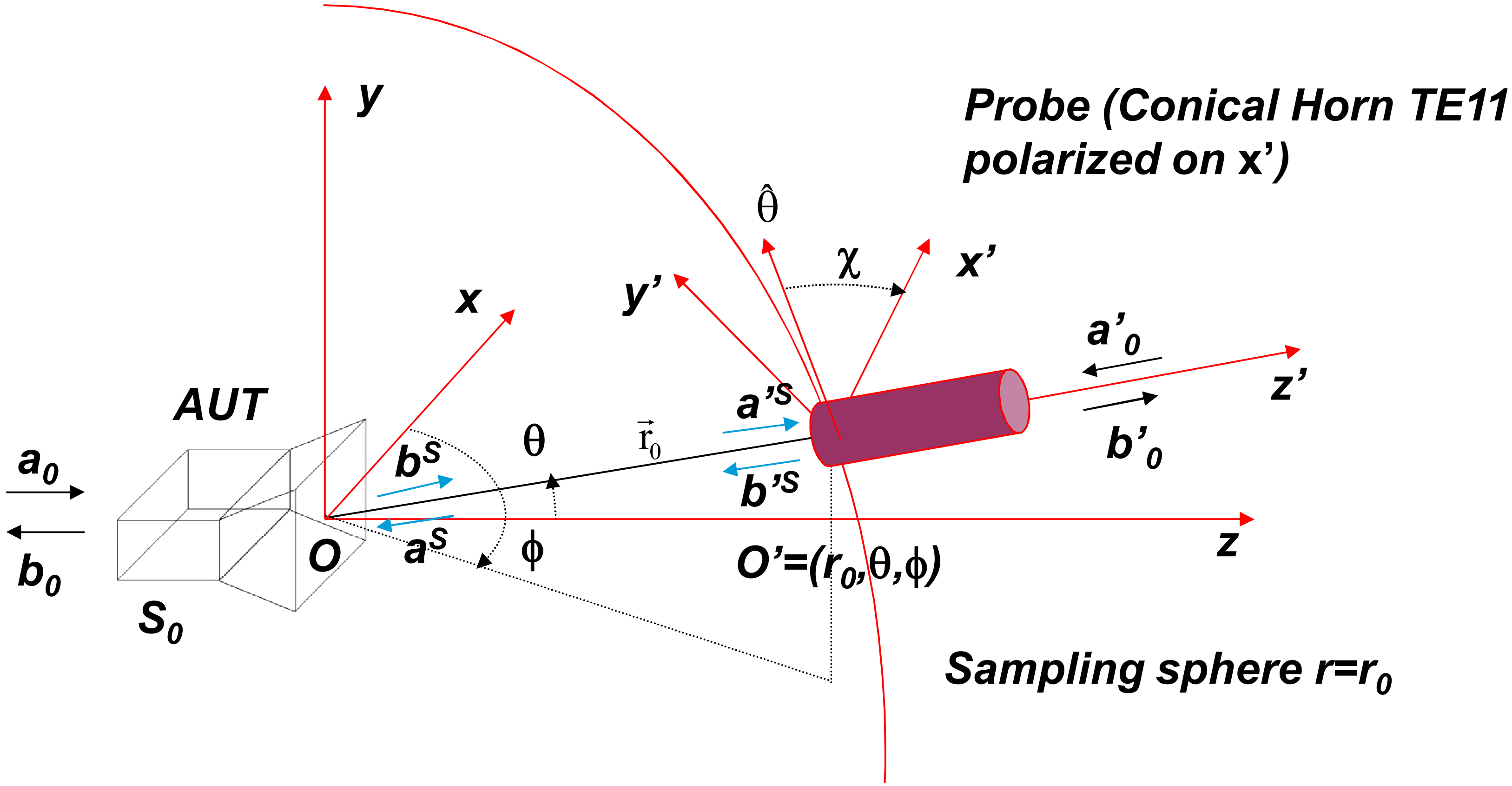

Spherical mode Decomposition

- Monocromatic Electrical Field by a Tx antenna in spherical modes.

1st kind Hankel's Function

Associated Legendre Polynomial

$$E(\vec{r}) = \sum_{n=1}^{\infty} \sum_{m=-n}^{n} T_{Mmn} \vec{M}_{mn}(\vec{r}) + T_{Nmn} \vec{N}_{mn}(\vec{r})$$

Modes TE

$$\vec{M}_{mn}(\vec{r}) = \frac{k}{\sqrt{\eta}} \left(\frac{-m}{|m|}\right)^m \sqrt{\frac{2n+1}{4\pi n(n+1)}} \sqrt{\frac{(n-|m|)!}{(n+|m|)!}} \begin{pmatrix} h_n^{(1)}(kr) \dfrac{jm}{\operatorname{sen}\theta} P_n^{|m|}(\cos\theta) \exp(jm\phi) \hat{\theta} - \\ - h_n^{(1)}(kr) \dfrac{dP_n^{|m|}(\cos\theta)}{d\theta} \exp(jm\phi) \hat{\phi} \end{pmatrix}$$

Modes TM

$$\vec{N}_{mn}(\vec{r}) = \frac{k}{\sqrt{\eta}} \left(\frac{-m}{|m|}\right)^m \sqrt{\frac{2n+1}{4\pi n(n+1)}} \sqrt{\frac{(n-|m|)!}{(n+|m|)!}} \begin{pmatrix} \dfrac{n(n+1)}{kr} h_n^{(1)}(kr) P_n^{|m|}(\cos\theta) \exp(jm\phi) \hat{r} + \\ + \dfrac{1}{kr} \dfrac{d\left(krh_n^{(1)}(kr)\right)}{d(kr)} \dfrac{dP_n^{|m|}(\cos\theta)}{d\theta} \exp(jm\phi) \hat{\theta} + \\ + \dfrac{1}{kr} \dfrac{d\left(krh_n^{(1)}(kr)\right)}{d(kr)} \dfrac{jm}{\operatorname{sen}\theta} P_n^{|m|}(\cos\theta) \exp(jm\phi) \hat{\phi} \end{pmatrix}$$

Spherical Modes

Mode $N_{1,5}$

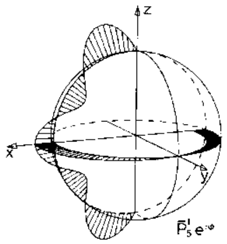

N_r

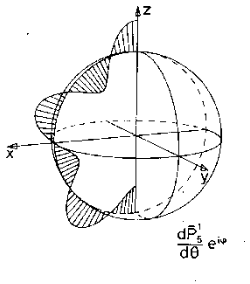

N_θ

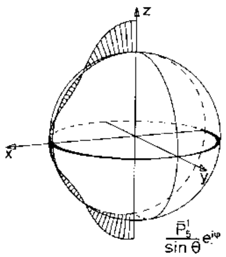

N_ϕ

Mode $N_{0,4}$

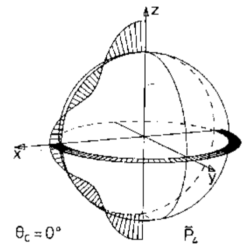

N_r

Mode $N_{6,10}$

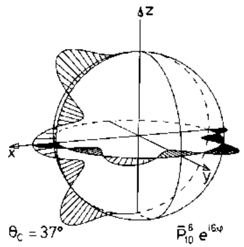

N_r

Mode $N_{20,24}$

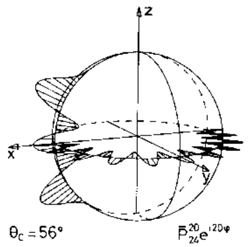

N_r

Received signal by the Probe

Modes Normalization

Radiated Power $= \frac{1}{2}\sum_{m,n}\left[\left|T_{Mmn}\right|^2 + \left|T_{Nmn}\right|^2\right]$

Probe Received Signal (as a multiport network)

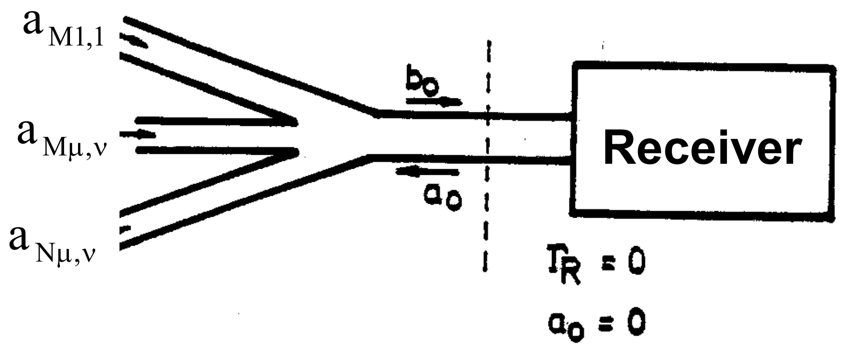

$$W = b_0' = \sum_{\mu,\nu}\left[a_{M\mu,\nu}P_{M\mu,\nu} + a_{N\mu,\nu}P_{N\mu,\nu}\right]$$

Spherical Mode Amplitude from AUT that inputs in probe system x'y'z'

Rx Scattering matrix of the probe

Coupling Equation

Received signal by the power:

$$W(r_0,\theta,\phi,\chi)=\sum_{mn\mu}\left(T_{Mmn}P_{M\mu n}(r_0)+T_{Nmn}P_{N\mu n}(r_0)\right)\exp(jm\phi)d^{n}_{\mu m}(\theta)\exp(j\mu\chi) \qquad \textbf{(1)}$$

where

$$P_{M\mu n}(r_0)=\frac{1}{2}\sum_{\nu}\left(C^{Mn}_{M\mu\nu}(r_0)P_{M\mu\nu}+C^{Mn}_{N\mu\nu}(r_0)P_{N\mu\nu}\right) \qquad P_{N\mu n}(r_0)=\frac{1}{2}\sum_{\nu}\left(C^{Nn}_{M\mu\nu}(r_0)P_{M\mu\nu}+C^{Nn}_{N\mu\nu}(r_0)P_{N\mu\nu}\right)$$

Multiplying (1) by $\exp(-jm\phi)\,d^{n}_{\mu m}(\theta)\exp(-j\mu\chi)\,\mathrm{sen}\,\theta$ **and integrating in χ,ϕ, y θ :**

$$T_{Mmn}P_{M\mu n}(r_0)+T_{Nmn}P_{N\mu n}(r_0)=\frac{n+\frac{1}{2}}{4\pi^2}\int_{\chi=0}^{2\pi}\int_{\phi=0}^{2\pi}\int_{\theta=0}^{\pi}W(r_0,\theta,\phi,\chi)d^{n}_{\mu m}(\theta)\,\mathrm{sen}\,\theta\, d\theta\,\exp(-jm\phi)d\phi\,\exp(-j\mu\chi)d\chi$$

Using two acquisitions for χ=0 y χ=90, at each couple (m,n) the integral for μ=1 and μ=-1, an system of 2 equations with 2 unknowns: T_{Mmn} y T_{Nmn}
Probe must be rotational symetry and excited with a cylindrical mode TE_{11} ($\mu=\pm1$, taht is to say expressed in terms of senϕ y cosϕ)

Propagation Cut Conditions of Spherical Modes

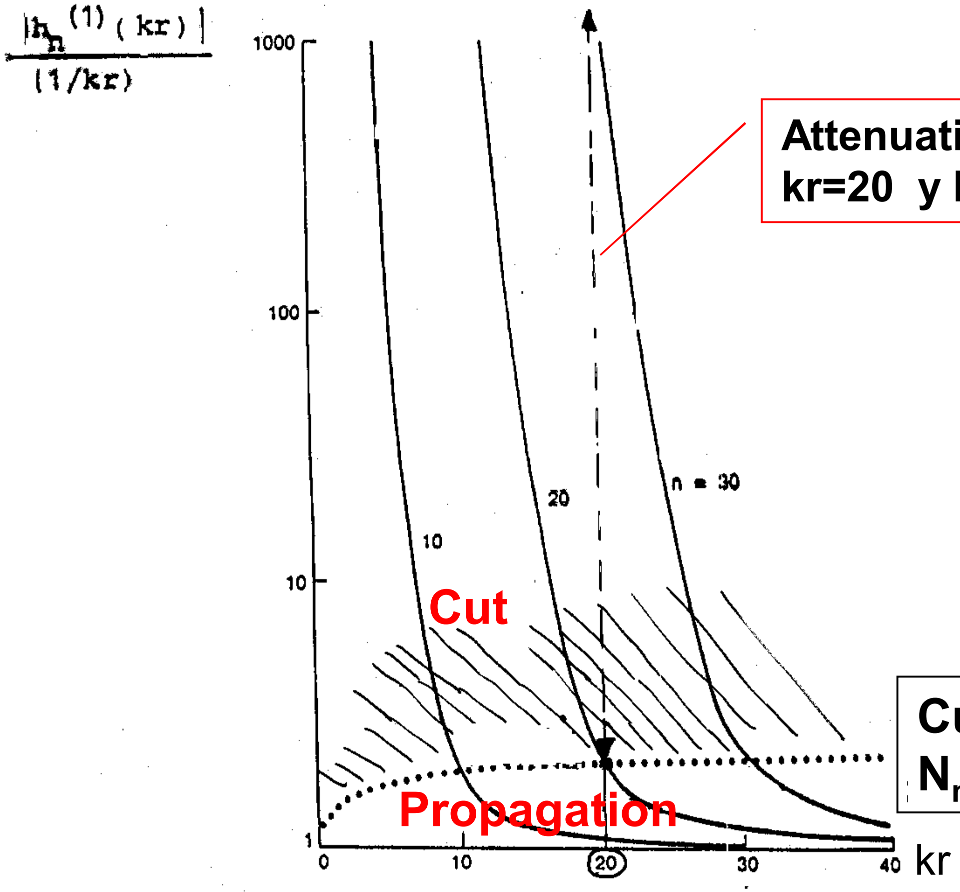

Attenuation of mode n=30 between kr=20 y kr=30 (>60 dB)

Cut Condition
$N_{max}=kR_0$

Sphere of minimum radius closing the antenna

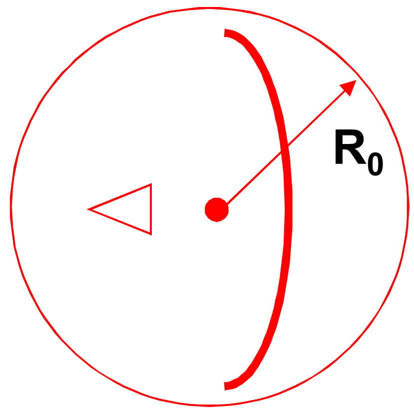

Near Field Sampling

- Near field is sampled on a regular grid (θ,ϕ) with steps $\Delta\theta$ and $\Delta\phi$ for χ=0 y χ=90. $\Delta\theta$ and $\Delta\phi$ are function of the minimum radius R_0 enclosing the antenna.
- Doing $N_{max}=kR_0+10=2\pi R_0/\lambda + 10$
- Angular steps are: $\Delta\theta \leq 180^o/N_{max}$ $\qquad \Delta\phi \leq 360^o/2N_{max}$
- Truncating the antenna to θ_1 $(0\leq\theta\leq\theta_1)$, the step $\Delta\phi$ can be reduced

$$M_{max} = N_{max}\,\text{sen}\,\theta_1 \qquad \Delta\phi \leq 360^o/2M_{max}$$

- ***The angular steps measured on the surface of the minimum radius are equivalent to the Samplig Theorem (separation of λ/2)***

Probe Correction

• **Polarization Correction**:
Se Q ratio at “Probe Calibration”

• **Pattern Correction**:
Necessary in case the tapering of probe pattern of the minimum sphere enclosing the antenna is larger than 0.5 dB.

Probe correction forces to compute probe spherical coefficients $P_{M\mu\upsilon}$ y $P_{N\mu\upsilon}$ processing it as an AUT.

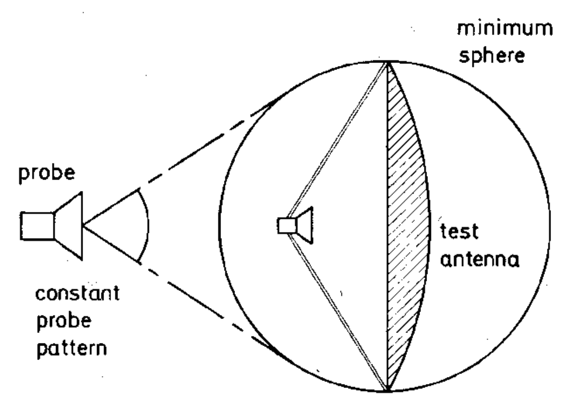

Probe having a constant pattern over the minimum sphere

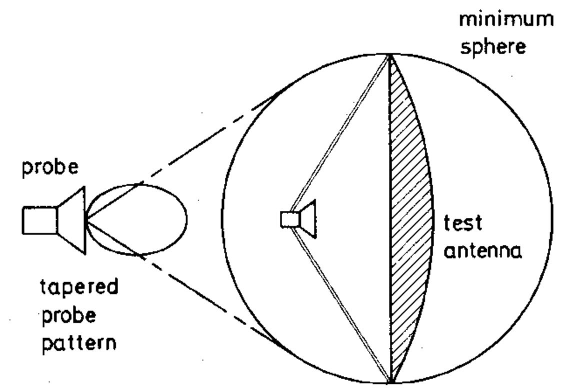

Probe having a tapered pattern over the minimum sphere

Probe Correction: Errors

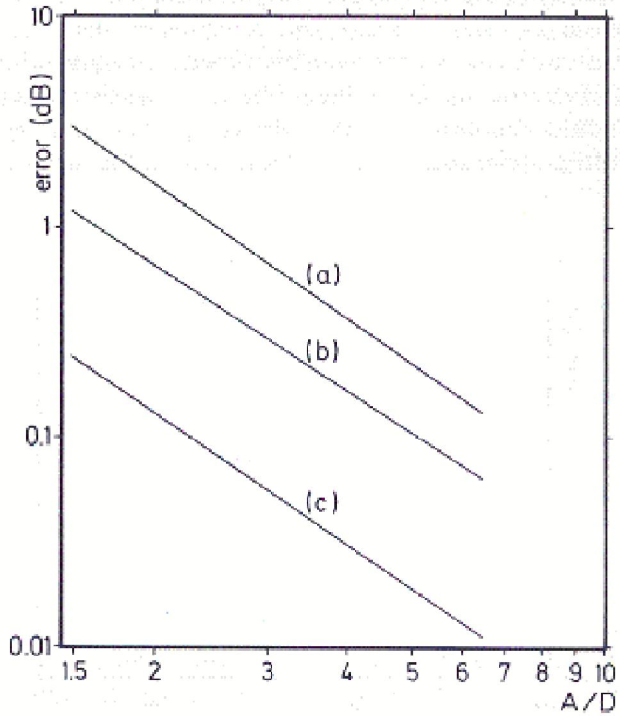

Error when probe correction is omitted versus relative measurement distances A/D. Probe directivity is 12.1 dBi.

(*a*) Inaccuracy of first side-lobe level (at −26.8 dB)

(*b*) Inaccuracy of cross-polar lobe (at −48.2 dB)

(*c*) Inaccuracy of main-beam directivity (at 38.4 dBi)

Both scales are logarithmic. Error in dB is seen to be proportional to $1/A^2$

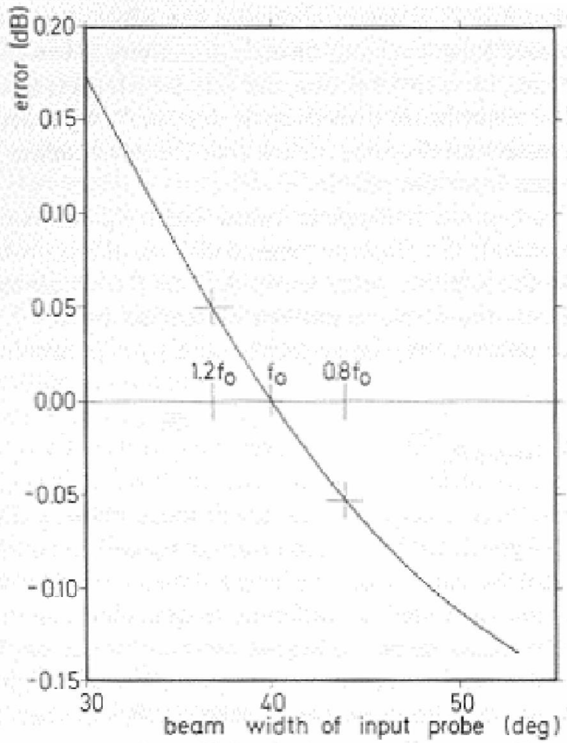

Error in main-beam directivity (at 38.4 dBi) when transformation probe is different from sampling probe, sample distance A = 15.1

Within the two horizontal lines the simulated probe changes are obtained by a frequency shift of ±20% from the nominal frequency f_0 of a probe of 6 hertzian dipoles. Outside the lines, the probe is changed by the number of elements in the probe

Source: J.E. Hansen. Spherical Near-Field Antenna Measurements

Acquisition Truncation

- When truncating the acquisition, the validation range is reduced as it is shown in the figure

θ_{tf} : Validation angle for Far Field

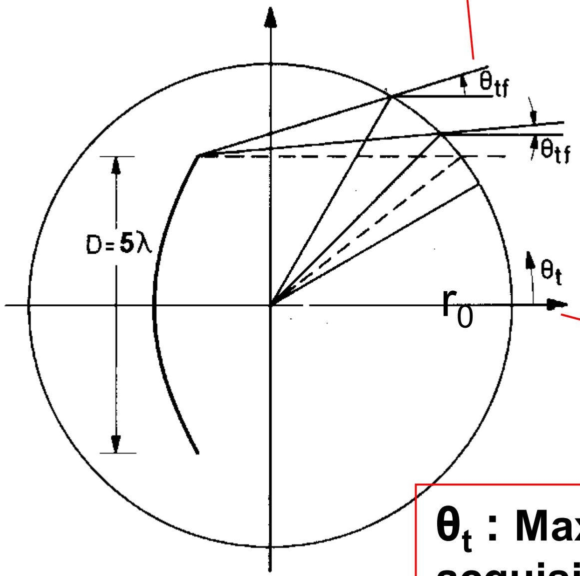

θ_t : Maximum acquisition angle

Measured Spherical Surface

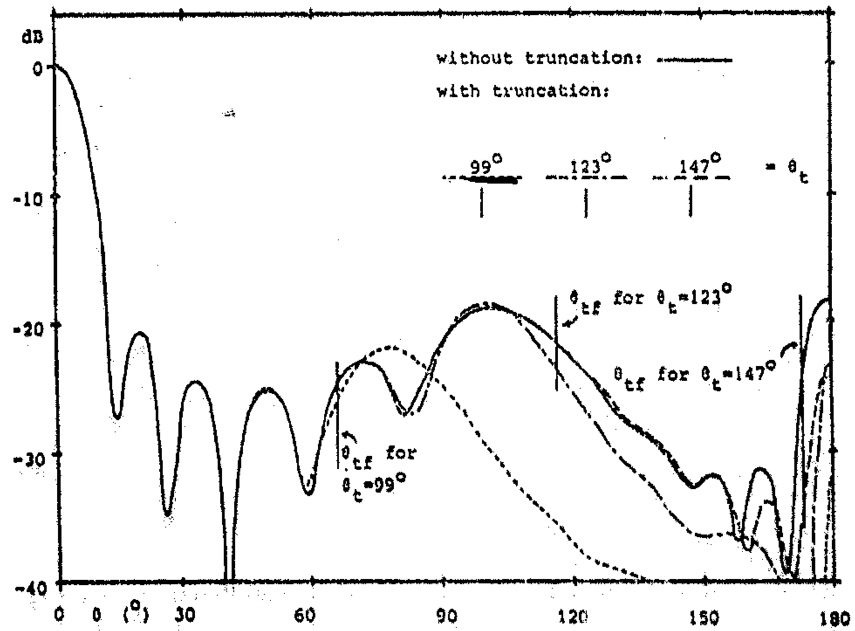

Simulated examples

Measurement Probe Selection

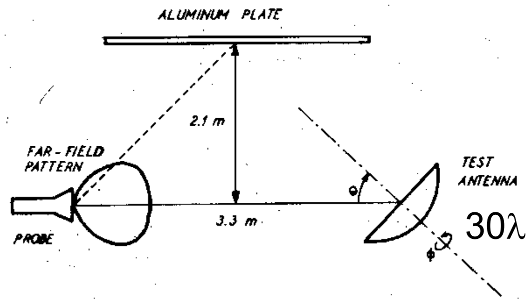

Cancelling of relected signals with directive probes.
Probe correction just corresponds to the signal coming from the measurement sphere of radius R_0 related to the transformation mode number N_{MAX}.

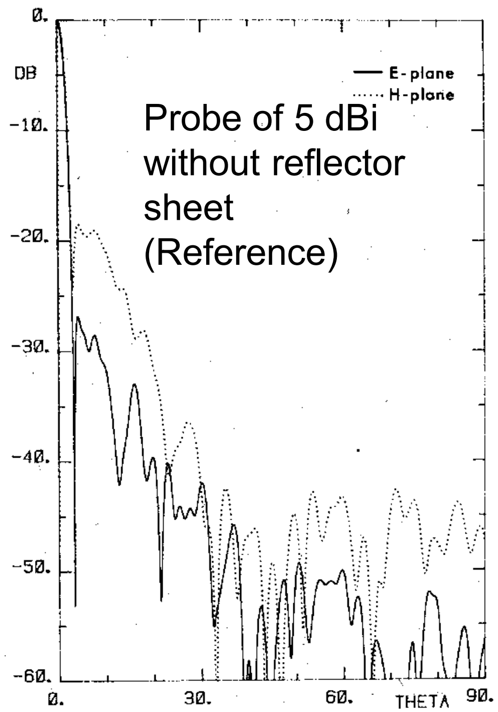

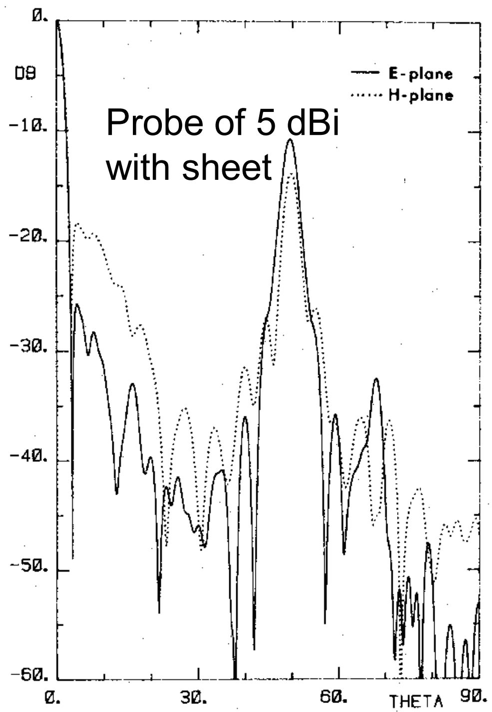

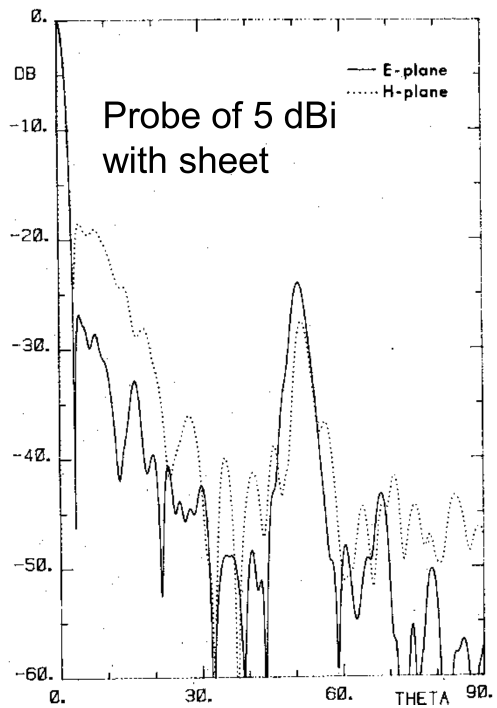

ISOFILTER™ Technique

- Las propiedades de corte de los modos esféricos también se pueden aprovechar para aislar la radiación de pequeñas antenas situadas sobre estructuras complejas.
- En la figura superior puede verse una pequeña bocina con la apertura situada a 7 pulgadas de un plano de masa de 36 pulgadas de diámetro, con distintas esferas de radio mínimo.
- La técnica pasa por adquirir los campos próximos asociados a la esfera de máximo tamaño y reducir luego el número de modos de la transformación de acuerdo con Nmax=kR_0+10 a la esfera deseada.
- Si se cambia el centro de la esfera hay que corregir los campos lejanos por el témino de fase asociado a la traslación, multiplicandolos por $e^{jk\vec{r}_o\cdot\hat{r}(\theta,\phi)}$, antes de obtener los modos sobre el nuevo sistema de representación para filtrarlos (reducir su número) y pasar de nuevo a campo lejano.

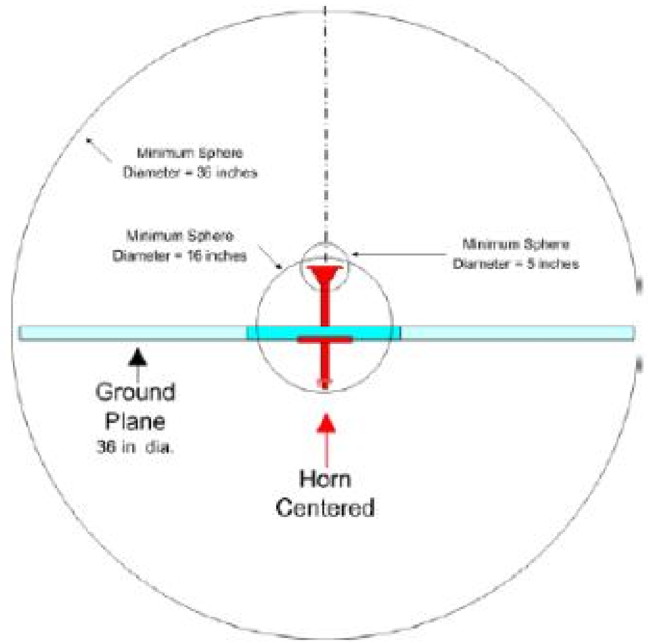

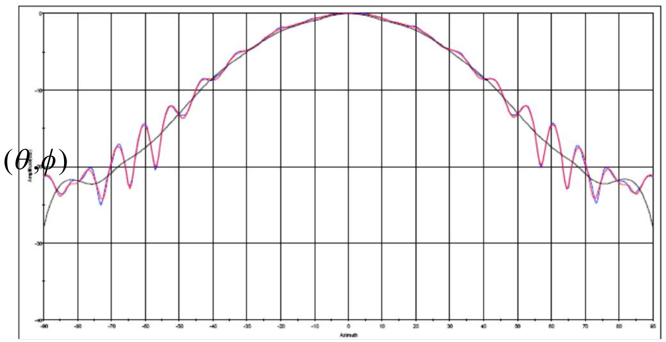

Campo lejano con rizado de plano de masa y filtrado

UPM Spherical System

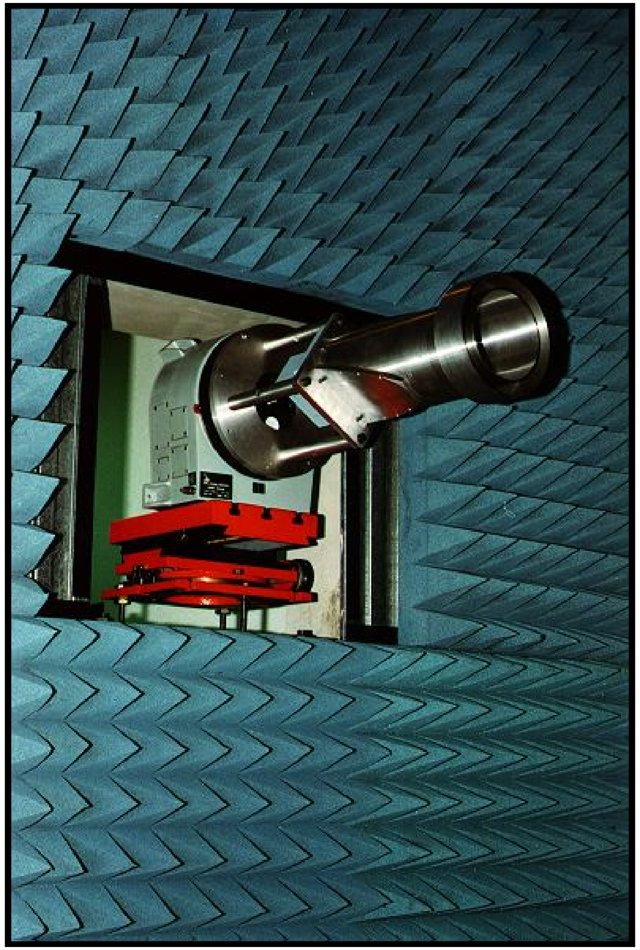

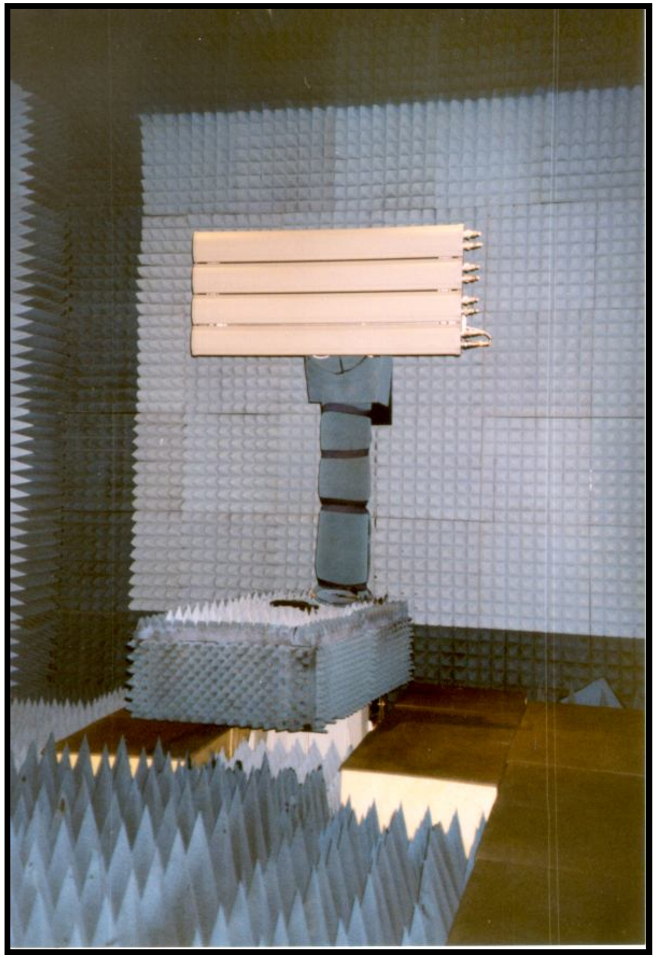

Alignment Procedure

Double colimation to fix the probe

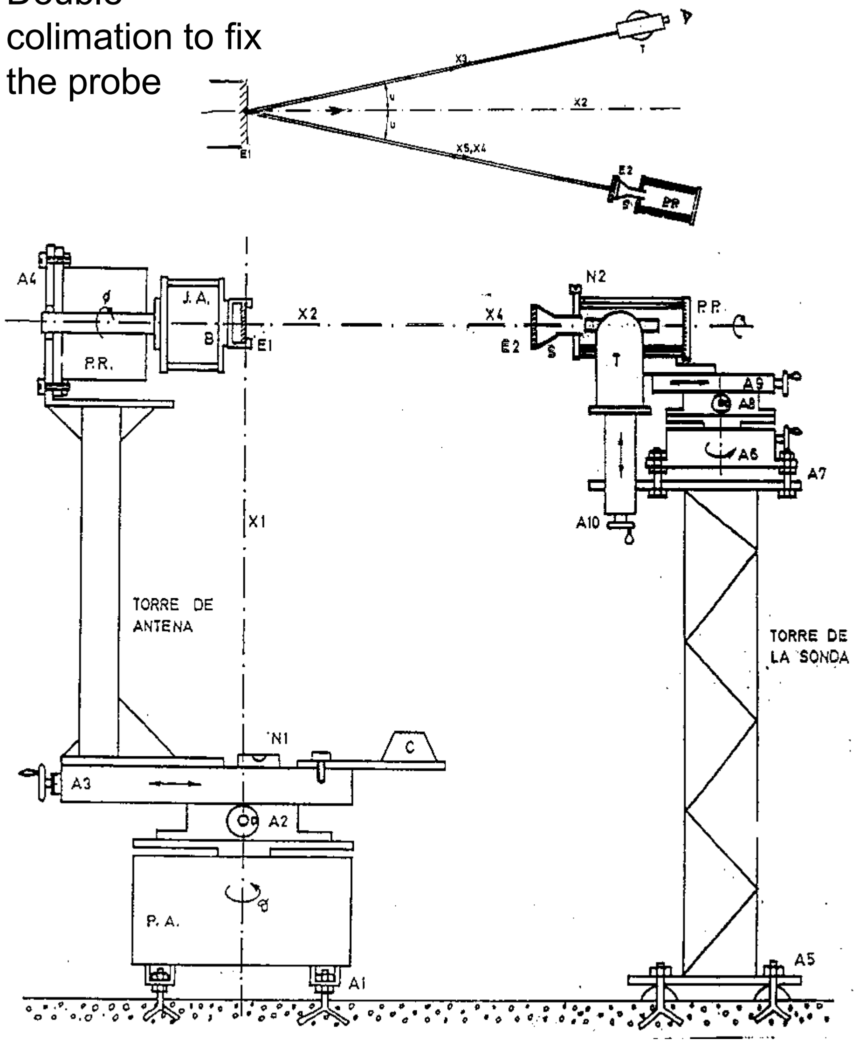

- Alignment Conditions:
  - Azimuth axis (X1) must be vertical.
  - Roll axis (X2) must be horizontal.
  - X1 and X2 must intersect to define the sphere measurement center.
  - Probe axis (X4) must be horizontal pointing at the sphere center.
  - Azimuth axis must be fixed to define θ=0º.
  - Polarization reference must be placed horizontal.

Mechanical Errors Effects

Table 6.1 *Influence on far-field pattern performances of typical mechanical inaccuracies (reflector antenna, D = 30λ). Dashes (—) indicate values below the level of numerical accuracy. The sign of the inaccuracies will in some cases change when the sign of the simulated error is changed.*

Mechanical inaccuracies	Main beam			First null	First side lobe	Cross-polar lobe
	Directivity	Cross-polar level	Beam width	Position	Level	Level
Reference far-field values	38.4 dBi	$-\infty$ dB	2.25°	2.95°	−26.8 dB	−48.2 dB
	Change in dB	Increased to (dB)	Change in degrees	Change in degrees	Change in dB	Change in dB
Elevation-over-azimuth set-up						
1. Non-intersecting axes (0.1λ)	0.07	—	0.02	0.02	0.07	0.05
2. Horizontal depointing (0.1°) at $\theta = 0$	0.03	—	—	—	1.2	0.03
3. Vertical depointing (0.1°) at $\theta = 0$	—	−75	—	—	—	—
4. Wrong measurement distance (0.1λ)	—	—	—	—	0.14	—
5. Horizontal probe misalignment (0.1λ)	0.04	—	—	0.01	1.6	0.03
6. Vertical probe misalignment (0.1λ)	—	—	—	—	—	—
7. Probe rotated (0.1°) around probe axis	—	−55	—	—	—	0.15
8. Angular resolution (±0.03°)	—	—	—	—	0.11	0.09

The reference field has a null for the cross polarization in the main beam direction. The table values show, relatively to the peak directivity, the level to which the cross polarization increases when the inaccuracies are introduced.

Source: J.E. Hansen. Spherical Near-Field Antenna Measurements

Block Scheme of UPM Range

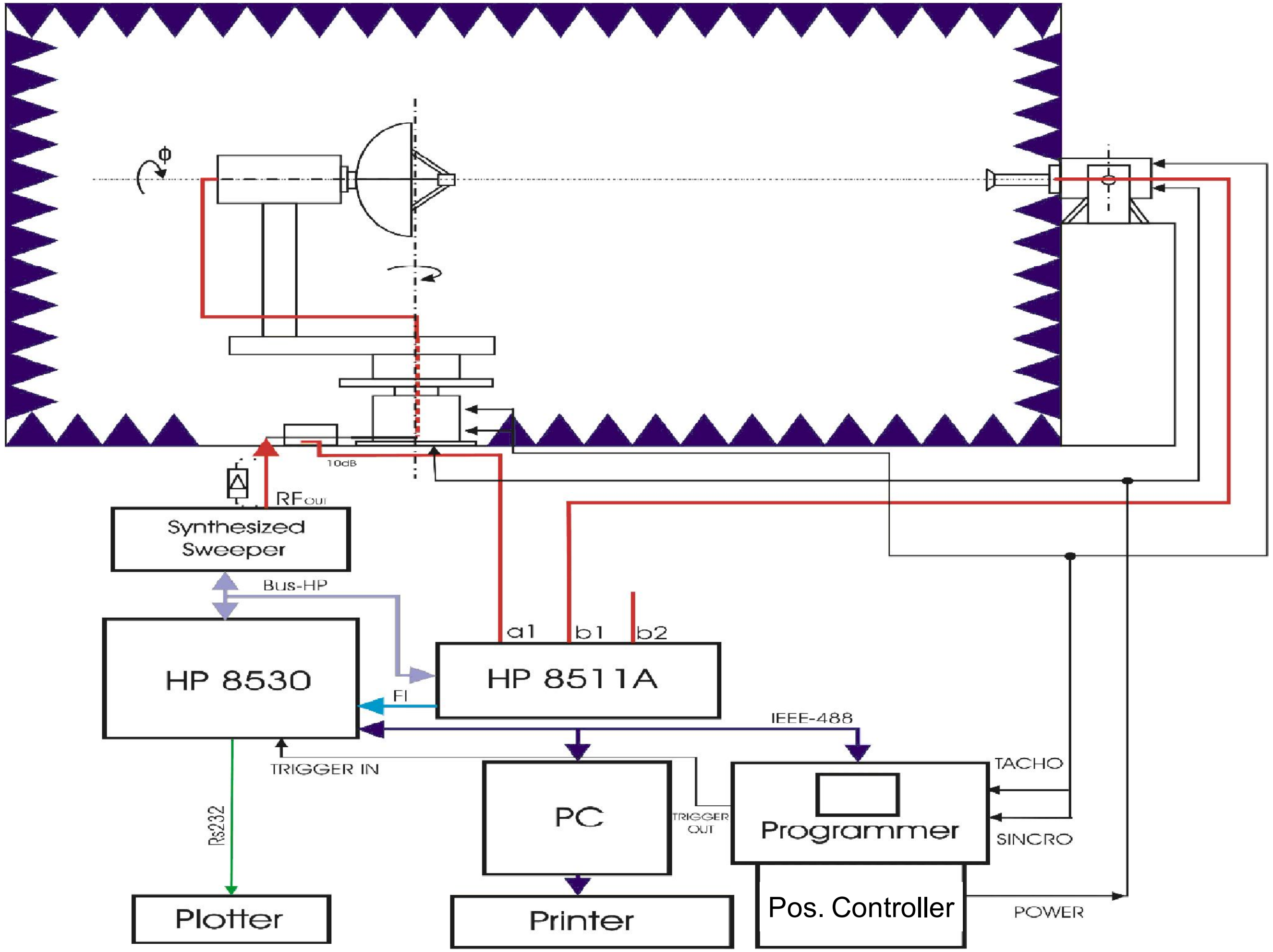

Software PROCENCA

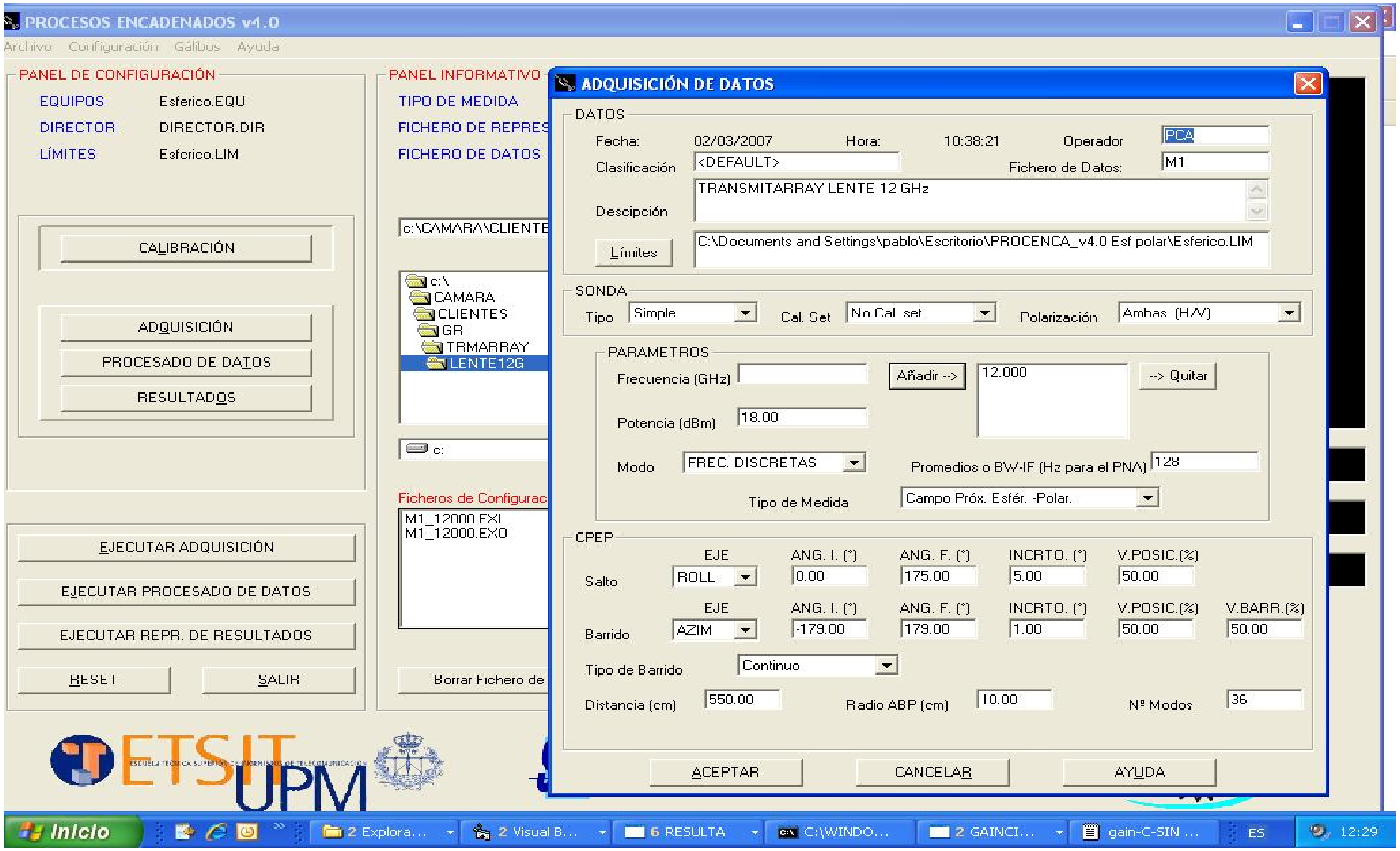

Measurement Definition

Software PROCENCA

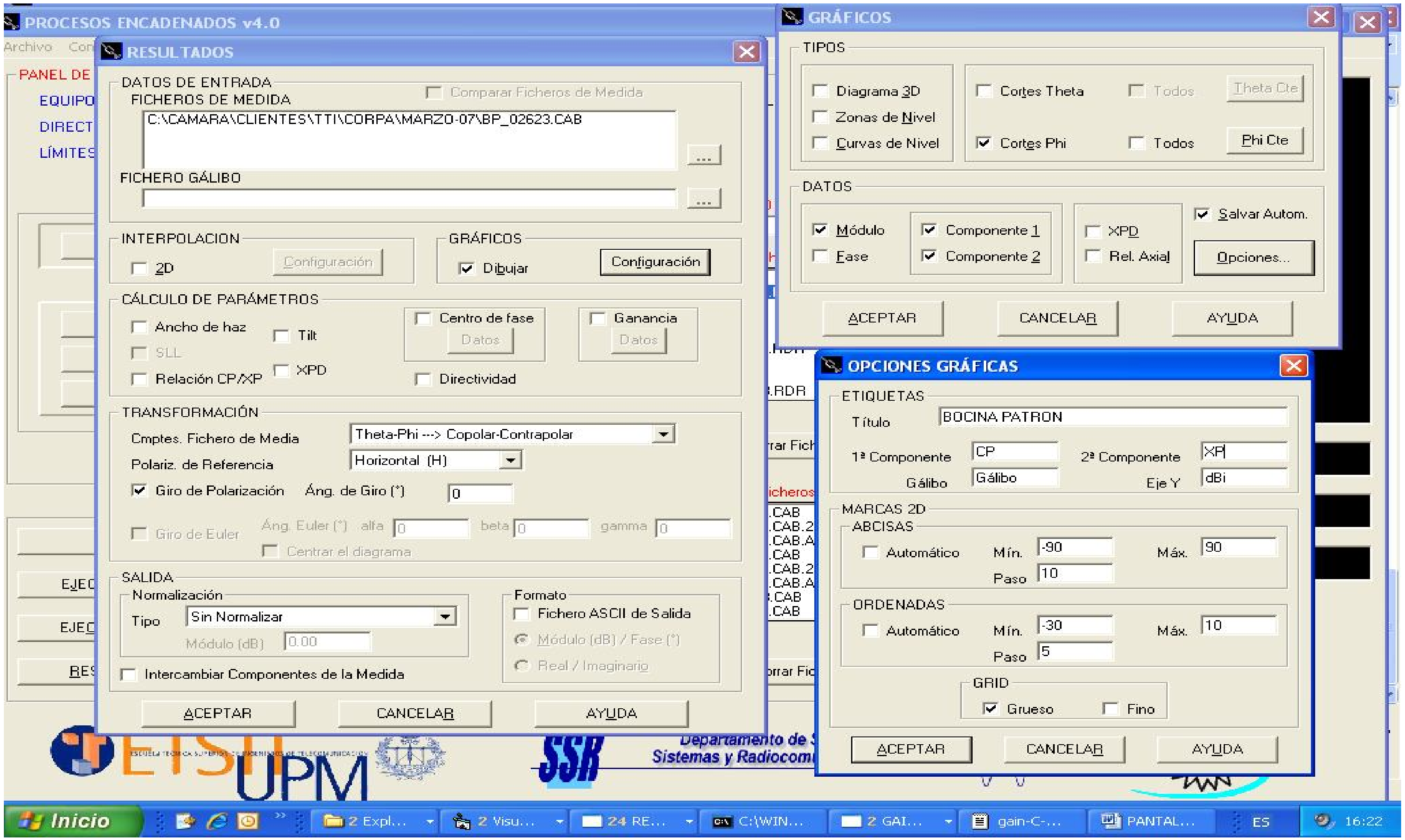

Results Definition

Software PROCENCA (GR-UPM)

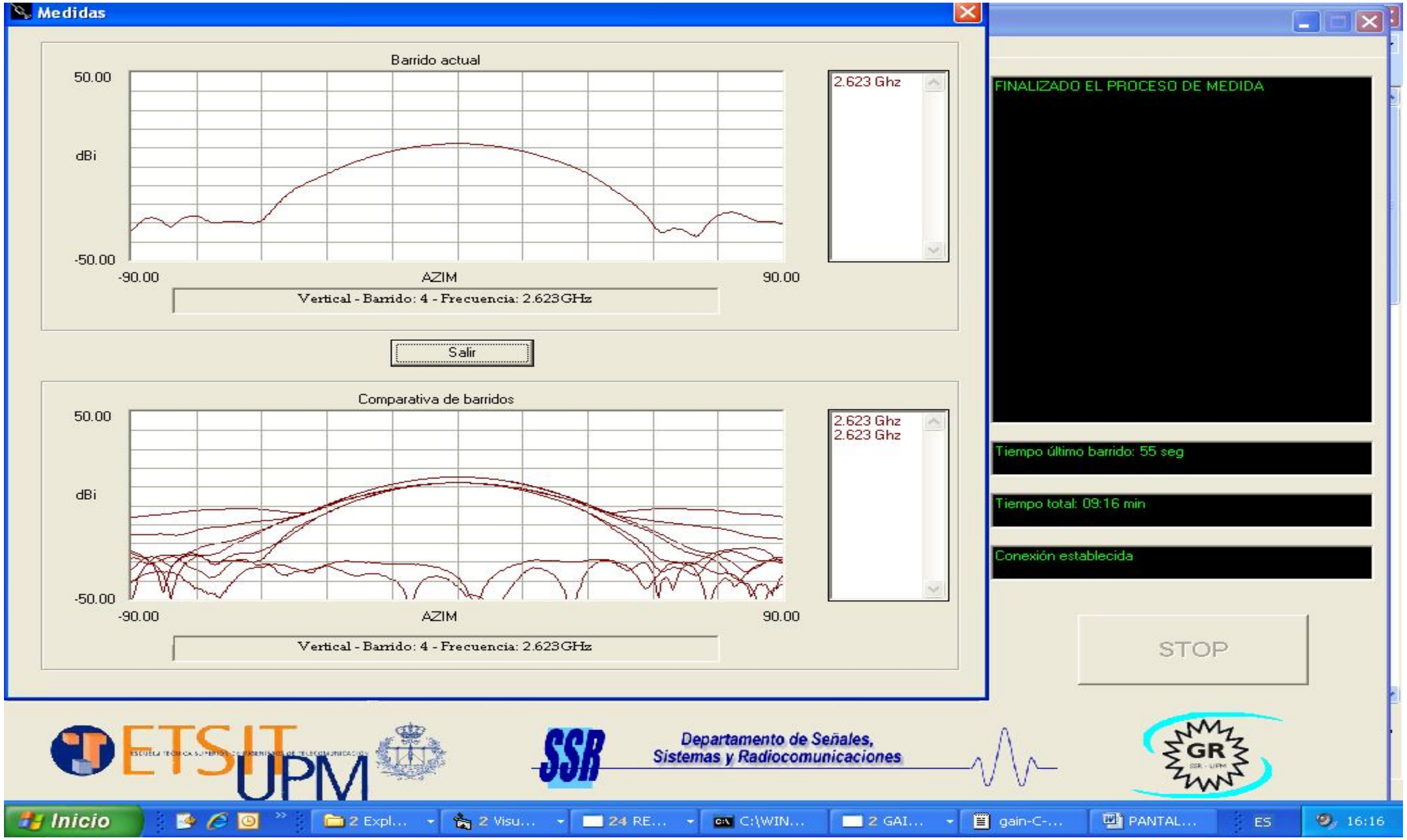

Acquisition Display

Software PROCENCA

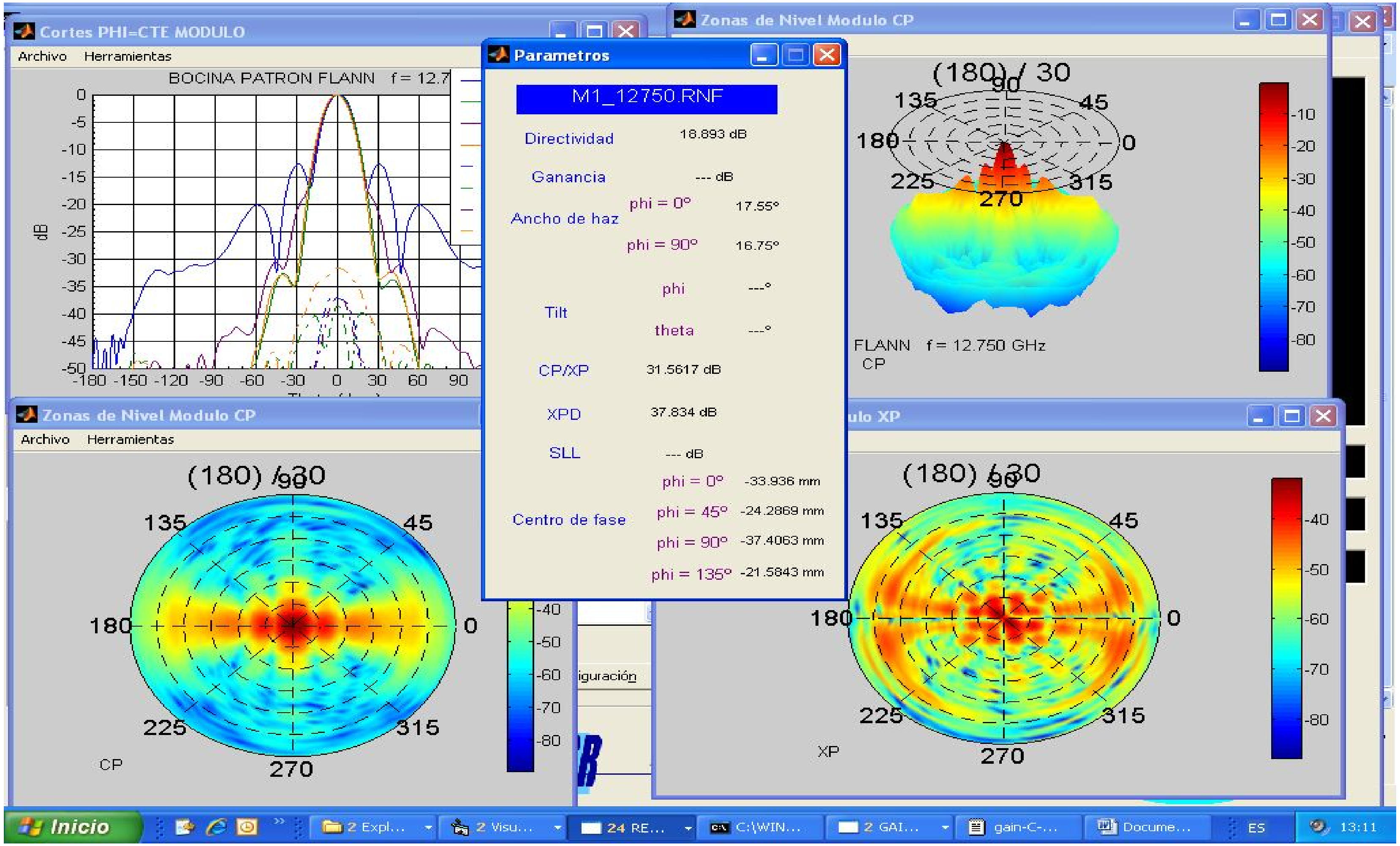

Results

Probe Calibration: Rotational Symmetry (TE_{11})

Measurement :

- ***Co-polar Pattern E_{PE1}, E_{PH1}***
- ***Axial Circular Polarization Ratio at every port:***

$$Q_i = \frac{E_{Ri}}{E_{Li}} = \frac{E_{xi} - jE_{yi}}{E_{xi} + jE_{yi}}$$

- ***Rx port ratio 1 y 2 : $A_{X/Y}$***

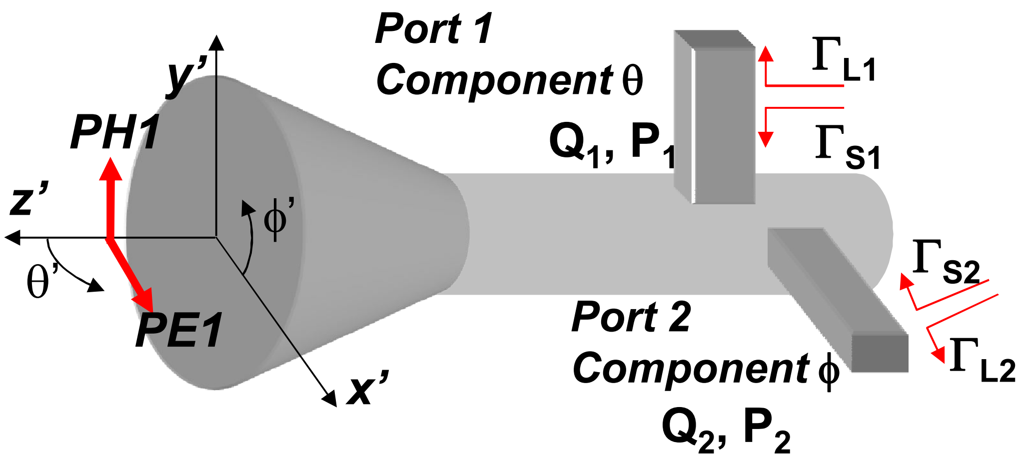

- ***Axial linear polarization Ratio***

$$P_1 = \frac{E_{y1}}{E_{x1}} = j\frac{Q_1 - 1}{Q_1 + 1} \qquad P_2 = \frac{E_{x2}}{E_{y2}} = -j\frac{Q_2 + 1}{Q_2 - 1}$$

- **Normalised Pattern of the Ideal Probe**

$$\frac{\vec{E}_1(\theta,\phi)}{\vec{E}_1(0^o,0^o)} = \left[\frac{E_{PE1}(\theta)}{E_{PE1}(0^o)}\hat{\theta} - P_1\frac{E_{PH1}(\theta)}{E_{PE1}(0^o)}\hat{\phi}\right]\cos\phi + \left[P_1\frac{E_{PE1}(\theta)}{E_{PE1}(0^o)}\hat{\theta} + \frac{E_{PH1}(\theta)}{E_{PE1}(0^o)}\hat{\phi}\right]sen\phi$$

$$\frac{\vec{E}_2(\theta,\phi)}{\vec{E}_2(0^o,0^o)} = \left[P_2\frac{E_{PE1}(\theta)}{E_{PE1}(0^o)}\hat{\theta} - \frac{E_{PH1}(\theta)}{E_{PE1}(0^o)}\hat{\phi}\right]\cos\phi + \left[\frac{E_{PE1}(\theta)}{E_{PE1}(0^o)}\hat{\theta} + P_2\frac{E_{PH1}(\theta)}{E_{PE1}(0^o)}\hat{\phi}\right]sen\phi$$

Gain Measurement by Comparison

$$G_{AUT}(\theta,\phi)=\frac{|W_{AUT}(\theta,\phi)|^2}{|w_{AUT}(\theta_1,\phi_1)|^2}\frac{|w_{AUT}(\theta_1,\phi_1)|^2}{|w_{SGH}(\theta_2,\phi_2)|^2}\frac{|w_{SGH}(\theta_2,\phi_2)|^2}{|W_{SGH}(0,0)|^2}G_{SGH}$$

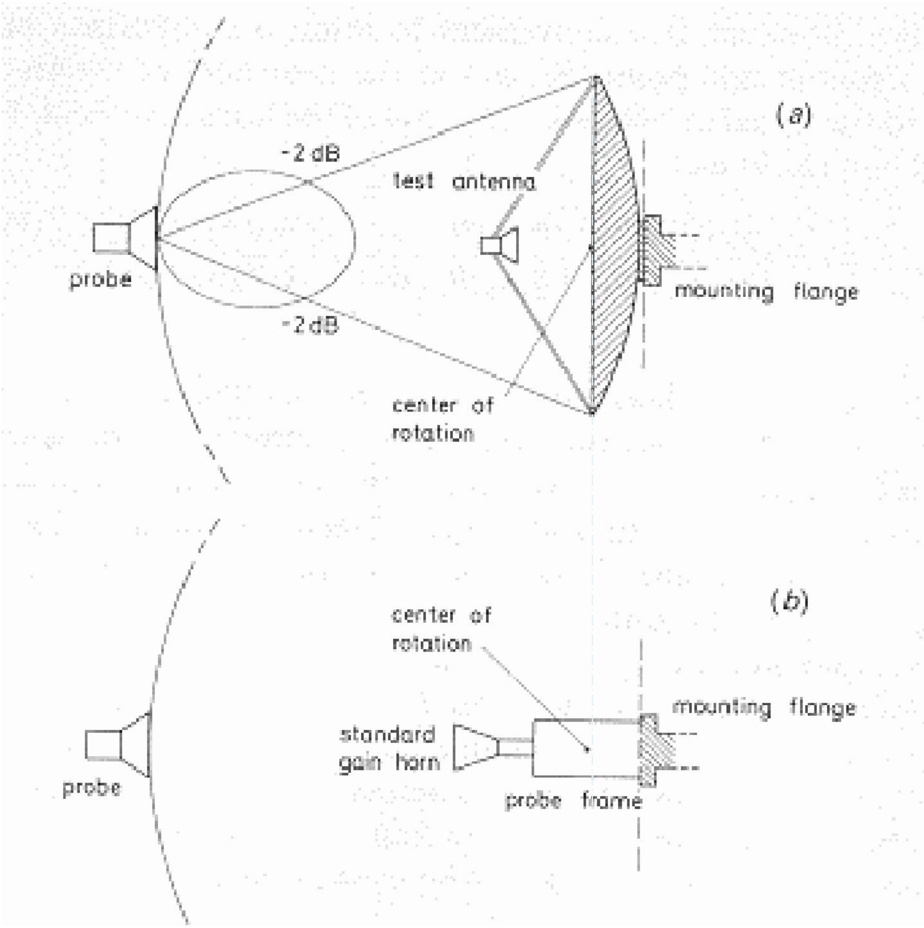

- Far Field Gain can be obtained measuring the near field of a SGH and computing:
  - Far field to near field Ratio of AUT
  - Comparison of near field between AUT and probe
  - Near field to Far Field ratio of the SGH probe
  - SGH gain.
- The distance between center of rotation of AUT and probe must be the same to the distance between enter of rotation of SGH and probe

Inter-comparison within ACE

Pattern results of the principal planes

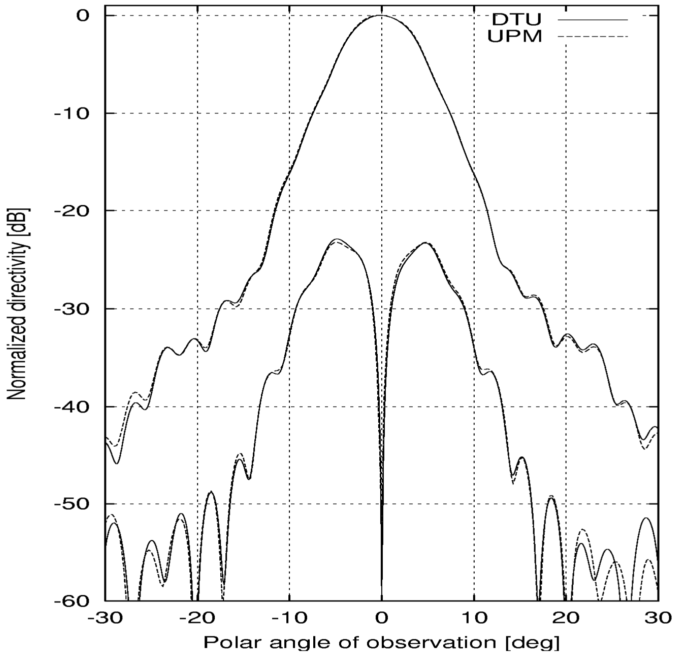

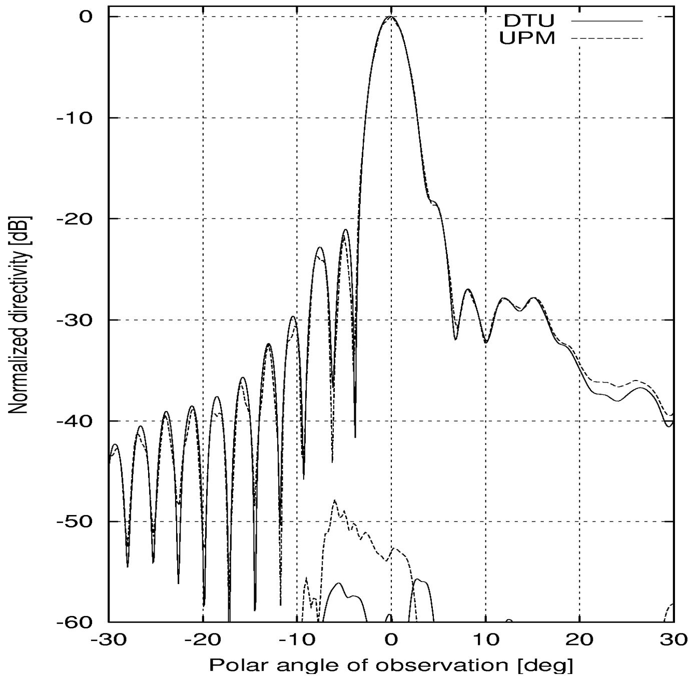

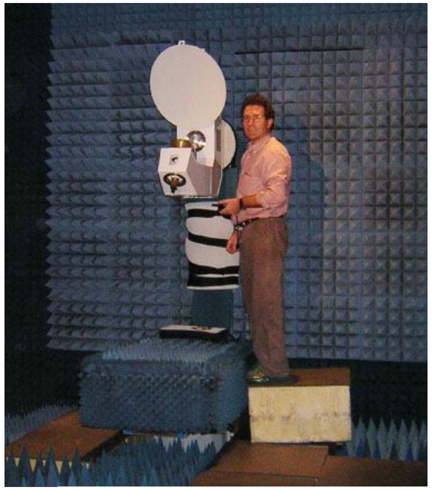

VAST12 antenna (ESA)

	Directivity	Gain
DTU	30.71	30.35
UPM	30.62	30.36
FTRD*	31.1	30.4

* Far Field Measurement in La Turbie - France Telecom

References

- J.E. Hansen. Spherical Near-Field Antenna Measurements. Peter Perigrinus. 1988.
- R.F. Harrington. Time-Harmonic Electromagnetic Fields. McGraw-Hill 1961.
- R.E. Collins. Field Theory of Guide Waves. McGraw-Hill 1960.
- Dan Slater. Near-Field Antenna Measurements. Artech House. 1991.
- The Handbook of Antenna Design. Chapter 8. A.W. Rudge et al (Ed.), Appel-Hansen J, et al. Peter Pelegrinus Ltd 1982.
- AMTA Proceedings.
- IEEE Trans. on Antennas and Propagation. Special Issue on Near-Field Scanning Techniques. June 1988.
- O. Breinbjerg, S. Pivnenko, M.Sierra Castañer, C. Savatier. Antenna Measurement Facility Comparison Campaign within the European Antenna Centre of Excellence. 2005 IEEE AP-S International Symposium. Washington, DC, USA. 2005.